MODELING SPARGING RELATED DEATH IN ANIMAL CELL BIOREACTORS

By

STEVEN J. MEIER

Bachelor of Chemical Engineering, 1992
University of Minnesota

Submitted to the Department of Chemical Engineering in
Partial Fulfillment of the Requirements for the Degree of

DOCTOR OF PHILOSOPHY IN CHEMICAL ENGINEERING
at the
MASSACHUSETTS INSTITUTE OF TECHNOLOGY
June, 1998

Author:_____
Department of Chemical Engineering
May 18, 1998

Certified by:_____
Daniel I.C. Wang
Institute Professor
Thesis Supervisor

Certified by:_____
T. Alan Hatton
Ralph Landau Professor of Chemical Engineering Practice
Thesis Supervisor

Accepted by:_____
Robert C. Cohen
St. Laurent Professor of Chemical Engineering
Chairman, Committee for Graduate Students

MODELING SPARGING RELATED DEATH IN ANIMAL CELL BIOREACTORS

by
Steven J. Meier

Submitted to the Department of Chemical Engineering on May 18, 1998, in partial fulfillment of the requirements for the degree of Doctor of Philosophy in Chemical Engineering

Sparging related death remains a problem for some cell culture systems. The bubble burst is most commonly cited as the direct cause of cell death. Surface active polymers reduce sparging related cell death, but their protection mechanisms were unclear. A killing volume model and some experiments in the literature suggest that death is independent of the bubble rise. Another group found that cells can attach to rising bubbles, yet cells attached to bubbles would be expected to die when the bubbles burst. This work seeks to reconcile such discrepancies.

Death associated with the bubble rise depends on a radius projected by the rising bubble. The projected radius was determined by analysis of liquid flow around the bubble, and it incorporates a cell-bubble attachment time. A short attachment time maximizes the projected radius, while a long attachment time minimizes it. In a literature report, the attachment time in a serum free medium was short, while the addition of Pluronic® F68 or methyl cellulose greatly increased the attachment time. Thus, additives such as Pluronic® F68 or methyl cellulose are expected to minimize rise-related death. This explains two literature observations: no rise-related death when using methyl cellulose, and cell attachment to rising bubbles when not using methyl cellulose. The model also predicts that smaller bubbles can cause an increase in rise-related death, consistent with several observations in the literature.

Several sets of experiments were conducted to verify that cell attachment to rising bubbles contributes to cell death. Rise-related death was found for a serum free medium. When either Pluronic® F68 or methyl cellulose was added to the medium, rise-related death was eliminated. The experimental data compare well with calculations based on published data and the rise-related death model. Rise-related death was found to be quite small for typical laboratory scale reactors, but it can become the dominant mode of cell death in taller reactors. It is necessary to use reactors over one meter tall in order to measure rise-related death reliably. Since Pluronic® F68 and methyl cellulose eliminate rise-related death, experimental death rates from short reactors can safely be used to scale-up cell culture processes when using these additives.

Thesis Supervisor: Daniel I.C. Wang
Title: Institute Professor

Thesis Supervisor: T. Alan Hatton
Title: Ralph Landau Professor of Chemical Engineering Practice

ACKNOWLEDGMENTS

I thank both my advisors, Professors Daniel I.C. Wang and T. Alan Hatton, for their expert guidance over the years. Professor Wang, you startled me with your ability to quickly evaluate information and assess its relevance. Your guidance kept me focused and gave me a new perspective on research. Professor Hatton, our discussions over the years have provided me with a broader view and opened avenues of inquiry that never would have occurred to me. I hope to emulate the dedication and insight you have both demonstrated. I also wish to thank the members of my thesis committee, Professors Daniel Blankschtein, Linda Griffith, and Paul Laibinis, for your input and effort over the years.

Thanks to the BPEC staff who have helped smooth my path over the years, Audrey Childs, Sonia Foster, Lynne Lenker, Joya Gargano, James Leung, John Galvin, Darlene Ray, Lorraine Cable, and Sara Puffer. I always enjoyed visiting the office, and I hope I didn't distract you from your work too much.

Thanks to both Robert Hubbard and Brett Iverson for the long hours they spent in the lab during the summer. I hope that neither of you got too bored counting dying cells all day. At least we tried to provide a few diversions with cards or computers.

I owe much of my learning over my years here, not to mention a lot of entertainment, to my coworkers. Besides all the technical education, I was fortunate gain experience in the important fields of sheepshead, darts, and poker. Thanks to Robert Balcarcel, David Chang, John Chung, Brian Follstad, Peter Frier, Joydeep Goswami, Sherry Gu, Bryan Harmon, Brian Kelley, Araba Lamousé-Smith, Dan Lasko, Kai-Chee Loh, Gautam Nayar, Chandra Papudesu, Martin Reinecke, Cliff Rutt, Anna Sanfeliu, Eric Scharin, Marc Shelikoff, Troy Simpson, Rahul Singhvi, Dave Stevenson, Inn Yuk, Liangzhi Xie, Jifeng Zhang, Craig Zupke, and finally Gregg Nyberg, master of the dart board.

I also want to thank the friends that have made the long haul a little more bearable. Thanks to Anita Parkinson, and Nancy and David Diggs for the movies and bridge. Scott

Lawing also provided frequent entertainment with the musical stylings of Gloryhound. Gregg and Gina Nyberg probably remember quite a few of those concerts, and thanks for the other fun as well: canoeing, skiing, and the occasional pint. Thank you Anat Shiloach. Many of my best memories from the last few years are because of you. Your support has made my life here a lot brighter, and I hope we remain friends for many years to come.

And finally, I would like to thank my family. I know you sometimes wondered why I didn't just get a job, but the Ph.D. was worth it. Mom and Dad, thank you for all the help and sacrifices that allowed me to get here. Carrie, talking to you was always a pleasure and helped me get through. Grandma, coming home to find a letter from you often made a tough day a lot better. Thanks to everyone for actually trying to read my papers (I know it couldn't have been easy), especially Grandma who actually caught the mistakes everyone else missed.

TABLE OF CONTENTS

LIST OF FIGURES

1. INTRODUCTION

1.1 Background

The manipulation of microorganisms for human benefit is older than recorded history. Microorganisms are traditionally used for the production of food and beverages. Yeast fermentation has long been used to produce beverages such as mead, beer, and wine from sugar rich liquids, while many important staple foods benefit from the action of bacteria and fungi, including bread, cheese, yogurt, and some meats. These uses probably arose accidentally, since they occurred before the discovery of microorganisms. Yet the traditional uses remain important, as they are still the major economic uses for microorganisms.

More recently, specific microorganisms have been exploited for other uses. In 1796, Edward Jenner used the material from a cowpox lesion as the first effective vaccine against smallpox. The growth of individual strains of microorganisms for use in the production of vaccines is still important today. The next major development in the use of microorganisms was Alexander Fleming's 1928 discovery of the antibiotic action of penicillin, a compound produced by filamentous fungi; the industrial production of penicillin and its derivatives remains a multi-billion dollar industry. The biotechnology revolution began with the development of recombinant DNA technology in the 1970s. For the first time, an organism could be designed to produce a specific product.

The ability to alter the genome of a microorganism directly has led to several applications. New genes can by introduced in order to make the organism produce a new chemical, such as an altered form of penicillin. The genetic structure can also be

manipulated to induce the organism to produce more amino acids or vitamins. The biotechnology industry has exploited recombinant DNA technology to induce microorganisms to produce foreign proteins which are important for use as therapeutic agents or as components in analytical techniques. Insulin and human growth hormone were the first major therapeutic proteins to be produced through genetic manipulation. Many other proteins have been added over the years, including erythropoietin, interferons, and tissue plasminogen activator. Some individual proteins have sales exceeding one billion dollars a year.

Bacteria are the simplest and quickest means of producing proteins, and they offer high productivities. They typically produce the protein as an inclusion body, which consists of aggregated protein. This complicates processing, since the aggregate must be dissolved, and the protein refolded to its native conformation. Bacteria are also unable to form intramolecular disulfide bonds or glycosylate a protein, important processing steps that are required for some proteins. Yeast still offer fairly rapid production, secrete soluble proteins, have high productivities, and are able to form intramolecular disulfide bonds, but they do not provide the correct glycosylation for use in human therapeutics. Thus, animal cells present the only currently available option for the production of some proteins. Animal cells are quite fragile, slow growing, and offer relatively modest productivities, but they secrete soluble proteins with correct disulfide bond formation and correct glycosylation. Animal cells and insect cells are also important for the production of viruses, which are used for producing vaccines and bioinsecticides, but which need a host cell to grow.

1.2 Motivation

Animal and insect cells are relatively large compared to bacteria and yeast. They also lack the protective cell wall found in those organisms, making them sensitive to disruption from fluid mechanical shear. Shear stresses on the cell membrane can cause death by disrupting the cell membrane. Animal and insect cells are most easily cultured as individual cells in suspension, but this subjects them to shear stresses. They also require oxygen to grow, but oxygen solubilities in cell culture media are quite low, requiring oxygen be supplied to the cell culture either semi-continuously or continuously. The metabolism of these cells also results in the buildup of carbon dioxide in the media, resulting in an increased acidity which can be toxic to the cells.

The problems of oxygen supply and carbon dioxide removal are most simply met through the use of sparging. Gas bubbles have a large surface area for mass transfer and avoid the problems associated with supplying oxygen across a membrane or neutralizing the acid from the carbon dioxide. Bubbles create a different problem, however, as gas sparging has been observed to cause significant cell death. Serum and some polymers have been found to reduce, but not eliminate, cell death from sparging. The evidence and theories in the literature are in apparent conflict on the roles of bubble size and protective additives in cell death. Thus, a more complete understanding of the mechanisms of sparging related death and the role of protective additives is required for the rational design of industrial bioreactors.

1.3 Research Objectives

This research is intended to clarify the mechanisms by which cells die in sparged bioreactors. An understanding of how factors such as reactor shape, reactor size, bubble size, cell size, and medium additives affect sparging related death should allow for better decisions regarding reactor scale-up and operation. With this in mind, this thesis addresses the following specific objectives:

1) How large a contribution to sparging related death does cell attachment to rising bubbles make?

2) How do protective additives affect cell attachment to rising bubbles?

3) What is an appropriate model for cell attachment to rising bubbles?

4) What are the design implications of cell attachment to rising bubbles?

1.4 Thesis Organization

This thesis is divided into seven major chapters. This, the first chapter, includes a brief discussion of the motivation for this thesis and the specific research objectives that it was designed to meet. The second chapter is a detailed literature review which focuses on several aspects of shear related cell death, protection from sparging related death, and previous models which attempt to explain sparging related death. The third chapter presents the material and techniques that were used to perform the experiments reported in this thesis. In chapter four, an improved model for sparging related death is presented. It incorporates cell attachment to rising bubbles, a mechanism that was not included in previous quantitative sparging death models. The model is also used to analyze and interpret previously published experimental data. Model predictions for reactor scale-up

are also analyzed. Chapter five presents the experimental evidence to support cell attachment to rising bubbles as a mechanism for sparging related cell death. It also presents data which shed further light on the role of protective surfactants in preventing sparging related cell death. In chapter six, a novel approach for providing oxygen to cell cultures is explored. The supply method avoids the problems involved with bubbles, provides a large surface area for mass transfer, yet does not encounter the problems with membrane fouling or rupture found in other bubble free oxygen supply systems. The seventh chapter contains the conclusions that are drawn from this work. The remaining chapters include recommendations for future work, nomenclature, and references.

2. LITERATURE REVIEW

2.1 Shear Sensitivity of Animal and Insect Cells

2.1.1 Laminar Shear for Cells on Surfaces

Stathopoulos and Hellums (1985) investigated the behavior of anchorage dependent embryonic kidney cells exposed to laminar shear. They found that as the shear stress and duration of exposure to shear stress increased, cell viability decreased. The decrease in viability became quite significant when the cells were exposed to a shear stress of 5.4 N/m^2 for more than eight hours. As the cells are exposed to higher shear stresses for longer durations, they begin to become elongated in the direction of fluid flow. Sato et al. (1987) also examined the behavior of anchorage dependent cells exposed to laminar shear. They used aortic endothelial cells in their study and analyzed cell response using micropipette aspiration and fluorescent staining of cytoskeletal F-actin filaments. They also observed cell elongation under laminar flow. When the cells subjected to the laminar flow were detached from the surface, they maintained their elongated shape, while cells from a stagnant culture reverted to a spherical shape. The maximum shear stress tested in their experiments was 8.5 N/m^2, above the level seen to cause death in the kidney cells. For cells exposed to laminar flow, the F-actin filaments aligned in the direction of fluid flow, while the F-actin filaments in cells from a stagnant culture seemed to form a cortical layer below the cell membrane. The micropipette aspiration experiments characterized cells using a stiffness parameter. The cells that were exposed to higher levels of shear stress exhibited greater stiffness. This is probably related to cell cytoskeleton changes induced by the shear stress. It is clear from these experiments that fluid shear produces an

elongational force on anchorage dependent cells. The force results in alteration of cell properties and can result in cell death if the shear stress is high enough. One might hypothesize from these data that suspension cells might undergo some internal alteration as a result of exposure to shear stress. However, one would not expect elongation to occur in suspension cells due to the fact that cell orientation to fluid shear is likely to change on fast time scales, while the orientation of anchorage dependent cells is fixed.

2.1.2 Laminar Shear for Cells in Suspension

Many studies of suspension cell behavior in laminar flow fields have been conducted. Most studies employ some type of Couette viscometer apparatus where the cell suspension is contained in a cylindrical annulus. Leverett et al. (1972) examined the response of red blood cells in such a device for an exposure time of 2 min. They found that above a shear stress threshold of 150 N/m^2, extensive shear damage to cells is observed, and the cells lyse. Petersen et al. (1988) examined the shear sensitivity of hybridoma cells grown in 1% serum under shear stresses of up to 5 N/m^2 for up to 10 min of exposure. They found that cells in exponential growth were less sensitive to shear stress than cells in either lag or stationary phase. Petersen et al. (1988) also compared cells that were grown under gentle shear conditions with cells that were grown under higher agitation intensities. They found that the cells grown at higher agitation rates were less sensitive to shear stress in the viscometer experiments. Petersen et al. (1990) extended the viscometric analysis for hybridoma cells grown in a 1% serum medium to batch, continuous culture, and fed batch systems. They found that as long as the cells were in exponential growth, the shear sensitivity was reduced. This was true for a wide

range of growth rates and metabolic yields. Michaels et al. (1991b) examined whether serum, Pluronic® F68, or polyethylene glycol (PEG) reduce the shear sensitivity of hybridoma cells in viscometric experiments using a 10 min exposure at a shear stress of 5 N/m^2. They found that for serum free adapted cells, short term (30 min) exposure to 5% or 10% serum media resulted in an approximately 5% to 10% improvements in viability. However, this difference was not statistically significant at the 95% confidence level, probably due to shear sensitivity variations that resulted from variation in culture age. To examine the effect of long term exposure to serum, serum was added at 1%, 5%, or 10% three doublings prior to the viscometric measurements. They found a statistically significant reduction in sparging damage for the 5% and 10% serum cases, with an average reduction in lysis of approximately 10%. Short term and long term exposure experiments were performed using 0.1% w/v Pluronic® F68 and the same exposure profiles used with serum. No statistically significant difference was seen in either case. Similar observations were found with the addition of 0.1% w/v PEG. Shürch et al. (1987) found significant cell death for hybridoma cells in 10% serum with 1.2% w/v carboxymethyl cellulose when exposed to 5 N/m^2 of shear stress for 10 min. Smith et al. (1987) investigated the behavior of hybridoma cells in 10% serum using a 15 hr exposure in a Couette viscometer. They found that at a shear stress of 0.32 N/m^2, no reduction in growth or increase in death was observed. While at a shear stress of 0.67 N/m^2, significant cell death was observed, and it was approximately equal to the normal growth rate of the cells. McQueen and Bailey (1989) used a converging and diverging tube apparatus to test shear sensitivity in laminar flow. They found that for myeloma cells in 10% horse serum, significant cell damage

occurs when the average wall shear stress increases from 150 to 200 N/m^2. This shear stress is much higher than the level found to cause damage in the Couette type viscometer experiments; however, the wall shear stress parameter is not directly comparable to the shear stress reported for the Couette viscometers. Also, the cell exposure time to the shear stress is very short compared to the Couette viscometers, and this may account for the higher threshold for shear damage.

Laminar shear stress studies have also been conducted for insect cells. Tramper et al. (1986) examined the response of cells isolated from *Spodoptera frugiperda* in a Haake cup and bob viscometer in a medium containing 10% serum and 0.1% w/v methyl cellulose. They found that at shear stresses above 1 to 4 N/m^2, cell viability begins to decrease dramatically after an exposure of 30 min to 2 hr; however, they apparently did not investigate behavior at lower shear stresses. Wudke and Shugerl (1987) investigated the response of *Spodoptera frugiperda* cells in a serum free medium using a Couette type viscometer. Over an exposure time of several hours or more, significant cell death was observed for shear stresses of 2.1 and 3.1 N/m^2. Goldblum et al. (1990) examined the shear stress response of *Trichoplusia ni* and *Spodoptera frugiperda* cells in a cone and plate viscometer. They tested cells grown in 10% serum media during late exponential growth. They also examined the effects of several additives. For systems with no additives and exposure times of 5 min or less, significant cell death was observed at all the shear stresses tested, all of which were above 0.12 N/m^2. The results of Goldblum et al. (1990) indicate a slightly lower threshold for shear damage in insect cells when compared with the data reported by Petersen et al. (1988), Petersen et al. (1990), and Michaels et al.

(1991b) for hybridoma cells. This could indicate that insect cells are slightly more sensitive in general, or that these specific cell lines were more sensitive. When Goldblum et al. (1990) added methyl cellulose or dextran to the media, they observed a significant decrease in shear damage when cells were exposed to the same levels and durations of shear stresses, perhaps explaining why Tramper et al. (1986) claimed to have observed a higher threshold for the onset of shear damage in *Spodoptera frugiperda*. Goldblum et al. (1990) also evaluated the effect of Pluronic® F68 and found that it significantly reduces shear damage in both cell lines when it reaches a concentration of 0.2 to 0.3% w/v.

One can begin to generalize from these data. It is clear that laminar shear stress can begin to damage animal and insect cells when it reaches the level 0.1 to 0.7 N/m^2. Cell damage may be manifested as either lowered viability or cell lysis. The damage may not be noticeable unless long exposures are conducted, but Goldblum et al. (1990) observed the effect in as little as 5 min. While experiments such as those of Petersen et al. (1988) did not observe significant cell death for shear stresses less than 5 N/m^2 at exposure times of 10 min, this may have been due to too short an exposure. As can be seen from the work of Smith et al. (1987), it may take exposure times of many hours to observe death. When higher shear stresses, such as 5 N/m^2 are reached, death is seen in several minutes in most cases. Leverett et al. (1972) did not observe death until reaching higher shear stresses; however, the two minute exposure time they used is extremely short. It may explain why they did not see damage at lower shear stress levels. McQueen and Bailey (1989) also did not see damage until reaching higher shear stress levels, but the possible reasons for that are noted above.

2.1.3 Turbulent Shear in a Capillary Tube

Augenstein et al. (1971) investigated the shear sensitivity of two anchorage dependent cell lines to turbulent shear in a capillary tube. The two cell lines, HeLa cells and mouse fibroblasts grown in 10% serum, were harvested and maintained in suspension for the duration of the experiments. The exposure time to the shear stress was on the order of milliseconds, and multiple passes through the capillary were necessary to observe cell death. The wall shear stresses examined in this study ranged from 100 to 2000 N/m^2. Significant cell death was observed for both cell lines at all shear stresses tested. McQueen et al. (1987) used mouse myeloma cells to determine a threshold shear stress value in a similar capillary flow apparatus. The cells were grown in 20% serum and were used in experiments after three days of exponential growth. They found a threshold wall shear stress for cell lysis of 180 N/m^2. This is slightly higher than some of the shear stress levels tested by Augenstein et al. (1971), but the difference may be due to cell line variations or flow variations stemming from slightly different geometries. The difference may also be due to the fact that wall shear stress is a poor method for characterizing the shear stress experienced by cells in these flow geometries. In a second publication examining turbulent shear in a capillary, McQueen and Bailey (1989) used both myeloma and hybridoma cells grown in 5% or 10% serum. The threshold value for wall shear stress was again found to be in the range of 150 to 180 N/m^2. Zhang et al. (1993b) also tested myeloma and hybridoma cells in a capillary flow device and found cell death at shear stresses of 86 to 433 N/m^2. Al-Rubeai et al. (1995b) investigated which cell populations are lysed during shear in a capillary tube. They used hybridoma, Chinese hamster ovary,

and *Spodoptera frugiperda* cells grown in 5% serum containing media. After several passes through the capillary tube, the cell cycle distribution of the population was determined and compared to the shear free control. The S and G_2 phase cells were preferentially destroyed. This is most likely due to their larger size. They would be more likely to experience the effect of turbulent eddies. It could also be due to differences in their cytoskeletal structure, related to preparation for division. The death observed in the turbulent shear systems is almost completely caused by cell lysis. The loss of viability observed in some of the longer term laminar flow experiments was not found in these systems and probably reflects the much more violent effect of turbulent eddies.

2.1.4 Turbulent Shear in Agitated Bioreactors

Many researchers have conducted studies evaluating the effects of shear stress in agitated bioreactors. This section will only address the effects of the agitation, the effects of sparging will be covered in a following section. Mizrahi (1984) studied lymphoblastoid cells grown in a 5% serum containing medium. Mizrahi found that the addition of Pluronic® F68 or Pluronic® F88 was able to increase the maximum viable cell density in agitated, surface aerated cultures. Ramirez and Mutharasan (1990) evaluated the sensitivity of hybridoma cells cultivated in a medium with 9% serum using 100 mL spinner flasks and a 600 mL working volume bioreactor. They found that for the bioreactor system, the maximum viable cell density decreased by 60% when the agitation rate was increased from 60 to 180 rpm. The same agitation rates in the spinner flasks produced a 15% decrease in maximum viable cell density. This difference is most likely due to the higher Reynolds number in the bioreactor, indicating harsher shear conditions.

In spinner flasks, a reduction in serum concentration caused an increase in shear sensitivity, however, this is at least partly due to a lack of adaptation time to the low serum environment. In a later study, Ramirez and Mutharasan (1992) again used a hybridoma cell line grown in 9% serum to examine shear sensitivity in 100 mL spinner flasks agitated at either 440 or 510 rpm. This study found that media supplemented with either high or low density lipoproteins had decreased shear sensitivity, even when serum levels were reduced.

Petersen et al. (1988) found that hybridoma cells cultivated in a 1% serum medium exhibited greater shear sensitivity depending on culture age. Cells from static cultures, obtained at different culture ages, were inoculated into a 100 mL working volume spinner flask operated at 400 rpm. Cells in mid-exponential growth had the highest shear resistance. Kunas and Papoutsakis (1989) used 1.2 L working volume bioreactors to examine the effects of agitation on hybridoma cells adapted to grow in a 1% serum medium. They found that when the agitation intensity was increased from 60 to 220 rpm, cells that had been seeded in media containing 5% serum or more were able to withstand the shear stress. Cell concentrations in reactors with lower serum levels decreased substantially after the onset of higher agitation rates. They suggest that the damage seen in this system might be the result of bubble entrainment due to the vortex caused by the impeller, and thus, the serum is actually preventing bubble damage, not damage from agitation. In a later study, using the same cells and cultivation medium, Kunas and Papoutsakis (1990a) found that variations in serum levels in 100 mL spinner flasks agitated at 120 rpm did not result in variations in observed cell concentrations or

viabilities. However, when the cells were agitated in the bioreactor mentioned above, they again found that increasing the serum level provided protection against the higher agitation intensity. The protection did not require adaptation to the higher serum levels, as the cells were directly seeded into the higher serum media. The bioreactor experiments had a bubble entraining vortex, while the spinner flask did not. They attribute the damage to bubbles, not agitation, and attempt to demonstrate this behavior in a later publication. In this case, the higher Reynolds number, and thus higher shear, in the bioreactor, as compared to the spinner flasks, cannot be ruled out as the explanation for the difference in culture responses in the different systems. To verify their hypothesis, Kunas and Papoutsakis (1990b) used the same cells, maintenance medium, and bioreactor. However, this time, they operated the bioreactor both as before and also without a gas headspace. They tested agitation rates up to 800 rpm in the absence of a vortex and entrained bubbles, and found that the cultures did not exhibit any significant damage.

Passini and Goochee (1989) examined the response of hybridoma cells cultivated in a serum free medium. They found that in a 1 L working volume bioreactor, no adverse effects were found at agitation rates of up to 300 rpm. In a 1.5 L working volume bioreactor, no detrimental effects were found at agitation rates of up to 400 rpm. When Gardner et al. (1990) agitated hybridoma cells grown in 5% serum using a 1.2 L working volume bioreactor, they saw no detrimental effects at an agitation rate of 200 rpm. For *Spodoptera frugiperda* cells cultivated in a 10% serum and 0.1% w/v methyl cellulose containing medium, Tramper et al. (1986) conducted experiments in an agitated 3 L bioreactor operated in a continuous culture mode. Cell concentration began to decrease at

220 rpm in one run, but in a second run, cell concentration did not begin to decrease until 510 rpm was reached. They estimated that the shear stress experienced by the cells at the 510 rpm agitation rate was approximately 3 N/m^2, similar to the threshold values for shear damage that were obtained in laminar flow experiments. In the absence of bubbles, agitation rates of several hundred rpm are necessary to alter cell growth or induce cell death in 1 L scale reactors. The estimated shear stresses for the agitated bioreactor data are all reasonably consistent with the laminar and turbulent shear stress data reported above.

Smith and Greenfield (1992) used a 2 L bioreactor to examine the response of hybridoma cells to high agitation intensities in the absence of vortex induced bubble entrainment. They found that for cells grown in a 10% serum medium, agitation rates up to 600 rpm did not affect cells. The effects of several supplements were examined for cells that were propagated in a serum free medium and exposed to the 600 rpm agitation rate. In all cases, the exponential growth phase of the culture mirrored the behavior of a static control. However, at the end of the exponential growth phase, the cells in the agitated system died rapidly, while the cells in static culture did not. Pluronic® F68, bovine serum albumin, and 10% serum (added at the start of the agitation) did not protect against this effect. The cells in the agitated environment showed higher glycolysis rates and were possibly dying from nutrient depletion or the buildup of toxic byproducts. It is also possible that the higher shear sensitivity of cells in stationary phase that has been observed by other researchers, such as Petersen et al. (1988), accounts for the more rapid death during the stationary phase. Since cells that were propagated in 10% serum did not

exhibit the same response as those that were supplemented with serum immediately prior to agitation, the researchers hypothesized that serum has a metabolic protective effect against shear. However, the serum free cultivated cells were only adapted to serum free growth for seven days. It is possible that this period was insufficient and explains the higher glycolysis rate the cells exhibited under shear stress. Oh et al. (1989) used a surface aerated, 1.4 L working volume reactor to examine agitation effects on three hybridoma cells lines grown in media containing 5% serum. They found no detrimental effects up to the highest agitation rate they tested, 450 rpm. When Al-Rubeai et al. (1990) examined the effect of serum deprivation on hybridoma cells using 100 mL spinner flasks they found that for cells normally cultivated in media with 5% serum, a 14 hr serum deprivation prior to agitation at 600 rpm resulted in a reduction in viable cell density compared to lower agitation rates. Cultures that did not experience serum deprivation showed no performance difference between high and low agitation rates.

Lakhotia et al. (1992) used Chinese hamster ovary cells grown in a 3% serum medium to examine the effect of agitation on the cell cycle. The experiments were conducted in a 1.3 L working volume bioreactor. When the agitation intensity was increased from 80 to 250 rpm, the viable cell concentration reached a plateau while the viable cell concentration in a control culture continued to increase. The agitated culture showed both a higher relative S phase population and an increased DNA synthesis rate. The relative number of cells in the G_1 phase was lower in the agitated culture. This behavior is the opposite of that seen by Al-Rubeai et al. (1995b) in turbulent capillary shear experiments. It suggests that long term, lower levels of shear stress affect cells

differently than brief, high intensity shear. Lower shear stress seem to alter the cell cycle distribution, while high intensity shear stress seems to selectively destroy a specific cell population. When Lakhotia et al. (1992) exposed the cells to an agitation intensity of 235 rpm, the cell cycle changes were still evident, but less pronounced, indicating that the cell cycle changes appear to be sensitive to the level of shear stress. The results could also be explained if the cells are preferentially induced to undergo apoptosis in the G_1/G_0 phase. This would also explain the relatively lower number of cells in the G_1 phase. Al-Rubeai et al. (1995a) used hybridoma cells grown a medium with 5% serum to examine bubble free agitation and its effect on cell cycle distribution. In a 1 L working volume reactor, they found that cell number was dramatically reduced in a reactor agitated at 600 rpm compared to one agitated at 100 rpm. Both necrosis and apoptosis were observed in the 600 rpm culture. In a second reactor operated at a working volume of 1.5 L and agitated at 1500 rpm (operated with no headspace to prevent bubble entrainment), rapid cell death was observed. Total cell viability remained high for the later case, but the total number of cells rapidly decreased over the course of several hours. The authors noted that during the course of exposure to the 1500 rpm rate, a population of small, apoptotic like bodies developed. They infer that the high agitation intensity induced apoptosis. It is more likely that turbulent eddies are causing cell fragmentation, and it is these cell fragments that the authors are interpreting as apoptotic bodies. There is some suggestion that the normal sized cell population became slightly enriched with G_1 phase cells. These cells are slightly smaller that the cells in the other phases, and thus, might be less susceptible to damage from turbulent eddies. This is analogous to the behavior seen by Al-Rubeai et al. (1995b)

for turbulent flow in a capillary tube. In summary, it seems that sub-lytic shear stress can induce apoptosis, while the turbulent eddies found at higher levels of shear stress result in cell disruption and preferentially disrupt larger cells.

2.1.5 Plasma Membrane Fluidity

Ramirez and Mutharasan (1990) investigated the role of plasma membrane fluidity (PMF) in affecting the shear sensitivity animal cells. They measured PMF using steady-state fluorescence anisotropy. This technique measures the change in polarization between the excitation and emission of a fluorescent probe which partitions to the plasma membrane. This non-destructive technique measures PMF at physiological conditions. These studies were conducted using a hybridoma cell line grown in a medium containing 9% serum. They investigated several parameters in order to correlate PMF with shear related cell death. Shear death was measured in a Couette flow device operating in the laminar flow regime or in an agitated bioreactor. PMF was manipulated using either benzyl alcohol or a temperature shift. As benzyl alcohol concentration increased, PMF was also found to increase. The increase in PMF correlated with a dramatic decrease in cell viability when exposed to a shear stress of 8 N/m^2 for 15 min. For the temperature shift case, lower temperatures were found to have lower PMF and higher viabilities, while higher temperatures were found to have higher PMF and lower viabilities (using a shear stress of 8 N/m^2 and a 20 min exposure). Again using the Couette flow device, they investigated the effect of increasing cholesterol. Cholesterol is known to be an important compound in regulating PMF. Increased cholesterol levels were found to correlate with decreased PMF and higher viabilities when the cells were exposed to a shear stress of 8

N/m^2 for 15 min. Pluronic® F68 at a concentration of 0.5% w/v was also added to the medium in a static batch culture and the PMF measured for the duration of the batch. The PMF was found to be consistently lower than in a control culture with no Pluronic® F68. Ramirez and Mutharasan (1990) argue that this decrease in PMF could explain the shear protective properties observed with Pluronic® F68. They also investigated the role of serum. The experiment compared a static culture to an agitated culture over a range of serum concentrations. The parameters they compared were: integrated viable cell density, initial growth rate, and specific death rate. As one might expect, the integrated viable cell density was higher at all conditions for the static culture. The two types of cultures were found to have the same initial growth rates, but the agitated cultures had higher specific death rates, especially at lower serum concentrations. Since lower serum levels correlated with lower initial growth rates, the authors speculate that this confirms a metabolic protective effect for serum. However, since no mention of adaptation to the lower serum conditions is mentioned, this difference could be solely due to the effect of the rapid environmental shift. When cells are properly adapted, this effect will most likely disappear. If it did not, serum free growth of hybridomas would not be possible, and that is not the case. The authors also argue that the difference in specific death rates between the static and agitated cultures can be explained by a shear protective effect from serum. They hypothesize that this difference partially results from serum causing a decrease in PMF, which their other work has shown correlates to a reduction in shear related death.

In a later work, Ramirez and Mutharasan (1992) investigated the effect of serum concentration on PMF using the same steady-state anisotropy technique mentioned

above. Increasing serum levels were found to decrease the PMF, which was found previously to result in higher integrated cell viability when grown in an agitated spinner flask. The authors speculated that the shear protective effect of serum could be linked to cholesterol. Cholesterol is one of the many components found in serum, and it is also known to play an important role in the plasma membrane. Culture media supplemented with either high or low density lipoproteins were found to result in lower PMFs. The supplemented cultures were also found to exhibit more shear resistance as measured in agitated spinner flasks. Thus, the authors conclude that one of serum's important shear protection mechanisms is to provide cholesterol to the plasma membrane, thereby decreasing its fluidity.

2.1.6 Membrane Bursting Tension

Zhang et al. (1991) have developed a novel technique for directly measuring the membrane properties of living cells. They place the cell between two parallel surfaces and measure simultaneously the force being imposed on the cell and the deformation of the cell. Zhang et al. (1992a) developed a model that allows one to use the force and distance data supplied by the technique to calculate three terms related to the cell: the membrane bursting tension, the membrane bursting pressure, and the elastic area compressibility modulus. This approach was developed to overcome the difficulties raised with other techniques, such as micropipette aspiration which only deforms a small area of the cell membrane, and thus may not be used to determine the membrane bursting tension. Since shear damage from turbulent shear results in destruction of the cell, the membrane bursting tension is a key parameter for predicting shear sensitivity. The technique showed

the membrane bursting tension and compressibility modulus are essentially independent of cell size for the cell size distribution within a culture. The significance of the compressibility modulus is that it may be used to predict cell distortion under shear stresses, and thus the membrane tension. This would allow one to predict whether a specific shear field would burst the cell. The technique uses low strain rates, however, so it may not be directly applicable to the high strain rates accompanying phenomena such as bubble bursts.

Using this new technique, Zhang et al. (1992b) examined the membrane bursting tension of hybridoma cells grown in 5% serum during the course of batch growth. They found that the membrane bursting tension rose during exponential cell growth. As viability began to decrease at the end of the batch, the membrane bursting tension also decreased. They note that this trend in membrane bursting tension follows the behavior of shear sensitivity observed in viscometer studies (Goldblum et al. 1990; Petersen et al. 1990). In those experiments, cells in exponential growth were found to be less sensitive to fluid shear than cells in the lag phase or stationary phase. In a study examining the effect of Pluronic® F68 on membrane bursting tension, Zhang et al. (1992c) found that hybridoma cells grown in continuous culture with 0.05% w/v Pluronic® F68 had a 60% higher membrane bursting tension than those that were grown without Pluronic® F68. When Pluronic® F68 was added to the medium immediately before the membrane bursting tension measurement, the bursting tension increased when the concentration of Pluronic® F68 was above 0.1% w/v. These observations are consistent with those of Goldblum et al. (1990) who found that exposure to Pluronic® F68 protects cells against laminar shear.

It is also consistent with the work of Ramirez and Mutharasan (1990) who found that Pluronic® F68 decreased plasma membrane fluidity. One might expect a stronger membrane to be more rigid and have a lower plasma membrane fluidity.

Zhang et al. (1993a) used their micromanipulation technique to compare variations in fragility between three different cell lines grown in media with 5% serum. They examined murine hybridomas, myelomas, and SF9 (*Spodoptera frugiperda*) cells. For all three cells lines, membrane bursting tension was highest during exponential growth and was lower during lag phase and death phase in batch cultures. In comparisons of relative membrane bursting tension between the cell lines, the myelomas were weakest. All cells in these tests were weaker than the hybridoma cell line tested in their previous work (Zhang et al. 1992b). The fact that hybridoma cells were stronger than the *Spodoptera frugiperda* cells may explain why the threshold for shear damage for unprotected *Spodoptera frugiperda* cells reported by Goldblum et al. (1990) is lower than the threshold for shear damage reported by Petersen et al. (1988) for hybridoma cells in 1% serum.

The membrane bursting tension measurements were used in predictive models for shear damage. Born et al. (1992) analyzed the laminar flow situation. The key assumption involved in their approach to modeling deformation in laminar shear involves the internal viscosity of the cell. The cells are treated as droplets that deform in the shear field in a manner that depends on their internal viscosity. The authors used an estimate for the internal viscosity of the hybridoma cells used in their experiments that was based on measurements made for blood cells at shear rates similar to those used in the hybridoma experiments. Using this approximation, the authors were able to predict the actual cell

lysis rate based on membrane bursting tension measurements and the model for cell deformation in laminar fluid shear. They were able to predict the lysis rate to within 30%, which is quite reasonable given the approximation of the cell as a liquid droplet with an estimated internal viscosity. The estimated internal viscosity and the fact that the influence of the cytoskeleton was neglected probably explain the discrepancy. Zhang et al. (1993b) extended the use of membrane bursting measurements for lysis prediction to turbulent flow. The model assumes that turbulent eddies on the order of the cell size can interact with the cell and cause surface deformations. The kinetic energy of the eddies was used to calculate the deformation of the cells. The model underestimated the specific lysis rate by 15%, but the general agreement is impressive. Thus, it appears that the membrane bursting tension measured by this technique is truly representative of the behavior of cells exposed to high fluid shear rates. These measurements should allow for reliable predictions of cell lysis rates when the fluid mechanics of the cells' environment can be characterized.

2.2 Sparging Related Death

2.2.1 Cell-Bubble Attachment

Orton (1992) observed that if a suspension of hybridoma cells in 5% serum was used to blow a bubble at the end of a capillary tube, many cells could be observed trapped in the bubble film when viewed under a microscope. Cherry (1991) made similar observations using *Spodoptera frugiperda* cells. However, when Orton (1992) added 0.2% w/v Pluronic® F68 to the medium, the cells were observed to rapidly drain from this thin film. Chalmers and Bavarian (1991) had similar findings for *Trichoplusia ni* and

Spodoptera frugiperda cells in a 10% serum containing medium. Cells became trapped in the thin film that forms between a bubble and the gas-liquid interface. They hypothesize that the cells caught in this film die when the bubble bursts, as the shear rates in the receding rim of the broken bubble are extremely high. Garcia-Briones and Chalmers (1992) again used microscopic visualization to study *Spodoptera frugiperda* cells in both a 10% serum medium and a serum free medium. They found that for both media, significant numbers of cells were trapped in the thin film between the bubble and the gas-liquid surface. When 0.2% w/v Pluronic® F68 was added to the media, no cells were observed in this thin film. Chattopadhyay et al. (1995a) also used *Spodoptera frugiperda* cells grown in either a 10% serum medium or a serum free medium and examined the influence of several additives on cell entrapment in the thin film. Cell entrapment was observed for both the serum and serum free cases when no additives were present. When 0.1% w/v polyvinyl alcohol, 0.1% w/v polyethylene glycol, or 0.5% w/v dextran were added, there was still visible cell entrapment. However, when either 0.1% w/v Pluronic® F68 or 0.3% w/v methyl cellulose was present, no cells were observed entrapped in the thin film. Michaels et al. (1995a) created thin films by withdrawing fluid from a biconcave drop containing a suspension of Chinese hamster ovary cells grown in a serum free medium. They found that for thin films formed with a serum free medium containing no additives, 0.1% w/v Pluronic® F68, 0.1% w/v polyvinyl alcohol, or 0.1% w/v methyl cellulose, cells moved out of the thin film in one to two seconds. The films were found to be on the order of 10 nm thick, also indicating the absence of cells in the films. When 3% serum, 0.1% w/v polyvinyl pyrrolidone, or 0.1% polyethylene glycol was added to the medium, cells

were trapped in the draining films. The films also drained much more slowly and never became as thin as the films made with the other additives. Cherry and Hulle (1992) formed thin films of a *Spodoptera frugiperda* cell suspension in a 5% serum medium using a wire loop. The films were allow to drain and burst over a vial of isotonic liquid. The medium remaining on the loop was rinsed off in the isotonic liquid. The number of cells remaining was then measured using a particle counter. They found that 20% of the cells disappeared, and they assumed that the cells lysed. They did not measure the viability of the remaining cells. When either 0.1% or 0.2% w/v Pluronic® F68 was added to the medium, no cell loss was observed. The same was true for the addition of 0.2% or 0.4% w/v Pluronic® F127. The thin film cell entrapment results appear to be similar for both insect and animal cells: cells become entrapped for most additive free systems, but when Pluronic® F68 of methyl cellulose is present, entrapment, and consequently death, is prevented.

Bavarian et al. (1991) made extensive studies visualizing the attachment of *Trichoplusia ni* and *Spodoptera frugiperda* cells to rising bubbles in a 10% serum medium. They found that for air bubbles of 1.5 to 1.8 mm diameter, both individual cells and cell clusters attached to the rising bubbles. Cells also attached to rising oxygen microbubbles that were 20 to 120 μm in diameter. The smaller bubbles allowed higher magnifications for better observation of cell-bubble attachment, and the smaller bubbles also moved at lower velocities, as they were in the Stokes' flow regime. The cells attached near the apex of the rising bubbles and were swept around to the rear of the bubbles. Cell-bubble detachment was never observed. Cells were also observed becoming trapped in the foam layer that

formed at the top of the reactor. They entered the foam either by becoming trapped by swarms of bubbles rising from below or by being pulled into the foam in the wakes of rising bubbles. Presumably, the cells that were already attached to the bubbles entered the foam layer as well. Bavarian et al. (1991) calculated the maximum rise-related shear stress encountered by the cells. This stress occurs when the cells are stationary relative to the bubble at the equator of the bubble. The shear stresses for the microbubbles were less than or slightly above the levels found to cause shear damage in a viscometer at an exposure time of 5 min by Goldblum et al. (1990). However, the cells do not really experience these levels of shear stresses during the bubble rise. They were observed to be swept along the bubble surface until they reached the rear stagnation point of the bubble. Thus, the highest level of shear stress the cells experience during the bubble rise is probably quite brief and is also less than the calculated values. Handa-Corrigan et al. (1989) also microscopically observed cell-bubble interactions. They used myeloma, hybridoma, lymphoblastoid, and baby hamster kidney cells in a 5% serum medium. Cells were observed to be trapped in the thin films between the bubble and the gas-liquid surface. When antifoam was added to this system, no cell entrapment was observed. When Pluronic® F68 was present, no cells were seen trapped in the thin films either. The cell-bubble attachment results reported by the various researchers for the serum containing media are generally consistent. Pluronic® F68 is also consistently reported to prevent cell-bubble attachment.

Chattopadhyay et al. (1995b) propose that cell-bubble attachment may be modeled using a free energy balance on the cell-liquid, gas-liquid, and cell-gas interfaces.

This model approach has been shown to work for the attachment of bacteria and animal cells to solid surfaces (Absolom 1988; Absolom et al. 1983). Chattopadhyay et al. (1995b) used the maximum bubble pressure method to determine the actual surface energy of the bubbles in various culture media. The surface energies of the cell-liquid and cell-gas interfaces were determined using contact angle measurements. The measurements were made for a variety of insect and animal cells lines in either 10% serum media or in serum free media. Cell-bubble attachment was predicted for all cells when in either serum or serum free media without extra additives. When 0.1% w/v Pluronic® F68 or 0.3% w/v methyl cellulose was added to the media, no cell-bubble attachment was predicted. This model assumes that the interfaces are essentially independent of each other. Since surfactant molecules are not irreversibly adsorbed at gas-liquid interfaces, the model cannot account for the possibility that it may be more thermodynamically favorable for a cell to adsorb to a gas-liquid interface, and this may displace surfactant molecules. Thus, this model could provide misleading predictions.

Michaels et al. (1995a) directly measured cell-bubble attachment in a well controlled system. They used Chinese hamster ovary cells grown in a serum free medium. They used an induction timer to measure the contact time necessary for cell-bubble attachment to occur. The induction timer consisted of tube attached to an electromechanical driver. A 1.2 mm diameter bubble was created at the end of the tube using a small syringe. Fresh bubbles were lowered into a settled slurry of cells for a series of different times. Cell-bubble attachment was measured by microscopically observing the bubble. For the serum free medium, cell bubble attachment began to occur at a contact

time of 10 ms, and at a contact time of 500 ms, nearly every bubble-slurry contact produced attached cells. When either 0.1% w/v polyvinyl pyrrolidone or 0.1% w/v polyethylene glycol was added, the attachment occurred at similar contact times. For the addition of 3% serum, cell attachment began at 100 ms and became significant at 1 to 5 seconds. With 0.1% Pluronic® F68, some attachment occurred at 50 ms, but significant attachment did not occur until contact times of 10 to 20 seconds. Polyvinyl alcohol at 0.1% w/v resulted in initial attachment at 1 second and significant attachment at 20 seconds. When 0.1% methyl cellulose was added, low levels of attachment did not even occur until a contact time of 10 to 30 seconds. If the model for cell-bubble attachment proposed by Chattopadhyay et al. (1995b) was correct, the Pluronic® F68, and methyl cellulose cases tested by Michaels et al. (1995a) should not have produced cell-bubble attachment. However, since attachment did occur, it seems that cell-gas contact is more thermodynamically favorable that surfactant-gas contact for the systems tested. What is different between the various additives is the kinetics of the cell-bubble attachment event.

Jordan et al. (1994) used a bubble on a micromanipulated capillary to examine the effects of cell-bubble contact. Using both Chinese hamster ovary cells and hybridoma cells in a serum free medium, they contacted a bubble to cells settled on a solid surface. When the cells were in fresh media, the contact of the bubble with the first few cells resulted in cell lysis. The next cells to contact the bubble merely attached. Attached cells could not be detached by moving the bubble through the liquid, consistent with the observations of Bavarian et al. (1991). After several days of culture in the medium, cell-bubble contact resulted in attachment, not lysis. They hypothesized that this difference

was due to the influence of biosurfactants produced by the cells. This could be from cell debris, such as lipids and proteins from lysed cells, or it could be from proteins secreted by the cells. When either 5% serum or 0.1% w/v Pluronic® F68 was added, no lysis or cell-bubble attachment was observed. This might be because insufficient time was allowed for cell-bubble attachment to occur. As seen in the work of Michaels et al. (1995a), it can take several seconds of contact for cell-bubble attachment to occur, depending on which additives are in the media.

Foam flotation experiments have been conducted for several cell/additive systems. Cherry and Hulle (1992) studied *Spodoptera frugiperda* cells in a serum free medium containing 0.1% w/v Pluronic® F68. They placed 10 mL of cell suspension in a 25 mL pipette that was held at a 45° angle. Gas was fed into the pipette and the foam effluent was captured. They found that the liquid from the foam was depleted in cells relative to the bulk liquid. Michaels et al. (1995a) used a 54 mL bubble column with a sintered glass sparger to examine the foam flotation of Chinese hamster ovary cells grown in either a serum free medium or in various serum containing media. They also examined foam flotation in a 1.85 L working volume reactor. They found that for the serum free medium, and serum free medium with either 0.1% w/v polyvinyl pyrrolidone or 0.1% w/v polyethylene glycol, cells were enriched in the foam. With serum free medium and 0.1% w/v polyvinyl alcohol, 0.1% w/v Pluronic® F68, or 0.1% w/v methyl cellulose, cells were depleted in the foam. For the serum containing media, increasing the serum concentration from 0.5% to 10% resulted in a switch from cell enrichment in the foam to cell depletion in the foam. When the additives used with the serum free medium were used with a 3%

serum containing medium, the behavior was similar to the serum free case. The bioreactor flotation experiments were consistent with the bubble column data mentioned previously. These data are all consistent with the previous data on cell-bubble attachment in the presence of various additives.

In summary, cell-bubble attachment was observed for both rising bubbles and between the bubble and the gas-liquid interface. Attachment was found in most serum and serum free systems. Additives such as dextran, polyethylene glycol, and polyvinyl pyrrolidone did not prevent cell-bubble attachment. However, polyvinyl alcohol, methyl cellulose, and Pluronic® F68 do slow cell-bubble attachment, and when the bubble is not long enough lived, they should entirely prevent cell-bubble attachment. The thermodynamic model proposed by Chattopadhyay et al. (1995b) does not adequately explain this behavior. This is probably because it does not account for surfactant displacement by cells. The important differences between additives results from the different cell-bubble attachment kinetics they produce. It appears that bubbles in fresh serum free media can directly lyse cells. However, after a few such events occur, or after the media have been exposed to cells for a while, this effect disappears. Thus, it is probably not a significant issue for industrial culture since it is not likely to result in large amounts of cell death.

2.2.2 Cell Death at the Bubble Burst

Chalmers and Bavarian (1991) observed that when a bubble bursts, the cells that are in the thin film between the bubble and liquid surface undergo rapid acceleration and experience high shear stresses. A liquid jet forms in the cavity left behind by the bursting

bubble. The jet may break into droplets depending on the size of the bubble. The shear rates associated with the jet are also quite large. Garcia-Briones and Chalmers (1992) used a glass slide positioned over a bursting bubble to capture *Spodoptera frugiperda* cells from either a 10% serum medium or a serum free medium. In some of the rising jets from burst bubbles, cells or cells clumps were observed using a large depth of field microscope. A microscopic view of the liquid captured from the bursting bubbles showed that nearly all the cells captured on the plate were dead by a trypan blue exclusion assay. When 0.2% w/v Pluronic® F68 was added to the media, very few cells were observed in the liquid captured from the bursting bubbles. This technique does not measure any cells which lyse upon the bubble burst, however. Garcia-Briones et al. (1994) used numerical simulations of the fluid flow around a bursting bubble to estimate the shear stresses that would be encountered by a cell that was near a bursting bubble. They found that the region of highest shear stresses was very small, and the rate of energy dissipation associated with bursting bubbles increased as bubble size decreased.

Trinh et al. (1994) extended this work using the same cells and media as above. They measured the number of cells killed per bubble by rupturing a number of 3.5 mm diameter bubbles in 1.05 or 2.25 mL of cell suspension. In the experiments with a 10% serum containing medium, an average of 1150 cells were killed per bubble burst. When 0.1% w/v Pluronic® F68 was added to the medium, there was no measurable cell death. The number of cells killed in the liquid droplets from the bursting bubble was measured as reported in Garcia-Briones and Chalmers (1992). For the 10% serum medium, an average of 1428 cells were captured per bubble burst, and an average of 74% of the cells were

killed in the burst. The number of cells captured in the liquid droplets when 0.1% w/v Pluronic® F68 was added to the medium averaged 260 cells per bubble, and essentially all the cells remained viable. The authors also note that the total volume of liquid droplets per bubble was larger when Pluronic® F68 was added to the system. The number of cells killed is in reasonable agreement between the two measurements; however, cells that lyse are not accounted for in the drop capture technique. In the bubble rupture method, it appeared that some cells were lysing, but the technique was unable to accurately measure the number of those cells. For the serum free medium, only droplet capture measurements were made. The results for those experiments were reasonably similar to the 10% serum system. The authors also made an attempt count the number of cells that are in the thin film between the bubble and the liquid surface by placing a slide onto the bubble and letting the liquid attach. They then counted the number of cells that were on the slide. They reported that an average of 292 cells were in this thin film. Presumably, they were reporting the 10% serum case; however, the authors do not make this clear. In any case, the number of cells that are in the thin film appears to be much less than the number of cells that are killed by the bubble burst. Chattopadhyay et al. (1995a) used the same cells, media, and bubble rupturing technique to test the effect of several additives. Two additives, 0.1% w/v polyethylene glycol and 0.5% w/v dextran, provided a small level of protection against death from the bubble burst. Polyvinyl alcohol at 0.1% w/v provided intermediate protection. Pluronic® F68 at 0.1% w/v and two grades of methyl cellulose at 0.3% w/v provided good protection.

Orton (1992) also hypothesized that the volume of droplets formed from bursting bubbles correlates to cells death in sparged bioreactors. Newitt et al. (1954) measured the number and diameter of droplets formed by air bubbles bursting in pure water at 25°C, 35°C, and 45°C. The measurements were made for bubbles in the range of 0.31 to 0.53 mm in diameter. The highest water temperature corresponded to the lowest volume of droplets per bubble. This is consistent with a lower surface tension resulting in fewer droplets. The data from Newitt et al. (1954) allows for a volume of droplets produced per volume gas ratio to be calculated for each bubble size. Orton (1992) used curve fits to interpolate between the bubble diameters measured by Newitt et al. (1954). The curve fits used for interpolation are not appropriate, but this does not introduce large deviations in the interpolations. However, Orton (1992) also uses the curve fits to extrapolate to smaller bubble diameters than those measured by Newitt et al. (1954). The curve fits that were employed predict that as the bubble diameter goes to zero, the volume of droplets per gas volume goes to infinity. This is obviously unreasonable.

Orton (1992) used hybridoma cells grown in a 5% serum medium at 37°C as an experimental system to compare whether cell death from sparging correlates to the volume of droplets produced by the bursting bubbles. This model assumes an isotropic distribution of cells between the bulk liquid and the droplets, and that all cells in the droplets are killed. Orton (1992) examined bubble diameters from 1.1 to 4.5 mm. The sparging death rates correspond well to the droplet volumes for pure water at 35°C at the bubble diameters measured by Newitt et al. (1954). No reasonable comparison can be made for the smaller bubbles since there is no data for droplet volumes, and there is no

mechanistic model for predicting the droplet volumes. It should be noted, however, that the surface tension of the medium in the experiments by Orton (1992) is significantly lower than that for pure water at the same temperature, due to the presence of antifoam and serum. Since even the slight variation in surface tension caused by a 10°C temperature change causes a measurable change in total droplet volume, the model of Orton (1992) would predict significantly lower death rates than observed. It is clear from the work of Garcia-Briones and Chalmers (1992) and Trinh et al. (1994) that there is some correspondence between the droplets formed from bursting bubbles and cell death from sparging, but the model of Orton (1992) does not capture the observed behavior. Since Garcia-Briones and Chalmers (1992) and Trinh et al. (1994) observed that the addition of Pluronic® F68 significantly affects the number of cells that are found in the liquid droplets, the isotropic cell distribution assumption made by Orton (1992) is incorrect.

2.2.3 Measurements of Growth Performance

Several researchers have made attempts to characterize cultures by measuring growth rates or maximum cell densities in the presence of sparging or bubble entrainment. Kilburn and Webb (1968) operated a 3 L culture of a mouse derived cell line using gas sparging to control the dissolved oxygen concentration. The medium contained 2% serum and 0.1% w/v carboxymethyl cellulose. They found that sparging produced substantially lower growth than in a surface aerated culture. The addition of 10% serum or 0.02% w/v Pluronic® F68 was found to prevent sparging related effects in their system. Gardner et al. (1990) examined hybridoma cells in a 5% serum containing medium using a 1.1 L working volume bioreactor. They found that when they sparged the culture, cell growth

was impaired. The addition of 0.1% w/v Pluronic® F68 did not provide protection; however, the addition of 0.4% w/v Pluronic® F68 did provide significant protection. When investigating hybridoma cells grown in a 5% serum containing medium, Oh et al. (1989) found that sparging a 1.4 L working volume reactor resulted in lowered cell growth. At a fixed gas flow rate, increasing the agitation rate diminished the number of cells that grew in the reactor. Under sparged conditions, cell growth was impaired in all these systems, but the addition of Pluronic® F68 was able to return the cultures to normal growth.

Passini and Goochee (1989) studied the effect of sparging on a hybridoma cell line grown in a serum free medium. They used a 1 L working volume bioreactor with a low agitation rate for the sparging experiments. Rapid cell death was observed when sparging without any additives. When 0.01% w/v Pluronic® F68 was added to the system, cell growth was observed, but the performance was worse that the non-sparged control. With the addition of 0.2% w/v Pluronic® F68, complete protection was observed. Murhammer and Goochee (1988) extended the work to *Spodoptera frugiperda* cells grown in a 5% serum containing medium. For a sparged 3 L bioreactor, cell death was observed when no additives were present. The addition of either 0.1% or 0.2% w/v Pluronic® F68 produced growth behavior similar to a non-sparged control. The results were similar when the cells were cultivated in a 570 mL airlift reactor. Murhammer and Goochee (1990a) examined a number of Pluronic® and reverse Pluronic® compounds for their effectiveness in the prevention of sparging damage for the insect cell and medium combination mentioned above. They found that compounds that did not inhibit growth in spinner flask culture

provided protection against sparging damage in the 3 L and airlift bioreactors mentioned above. The common features of these compounds were relatively short polypropylene oxide blocks and relatively long polyethylene oxide blocks. Murhammer and Goochee (1990b) also examined the protection provided by Pluronic® F68 in a vortex induced bubble entraining system and in two airlift bioreactors. *Spodoptera frugiperda* cells grown in a 5% serum containing medium were again used. A supplement of 0.2% w/v Pluronic® F68 was able to prevent growth inhibition in the vortex induced bubble entraining system. Two airlift bioreactors were tested at essentially the same volumetric gas flow rate and bubble size. Pluronic® F68 was able to protect the cells against sparging effects in one reactor, but not the other. The reactor that was more damaging to the cells had a slightly greater pressure drop across the sparger, and the authors hypothesize that the difference in performance between the two reactors might be the result of higher shear stresses during bubble formation.

Handa et al. (1987a) examined myeloma and hybridoma cells grown in a 5% serum containing medium. They used 500 mL bubble columns with sintered disc spargers to determine the effects of sparging. Under identical sparging conditions, some cell lines showed satisfactory growth, while others did not. In the absence of sparing, the cells behaved in a similar manner. They also found that decreasing the size of the bubbles at a fixed gas flow rate reduced the growth curves of the cells. When increasing gas flow rates while using the same sintered disc sparger, the maximum cell density achieved by the cultures dropped. The addition of 0.1% w/v Pluronic® F68 was able to prevent the reduction in maximum cell density seen when increasing the gas flow rate previously. A

concentration of 0.1% to 0.2% w/v Pluronic® F68 provided optimal protection against sparging damage. Using hybridoma cells grown in serum free or various serum containing media, Handa et al. (1987b) examined the effects of serum concentration, Pluronic® F68, polyvinyl pyrrolidone, polyethylene glycol, carboxymethyl cellulose, dextran, and reactor height on sparging related damage in bubble column bioreactors. The serum free and 2% serum cases showed a decrease in maximum viable cell density compared to the non-sparged control. Serum concentrations of 5% or 10% provided good protection, especially in the taller bioreactor. Pluronic® F68 at a concentration of 0.1% w/v was able protect the cells against sparging damage for serum levels between 0% and 10%. Polyvinyl alcohol, polyethylene glycol, and polyvinyl pyrrolidone were also able to protect cells when added at a concentration of 0.1% w/v, while carboxymethyl cellulose and dextran were not able to protect cells. At a fixed gas flow rate, increasing the reactor height while keeping the cross section constant resulted in a reduction in sparging damage as measured by maximum viable cell density. Handa-Corrigan et al. (1989) extended the bubble column experiments to a variety of animal cells lines and saw behavior similar to that reported above. Serum and Pluronic® F68 were found to have a concentration dependent protective effect on cells. Smaller bubbles were found to cause greater damage at the same volumetric gas flow rate. At fixed reactor cross section and gas flow rate, taller reactors produced higher maximum viable cell densities than shorter reactors.

S. Zhang et al. (1992) studied the effects of antifoam and Pluronic® F68 on hybridoma cells grown in both a 5% serum containing medium and a serum free medium. At a concentration of 10 ppm antifoam C in the 5% serum medium, cell growth was

similar to the no antifoam case (foam was present in both systems). When the antifoam concentration was increased to 50 ppm, cell growth was slightly worse in the sparged culture, and some foam was still present. At 100 ppm antifoam, cell growth was still slightly worse in the sparged system, but all foam formation was suppressed. At the highest antifoam concentration, 200 ppm, sparging damage was worse, and the control culture also performed substantially worse that the previous control cultures. The same antifoam concentrations were tested with 0.2% w/v Pluronic® F68 in the 5% serum medium. The behavior was similar to the previous cases, except the sparged culture performed closer to the control culture. A reduction in maximum cell density for both the sparged and control cultures was observed at an antifoam concentration of 200 ppm. Cells grown in the serum free medium were much more sensitive to sparging damage, but 0.2% w/v Pluronic® F68 completely eliminated differences between the sparged and control cultures. Antifoam was not used in the serum free system.

Kunas and Papoutsakis (1989) studied hybridoma cells grown in serum containing media in a 1.2 L working volume bioreactor. They hypothesized that the impaired cell growth rates observed during agitation resulted from bubble entrainment caused by a vortex at the impeller. They found that increasing the serum concentration limited the damage. Kunas and Papoutsakis (1990a) observed similar behavior in other experiments with the same cell/media systems. Growth impairment was only found at lower serum levels. To confirm the growth impairment through bubble entrainment hypothesis, Kunas and Papoutsakis (1990b) operated a bioreactor both with and without a gas headspace. Growth impairment was only seen when the headspace was present. Without a gas

headspace, agitation rates of over 700 rpm were achieved without impairing cell growth. Michaels et al. (1991b) used hybridoma cells grown in a serum free medium to evaluate polyethylene glycol and Pluronic® F68 for protection against cell damage caused by entrained bubbles. They found that both polyethylene glycol and Pluronic® F68 prevented growth impairment at agitation rates that caused bubble entrainment. In other studies using the same approach, Michaels and Papoutsakis (1991a) found that polyvinyl alcohol, polyethylene glycol, and Pluronic® F68 all protected cells against growth impairment from agitation induced bubble entrainment. They found that polyvinyl alcohol worked best, followed by polyethylene glycol, and finally, Pluronic® F68. Subsequent work (Michaels et al. 1992) also evaluated dextran, methyl cellulose, and polyvinyl alcohol. The several grades of methyl cellulose that were tested appeared to be effective. Dextran increased growth impairment under conditions of agitation induced bubble entrainment. The addition of polyvinyl alcohol was able to overcome the detrimental effects of dextran. All these studies found that serum apparently had both a fast acting and long acting protective effect, implying that it protects by both a physical and biological mechanism. The other protective additives had only a fast acting, physical protective effect. The major problem in using these results to rank the relative protection levels afford by protective additives is that the bubbles were not characterized. The addition of surfactants has a profound influence on bubble formation. Thus, the different levels of protection provided by the different agents may only reflect their influence on the formation of bubbles.

Michaels et al. (1996) made an attempt to determine whether cell-bubble interactions in the bulk liquid influence observed cell growth rates. Using Chinese hamster ovary cells grown in a 3% serum medium and a serum free medium, they examined the growth of the cells in a sparged and agitated 1.8 to 2.0 L working volume bioreactor. The reactor was operated without a gas headspace. They provided the reactor with a bubble escape system that consisted of a bottle above the reactor and a tube that connected it to the reactor. Enough medium was added to the system so that the liquid partially filled the tube and bottle system. Any bubbles produced by sparging exited the reactor through this apparatus and burst within it. First, the researchers operated the reactor at relatively low agitation intensities (no vortex) and with a gas headspace. They found that for the 3% serum medium, total cell number began to decline with the onset of sparging. When sparging without the gas headspace, they observed growth rates that were similar to or even greater than the no sparging controls. However, the growth rates between replicate experiments varied by as much as 50%. They conclude that these data demonstrate that bubble-cell interactions in the bulk cause little damage. This may very well be the case, however, these experiments do not provide a well controlled system for comparison. When the tube/bottle apparatus is used, significant bubble coalescence can occur within the tube. Thus, when operating the reactor with no headspace, the performance improvement may merely be due to the fact that larger bubbles are bursting, and there is some evidence that larger bubbles result in less cell death (Orton 1992; Wu and Goosen 1995). The authors suggest the difference between the headspace and no headspace systems may be the formation of a foam layer in the tube/bottle apparatus. If the bursting

bubble is isolated from the bulk liquid, it is unable to form the liquid jet observed by many researchers, including Chalmers and Bavarian (1991). Thus, the cell death attributable to the liquid jet is probably prevented.

In summary, many animal and insect cell lines experience impaired growth when exposed to bubbles produced by either sparging or entrainment from a vortex. Serum is able to provide some protection against bubble damage, and the protection is dependent on serum concentration. Pluronic® F68 also consistently provided protection against bubbles when at sufficient concentrations. Polyvinyl alcohol and methyl cellulose also consistently provided protection against bubbles. These results are also consistent with the previously presented data indicating that these additives help prevent cell-bubble attachment. Dextran and carboxymethyl cellulose did not provide protection. Polyvinyl pyrrolidone and polyethylene glycol did seem to provide protection against bubbles, but the cell bubble attachment data indicate that they might increase cell-bubble attachment. The data also indicate that smaller bubbles or higher specific gas flow rates are more damaging to cultures. The data do not allow one to make a good evaluation of the relative protection provided by good protective additives such as serum, Pluronic® F68, methyl cellulose, and polyvinyl alcohol. The data were not controlled for bubble size or frequency, and thus, meaningful comparisons are not possible.

2.2.4 Measurements of Death Rates and a Killing Volume Model

The experiments reported above begin to explain the mechanisms of sparging related death. However, experiments which measure changes in growth rates or maximum viable cell densities are poor methods for characterizing sparging damage. In order to

understand sparging related death, well controlled experiments that measure both bubble sizes and specific death rates are necessary. Tramper et al. (1986) conducted a series of sparging experiments using *Spodoptera frugiperda* cells grown in a 10% serum, 0.1% w/v methyl cellulose, and antifoam containing medium. The experiments were conducted in a bubble column which was operated at gas flow rates that were high enough to produce cell death rates substantially greater than the average cell growth rates. They observed that the specific death rate was linearly proportional to the volumetric air flow rate. The reactor volume was fixed, and the bubble sizes were similar at the various gas flow rates. Tramper et al. (1987) hypothesized a killing volume related to each bubble, but its location is not specified. The specific death rate is modeled as being directly proportional to the killing volume and the gas flow rate. The specific death rate is also assumed to be inversely proportional to the bubble volume, reactor cross section, and the reactor height. Using the same cells and medium as above, Tramper et al. (1987) varied the reactor height at fixed gas flow rate, bubble diameter, and reactor cross section. They found that as height increased, the specific death rate decreased. This mirrors the observations of Handa et al. (1987b) and Handa-Corrigan et al. (1989) for growth performance, but since specific death rates were measured by Tramper et al. (1987), the quality of the correlation is better. Using the same cells and medium as above, Tramper et al. (1988a) studied the effects of bubble diameter and reactor diameter. At a fixed reactor height, gas flow rate, and bubble diameter, they observed a linear decrease in specific death rate when plotted versus the square of the reactor diameter. When they varied bubble diameter at a fixed gas flow rate and fixed reactor geometry, they observed no correlation between bubble

diameter and specific death rate. Handa et al. (1987a) and Handa-Corrigan et al. (1989) observed that smaller bubbles seemed to be more damaging that larger bubbles, however, they did not use methyl cellulose when varying bubble diameter, while Tramper et al. (1988a) did use methyl cellulose. Since much of the work reported in previous sections suggests that methyl cellulose has a protective effect against sparging damage, it seems reasonable to suggest that the difference in the effects of bubble diameter on sparging damage could result from the presence of methyl cellulose. The sparging rates used by Tramper et al. (1988a) are much higher that those reported by the other workers who found a protective effect from methyl cellulose. Thus, it seems that the protection afforded by methyl cellulose is limited. Tramper and Vlak (1988b) used the experimental data reported in this section to make design recommendations for the scale-up of insect and mammalian cell cultures. They proposed that increasing the height of the reactor and using a narrow reactor diameter should minimize sparging related death. This thesis will demonstrate that their recommendation is only applicable to systems with the appropriate protective agents.

Jöbses et al. (1991) extended the sparging death studies to hybridoma cells grown in a 1% serum medium with antifoam. They found a linear decrease in specific death rate with increasing reactor height when reactor diameter, gas flow rate, and bubble diameter were fixed. They also saw a linear decrease in specific death rate when plotted versus the square of reactor diameter at fixed reactor height, gas flow rate, and bubble diameter. An increase in gas flow rate with fixed reactor geometry and bubble diameter also yielded a linear increase in specific death rate. These observations all mirror what was seen with

insect cells previously. They also found that the specific death rate decreased when the concentration of Pluronic® F68 was sequentially increased from 0% to 0.1% w/v. The level of protection seemed to plateau around 0.1% w/v Pluronic® F68, but the protection was not complete, since some cell death was still observed. Martens et al. (1992) conducted similar studies on reactor height and gas flow rate using hybridoma cells grown at various serum concentrations and sparged in an airlift reactor. They found results that were similar to Jöbses et al. (1991).

Two other studies have been conducted where changes in specific death rates were measured at different bubble diameters. Wu and Goosen (1995) studied insect cells sparged in a 5% serum medium with antifoam. With other variables held constant, they found that specific death rate increased as bubble diameter decreased. Orton (1992) conducted similar experiments using hybridoma cells sparged in a 5% serum medium with antifoam. The experiments were conducted at slightly different gas flow rates, so the data were normalized by gas flow rate. According to the model proposed by Tramper et al. (1987), this should not introduce significant artifacts. With the other relevant parameters held constant, the specific death rate in the hybridoma system also increased with as the bubble diameter decreased. Observations from both these systems are consistent with the findings of Handa et al. (1987a) and Handa-Corrigan et al. (1989). All the systems that produced an increase in sparging damage with decreasing bubble diameter did not have protective additives, such as Pluronic® F68 or methyl cellulose, present. The experiments by Tramper et al. (1988a) that showed no death rate dependence on bubble diameter were conducted with 0.1% w/v methyl cellulose. When normalizing the data using the model of

Tramper et al. (1987), except for the bubble diameter term, the death rates found by Wu and Goosen (1995) and Orton (1992) are higher. This suggests the lower sparging death rates in the various experiments by Tramper et al. and the different behaviors with regard to bubble diameter might be explained by a protective effect from methyl cellulose.

The effect of serum concentration on the sparging sensitivity of hybridoma cells was examined by van der Pol et al. (1990). They cultured the cells in various levels of serum, in a concentration range from 2.5% to 10%. They found that when sparged in a bubble column, the cells grown at higher serum concentrations died with lower specific death rates. When the serum concentrations of the lower serum cases were supplemented to a final serum concentration of 10% immediately before sparging, the sparging death rates were nearly the same, except for the cells grown in 2.5% serum which had a slightly higher specific death rate. The authors interpreted this behavior as an indication that serum has a mainly physical protective effect, but a slight metabolic protective effect could be present in the 2.5% serum case. A similar set of experiments were conducted for cells grown at serum concentrations ranging between 0% and 2.5% (van der Pol et al. 1992). They found that decreased serum concentrations increased the specific death rates. When all cultures were supplemented to a serum concentration of 2.5% immediately before sparging, no differences in specific death rates were observed. This was interpreted as indicating that serum was only having a physical protective effect. When using an airlift reactor system and hybridoma cells, Martens et al. (1992) found that reductions in serum concentrations resulted in similar increases in specific death rates. Bubble diameters were not measured in any of these experiments, however, and the variations in serum

concentration could have affected bubble diameters and produced the observed results. However, this is unlikely.

The effect of silicone antifoam on sparging sensitivity was investigated by van der Pol et al. (1993) for a hybridoma cell line grown in either a 5% serum medium or a serum free medium. With the other variables held constant, increasing levels of silicone antifoam resulted in higher specific death rates for the 5% serum medium case and for the 0.1% w/v polyethylene glycol supplemented serum free medium case. The serum free medium had slightly higher specific death rates that the 5% serum system. When no polyethylene glycol was present, the specific death rates in the serum free medium were significantly higher. For this case, increasing antifoam concentrations produced slightly decreasing specific death rates. Van der Pol et al. (1995a) also studied the effects of sparging when using various concentrations and molecular weights of polyethylene glycol. They used hybridoma cells in a serum free medium without antifoam as the experimental system. In general, increases in polyethylene glycol molecular weight or concentration resulted in a lower specific death rates. The different molecular weight and concentration combinations reached a plateau of lowered specific death rates. In subsequent work, van der Pol et al. (1995b) examined various weights and concentrations of dextran as a sparging protective agent in a hybridoma/serum free medium with antifoam system. Low molecular dextran did not have a protective effect. However, the high molecular weights of dextran (222 to 2000 kDa) have a concentration dependent protective effect. The problem with using dextran as a protectant is that the same molecular weight/concentration combinations of dextran that were protective produced an order of magnitude decrease in the oxygen mass

transfer coefficient. Most likely caused by the order of magnitude increase in medium viscosity caused by the dextran. The levels of dextran that were found to be protective were in the range of 10% to 20% w/w. These are much higher concentrations than were tested by other researchers and required special medium preparation to avoid osmolarity problems. Thus, while these results show that previous workers who found dextran to be a poor protective agent did not use high enough concentrations to see the effect, dextran is a poor choice for sparging protection due to the mass transfer impairment it causes. All these experiments also lack measurements of the bubble diameter, which may have changed due to the addition of the additives. Thus, the protective effects that were observed cannot conclusively be attributed an effect that is independent of bubble size. Again, however, this is not a likely explanation.

In summary, the systematic measurements of specific death rates that were reported in this section demonstrate that the model proposed by Tramper et al. (1987) is a reasonable explanation of the lab scale data presented. A difference in the dependence of specific death rate on bubble diameter was observed, however. It seems that the addition of methyl cellulose eliminates the death rate/bubble diameter dependence observed in serum/antifoam systems. The model also seems to acceptably explain the behavior of both insect and animal cell systems. The experiments reported in this section also indicate that serum, Pluronic® F68, polyethylene glycol, methyl cellulose, and dextran prevent sparging damage. However, dextran is a poor choice because it severely reduces mass transfer rates. These experiments do not provide significant help in elucidating where the sparging damage is occurring. It does seem that for the lab scale systems tested, there is

no significant cell death correlating with the bubble rise. The data do not allow one to distinguish whether the bubble injection or the bubble burst is the event that causes cell death; however, the results presented in previous sections indicate that the bubble burst is the most likely source of cell death from sparging.

2.2.5 An Alternate Model for Sparging Related Death

Wang et al. (1994) proposed a more general model to account for cell damage resulting from bubble exposure. They consider bubble breakup or coalescence in the bulk liquid, and the bubble burst at the liquid surface. The model hypothesizes that the specific death rate will show a linear correlation with the specific surface area of the bubbles. Such a correlation is cited by the authors in the work of Oh et al. (1989). The model is based on generalized inactivation volumes which are related to cell death. The authors argue that the high energy dissipation rates associated with the phenomena they include in the model are sufficient to damage cells. Their model hypothesizes that the inactivation volume is a thin film around the bubble. They also assume that the thickness of the inactivation volume is not a function of bubble diameter. This model is essentially equivalent to the killing volume model proposed by Tramper et al. (1987), all it does is explicitly state that the inactivation volume results from two mechanisms and that the inactivation volume is a thin film around the bubble. The model makes no attempt to separate these two volumes when analyzing data, so in practice, it is one inactivation volume. The assumption made by Wang et al. (1994) acceptably explains that data of Oh et al. (1989); however, it is in direct conflict with the data presented by Tramper et al. (1988a) which shows that for some conditions, specific death rate is not proportional to

the specific surface area of the bubbles. This model does nothing to further the understanding of sparging related death and conflicts with some of the data in the literature. It is surprising that it was accepted for publication.

2.3 Summary

Laminar shear stress has been observed to cause cell death for both insect and animal cells on surfaces and in suspension. The threshold for shear damage was typically near 5 N/m^2, although shear stresses can begin to cause damage at levels of 0.1 to 0.7 N/m^2 if the cells are exposed for a long enough time. Shear stress thresholds of 150 N/m^2 were observed in systems that had very short exposure times. Many additives were examined to determine whether they can protect suspension cells exposed to laminar shear stresses. Serum was found to reduce shear sensitivity in laminar flow. Methyl cellulose and dextran were also found to reduce shear sensitivity. Pluronic® F68 was found to provide some protection against laminar shear stresses, but not in all studies. Polyethylene glycol did not provide protection against laminar shear stresses. Turbulent shear stress experiments in capillary tubes found that the threshold wall shear stresses necessary for damage were in the range of 100 to 2000 N/m^2 for several different cell lines. The higher shear stress thresholds in the capillary experiments are probably related to the much shorter duration of shear stress exposure in those systems. While some variation in shear sensitivity was found between cell lines, most cells responded to shear stresses similarly. The longer durations and lower shear stresses in the laminar flow experiments caused lowered viability and some lysis. The higher shear stresses in turbulent, capillary shear systems

resulted in cell lysis, and cells that were in the S and G_2 phases of the cell cycle seemed to be more susceptible to damage, perhaps due to their larger size.

Agitated bioreactors operated with surface aeration were also found to cause cell damage related to shear stress. Both insect and animal cells were affected. Cell sensitivity to shear damage was found to be highest in the lag and stationary phases of cultures. Serum seemed to reduce the shear sensitivity of the cells, as did high and low density lipoproteins. Cell death was observed to occur through both necrosis and apoptosis in these systems. Cells that were agitated at rates in the 600 rpm range showed a depletion of cells in the G_1 phase of the cell cycle. For the extremely high agitation rate of 1500 rpm, the culture had a slight relative enrichment of cells in the G_1 phase. This may reflect different damage mechanisms at the different agitation rates. At the lower levels of agitation, shear stresses might be inducing apoptosis, which is perhaps more likely to occur in cells that are in the G_1 phase. At the high agitation rate, cell death may be occurring through disruption by turbulent eddies. This would favor disrupting cells in the S and G_2 phases, since they are slightly larger.

Measurements of plasma membrane fluidity and membrane bursting tension indicate that serum, high and low density lipoproteins, and Pluronic® F68 can increase the strength of cell membranes. This suggests that these compounds protect cells from shear damage by strengthening the cell membrane. Models of cell death rates caused by lysis in laminar and turbulent flow that were based on membrane bursting tension measurements showed good agreement with experimental death rates. These results are generally in good

agreement with the experimental data obtained for laminar flow, turbulent flow in capillaries, and surface aerated, agitated bioreactors.

Cells have been observed to attach both to rising bubbles and to the thin films that form between bubbles and the gas-liquid interface. Cell-bubble attachment can occur in systems with either serum containing or serum free media. The addition of compounds such as polyvinyl alcohol, methyl cellulose, and Pluronic® F68 prevented cell bubble attachment or greatly increased the time required for attachment. Polyethylene glycol and polyvinyl pyrrolidone did not prevent cell-bubble attachment. A thermodynamic model for explaining cell-bubble attachment that was proposed in the literature conflicts with other published measurements. Those measurements show that cell-bubble attachment will occur in all the systems that were examined with the thermodynamic model, but additives that protect cells against sparging damage typically have very long cell-bubble attachment times.

Bursting bubbles have been observed to kill cells by two mechanisms. The rupture of a thin film will kill nearly all the cells that are attached to the film surface. The shear stresses produced in these rupturing films are very large. Cell death from the bubble burst can also result from the high shear stresses that are produced in the liquid beneath the bubble. Many attempts have been made to determine the influence of protective additives on cell death from bursting bubbles. Experiments that measured cell growth impairment caused by bubble entrainment found that serum, polyvinyl alcohol, polyethylene glycol, polyvinyl pyrrolidone, methyl cellulose, and Pluronic® F68 protected cells against bubble

related shear damage. Carboxymethyl cellulose and dextran did not provide protection at the levels tested.

A series of experiments that provide well controlled measurements of specific death rates are also available in the literature. For systems with only serum and antifoam, specific death rates were observed to increase as the bubble diameter decreased. For a system with methyl cellulose, specific death rates were independent of bubble diameter. Pluronic® F68 and methyl cellulose reduced specific death rates relative to systems containing only serum or no protective agents. A killing volume model which hypothesizes that some volume associated with each bubble results in cell death adequately explains the sparging death rate measurements that were available. However, this model does not adequately explain the observations of cell attachment to rising bubbles that were seen in a serum containing system. Cells that are attached to bubbles would be expected to die when the bubbles burst, yet death from this mechanism should increase as reactor height increases (reactor volume, gas flow rate, and bubble diameter fixed). This behavior was not observed in any of the published experiments, perhaps because at the reactor heights tested, this effect is small.

3. MATERIALS AND METHODS

3.1 Cells and Media

These studies used the mouse/mouse hybridoma CRL-1606 (American Type Culture Collection, Rockville, MD). The initial culture was grown in Iscove's Modified Dulbecco's Medium (IMDM), 5% v/v fetal bovine serum (FBS), and 0.1% v/v penicillin-streptomycin-neomycin solution (Sigma Chemical Co., St. Louis, MO). The initial stock of these cells was obtained from a frozen 1 mL aliquot of unknown passage number. The initial stock of cells was propagated in T-flasks at 37°C in a 95% relative humidity, 10% carbon dioxide atmosphere. The cells were diluted as necessary to maintain the cell number below 8 x 10^5 cell/mL, but not diluted below 1 x 10^5 cell/mL. After two weeks of growth, a fraction of the cells was frozen to provide a cell bank. The cells were frozen in ten 1 mL aliquots containing 5 x 10^7 cell/mL. The freezing medium consisted of IMDM, 5% v/v FBS, and 10% v/v dimethyl sulfoxide (Sigma Chemical Co., St. Louis, MO). The cells were placed in an isopropyl alcohol bath, and then placed in a freezer at -70°C for 12 hours. The alcohol bath ensured a gradual cooling rate of about 1°C per minute, as recommended by Freshney (1987). After the cells were frozen, they were transferred to a liquid nitrogen cell bank.

Since serum is known to be somewhat variable, and also influences the shear sensitivity of animal cells, it was desirable to adapt the cells to serum free growth. The serum free medium consisted of IMDM, 10 mg/L bovine insulin, 5 mg/L human transferrin, 12 mg/L bovine albumin, 3.5 μL/L 2-mercaptoethanol, 2.4 μL/L ethanolamine, and 0.1% v/v penicillin-streptomycin-neomycin solution (Sigma, St. Louis, MO). To

adapt the cells to serum free growth, the level of FBS in the medium was gradually reduced by diluting cells that were growing in the original 5% FBS medium from 8 x 10^5 cell/mL to 2 x 10^5 cell/mL. This five fold dilution maintained enough serum in the culture for cells to grow at their previous growth rate and maintained cell viabilities greater than 95%. After this batch of cells had grown to 8 x 10^5 cell/mL, they were again diluted five fold. This process was repeated until the original amount of serum was reduced to insignificant levels. Throughout this process, cell growth rates and viabilities remained similar to the initial culture. When the cells were fully adapted to the serum free medium, thirty 1 mL aliquots were prepared and frozen as above, except 1 mg/mL of bovine albumin (Sigma Chemical Co., St. Louis, MO) was substituted for the FBS. This served as the cell bank for all subsequent experiments. Every two to three months, a new aliquot of cells was thawed and expanded for use in experiments.

The cells were cultured in a consistent, reproducible fashion in T-flasks at 37°C in a 95% relative humidity, 10% carbon dioxide atmosphere. The cells were diluted into fresh medium to achieve concentrations of approximately 2 x 10^5 cell/mL, and then used in experiments after two days of growth. This typically allowed cells to reach concentrations of 8-10 x 10^5 cell/mL. The growth rate for these cells averages 0.03-0.04 hr^{-1}. All cells used in experiments were at greater than 95% viability. Prior to experiments, the cells were centrifuged at 800 rpm in an IEC Centra-4B Centrifuge (International Equipment Company), the supernatant was decanted, and the cells were suspended in the experimental medium at approximately 8 x 10^5 cell/mL.

3.2 Cell Enumeration

Cell viability was measured using an isotonic solution of 0.4% w/v trypan blue to dilute cell culture samples. The cells were then placed on a hemocytometer slide. Under a microscope, the viable cells appear bright white, while non-viable cells are stained blue. Trypan blue is not able to cross intact cell membranes, and thus it is a conservative measure for non-viable cells. Some non-viable cells could be missed by trypan blue staining. To determine if the trypan blue assay was underestimating cell death, the samples were periodically compared using an alternate staining technique which is described below.

Using a combination of the stains acridine orange and ethidium bromide allows one to measure the number of cells in a culture that die by each of two mechanisms: necrosis and apoptosis (Mercille and Massie 1994). Cells were diluted into an isotonic solution containing 100 μg/mL of acridine orange and 100 μg/mL of ethidium bromide. Both acridine orange and ethidium bromide are DNA intercalating dyes which fluoresce under ultraviolet excitation. Acridine orange (which fluoresces green) crosses cell membranes regardless of integrity, while ethidium bromide (which fluoresces orange) will only cross membranes which have lost their integrity. The combination of the two dyes allows four cell morphologies to be identified. Viable cells stain bright green and posses normal nuclei which do not show condensed chromatin. Early apoptotic cells stain green, but show a fragmenting nucleus with condensed chromatin. Late apoptotic cells stain orange and show a fragmented nucleus with condensed chromatin. Necrotic cells show a normal nucleus, but stain orange. The trypan blue assay misses the cells which are in the early

apoptotic stage of death. This technique showed that under the culture conditions used in this work, very low levels of apoptosis were occurring and the trypan blue staining technique did not significantly underestimate cell death.

Cell number was determined using a Coulter Z_F Electronic Particle Counter (Coulter Electronics, Hialeah, FL). Cells were diluted into an isotonic solution and counted using a 100 μm orifice on the counter. Using a Channelizer (Coulter Electronics, Hialeah, FL) connected to the counter, it is possible to measure the relative volume distribution of the cells. By calibrating the equipment using latex beads of a known volume distribution, it is possible to determine the cell volumes. From the cell volumes, the Sauter mean diameter of the cells can be calculated.

3.3 Physical Property Measurements

3.3.1 Equilibrium Surface Tension

Surface tension was measured with a Krüss Tensiometer K10T (Krüss, Hamburg, Germany) using the Wilhelmy Plate method. This technique measures the surface tension of an interface that has reached thermal and surface concentration equilibrium. Approximately 30 mL of sample is placed in a flat bottomed cup. The cup is surrounded by a water jacket that is used to control the temperature of the sample. A platinum plate is slowly lowered until it just makes contact with the liquid surface. The surface tension is then recorded for 20 min to 1 hr. The surface tension eventually reaches a plateau that represents the equilibrium value.

3.3.2 Viscosity

The viscosity was measured using a capillary viscometer. The time it takes a liquid to flow through a narrow capillary is recorded. Since the capillary is calibrated for a know standard, one can then calculate the viscosity from these data. The apparatus is submerged in a water bath to maintain a controlled constant temperature.

3.3.3 Molecular Weight Distribution

A Waters 410 Differential Refractometer in combination with a 515 HPLC Pump, a 746 Data Module, and a gel permeation column (Millipore Corporation, Waters Chromatography Division, Milford, MA) was used to measure the molecular weight distribution for two Pluronic® F68 batches. The system uses water based gel permeation chromatography. Each sample of polymer was dissolved at approximately 3 mg/mL in a solution of water with 0.02% w/v sodium azide and 0.5 M sodium nitrate. The polymer elution time is related to its molecular weight. Longer polymers elute at shorter times. The size distribution information provided by the equipment allows for the determination of the polydispersity of the polymer sample.

3.3.4 Bubble Diameter and Bubble Frequency

Bubble frequency and velocity were determined directly using a Kodak Ektapro 1000 High Speed Video System (Eastman Kodak, Rochester, NY) for serum free medium with antifoam and for serum free medium with antifoam and Pluronic® F68 at 37°C. The video system allows for the shutter rate to be set at up to 1000 frames per second. The output recording may be advanced frame by frame in order to make accurate measurements. Each frame has a time index that allows for direct assignment of times.

Two orifice sizes were examined. The gas flow rate was 43 ± 2 mL/min for both the 16 gauge and 24 gauge needles. For the 24 gauge needle, the video system was used to measure the time it took 25 bubbles to pass a fixed point approximately 10 cm above the sparger. At least three independent measurements were made for each case. For the 16 gauge needle, the time it took 10 bubbles to pass a fixed point was used. This is because the video system only records two seconds of data, and the bubble frequency with the 16 gauge needle was very low. During normal reactor operation, the bubble frequency was measured using a strobe light (Pioneer Electric and Research Corp., Forest Park, IL) to find the natural frequency of the bubbles. This technique agreed with the direct measurements made with the high speed video system. These measurements allowed the average bubble radius to be calculated using the bubble frequency and gas flow rate.

3.3.5 Bubble Rise Velocity

Bubble velocity was measured in the 1.3 cm radius, water jacketed reactor using the high speed video system and the conditions reported above. By determining the average time it took a bubble to traverse 31 mm, the rise velocity could be calculated. The measurement distance was approximately 10 cm above the sparger in order to allow the bubbles to approach their terminal rise velocity. For both the 16 gauge and 24 gauge needles, the transit times for 30 bubbles were measured. The transit times were then averaged, and the velocity was calculated by dividing distance by the average transit time.

3.4 Bioreactor Experiments

3.4.1 Reactor Configurations

Cell death rates were measured for two types of reactor system. Cell death was found to follow first order kinetics in all cases. One reactor consisted of a Tygon® tube, 0.64 cm in radius and 180 cm in height. A 24 gauge stainless steel needle was used as the sparger for this reactor. It was inserted into a silicone rubber stopper and was held in place using Red RTV 106 silicone adhesive (General Electric, Waterford, NY). This adhesive is known to be non-toxic to animal cells. The stopper and needle were inserted into one end of the Tygon® tube and form the base of the reactor. The reactor was held in place using several clamps and plumbed using a spirit level. The needle was fed with a gas mixture consisting of 5% carbon dioxide, 21% oxygen, and 74% nitrogen. The gas flow rate was controlled using a rotameter, and a 0.2 μm filter was placed between the rotameter and the needle. The experiments conducted in this reactor were of short enough duration that sterilization of the apparatus was not necessary.

The second reactor (Figure 3-1) consisted of a water jacketed glass column (Ace Glass, Vineland, NJ). The reactor was 1.3 cm in radius and 30 cm tall. Each end of the reactor had a threaded Teflon cap that was sealed using a silicone rubber O-ring. The bottom cap had either a 24 gauge or 16 gauge stainless steel needle that was held in place and sealed with silicone adhesive. The needle was attached to an in-line 0.2 μm filter. The gas supply is the same as above. The top cap of the reactor had two 16 gauge stainless steel needles. One was used as a sample port, and the other was attached to another 0.2 μm filter that served as the gas outlet. Temperature was controlled using a RM6 Lauda

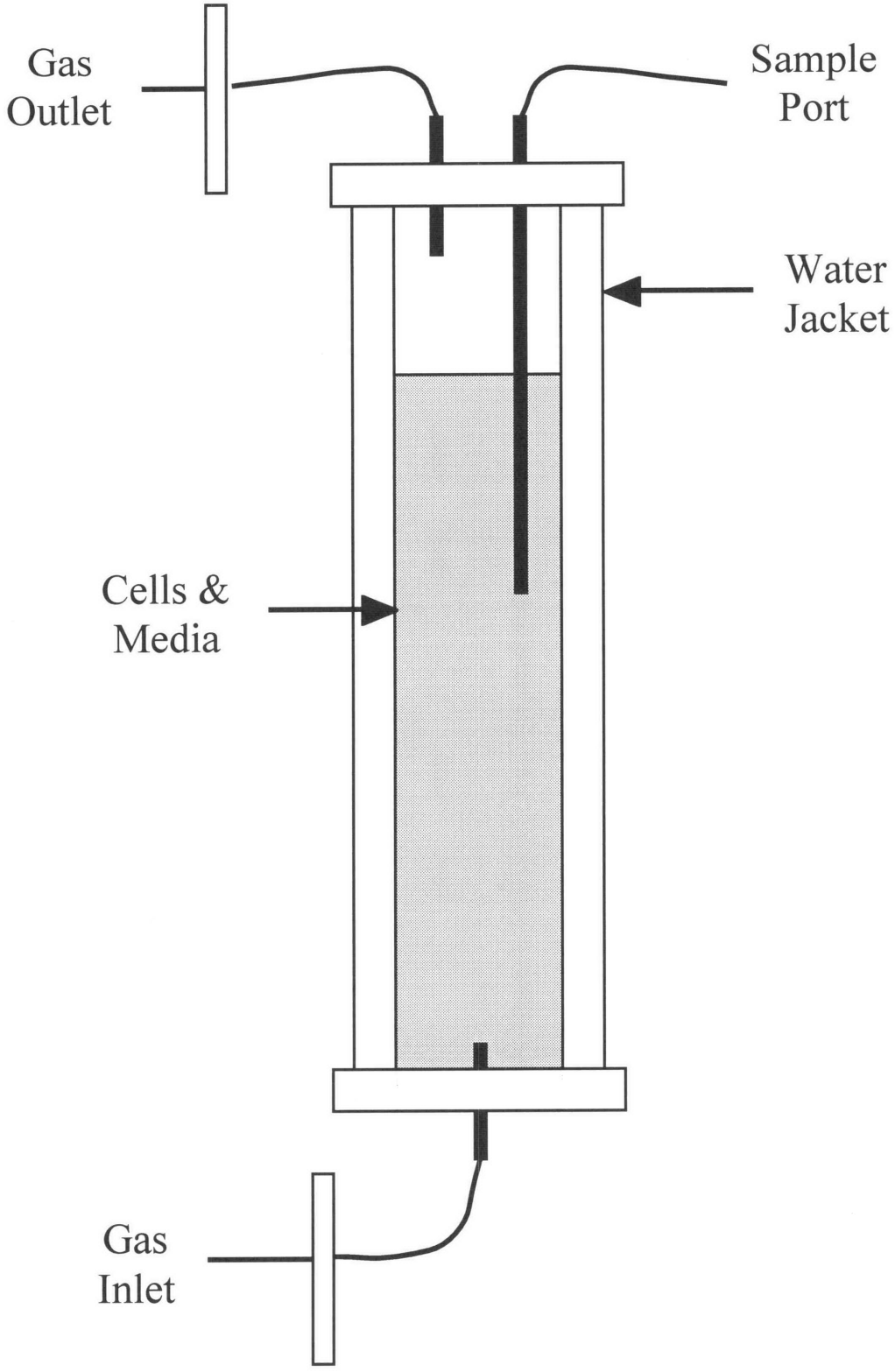

Figure 3-1 Reactor configuration for water jacketed reactor.

circulating water bath (Lauda and Co., Germany). This reactor can be sterilized by autoclave when necessary. For both reactor systems, gas humidification was unnecessary. No significant changes in culture volume were observed over the course of the experiments.

3.4.2 Culture Conditions Varied

Three different culture variables were tested for their effect on sparging related death rates. First, the cells used to inoculate the sparging experiments were grown under two conditions. One group of cells were grown for several generations in serum free medium supplemented with 5% v/v fetal bovine serum (FBS). The other group of cells were grown in serum free medium alone. These experiments were performed at 100 mL in culture volume, using a 1.3 cm radius reactor operated at 37°C. The gas flow rate was 43 ± 2 mL/min (the variance represents the standard error unless otherwise noted), resulting in 1.60 ± 0.05 mm bubbles. Prior to experiments, all cells were centrifuged, rinsed in phosphate buffered saline, centrifuged again, and suspended in serum free medium with 100 ppm Sigma antifoam A. This preparation was then used in the sparging experiments. Second, the effect of temperature on sparging death rate was measured for three different medium compositions. Sparging death rate measurements were made in reactors operated at either 24°C or 37°C. The media tested consisted of serum free medium with antifoam, and serum free medium with antifoam and either Pluronic® F68 (Sigma) or methyl cellulose. The 1.3 cm radius reactor was operated at a gas flow rate of 43 ± 2 mL/min and a culture volume of 100 mL. The 24 gauge needle was used as the sparger. The bubbles varied from 1.40 ± 0.05 mm to 1.60 ± 0.05 mm in radius, depending on which medium

was used. The temperature change did not affect the bubble radius, only medium composition did. Since the comparisons are only made for the same medium at two different temperatures, the variation in bubble radius is not relevant. Third, two batches of Pluronic® F68, one from Fluka and one from Sigma, were tested at the same reactor conditions to determine the effect of Pluronic® F68 variability on protection. The 1.3 cm radius reactor was operated at 24°C with a gas flow rate of 43 ± 2 mL/min. The 24 gauge needle was used as the sparger and produced bubbles 1.40 ± 0.05 mm in radius. The medium consisted of serum free medium with antifoam and 0.1% w/v Pluronic® F68. For the batch of Pluronic® F68 supplied by Fluka, the reactor was operated at a culture volume of 100 mL. For the batch of Pluronic® F68 supplied by Sigma, the reactor was operated at 180 mL.

3.4.3 Reactor Height Varied

In this set of experiments, two reactors with different aspect ratios were compared. Culture volume was kept constant at 180 mL. The reactors were operated at 24°C to ensure that no cell growth occurred during the experiments. The gas flow rate was set at 43 ± 2 mL/min. A single 24 gauge stainless steel needle was used as the sparger in each reactor. The sparger produced single, non-interacting bubbles of consistent radii. One reactor consisted of a Tygon® tube, 0.64 cm in radius and 142 cm in culture height. The other reactor consisted of a glass column, 1.3 cm in radius and 34 cm in culture height. In control experiments with no sparging, no growth or death was observed in either reactor. The death rates were measured for three different media: serum free medium with 100 ppm antifoam A (Sigma); serum free medium with antifoam and 0.1% w/v Pluronic® F68

(Sigma); and serum free medium with antifoam and 0.1% w/v 15 cP grade methyl cellulose (Sigma). The fluid motion induced by the rising bubbles was sufficient to keep the cells in suspension, and no mechanical agitation was required.

3.4.4 Reactor Volume Varied

In the second set of experiments, a 1.3 cm radius water jacketed glass column was used as the reactor. Three medium compositions were tested: serum free medium with antifoam, serum free medium with antifoam and 0.1% w/v Pluronic® F68 (Fluka), and serum free medium with antifoam and 0.1% w/v methyl cellulose (Sigma). The gas flow rates for the 16 gauge and 24 gauge needle were the same as above. Death rates were measured for 5 different reactor volumes: 100, 140, 180, 240, and 300 mL. The reactor was operated at 37°C. For serum free medium with antifoam, the death rates were significantly greater than the typical growth rates for these cells. For the media with either Pluronic® F68 or methyl cellulose, the death rates were the same order of magnitude as the growth rates, so a control was necessary. The control culture consisted of a 20 mL sample of cells and medium from the inoculum for each reactor. The control culture was grown in a 50 mL shake flask operating at 80 rpm, in a 37°C, 5% carbon dioxide atmosphere. Thus, true death rates for the reactors could be calculated.

3.4.5 Novel Oxygen Supply

Expanded polystyrene foam obtained from tube racks supplied with sterile 50 mL test tubes (Corning) was used as the oxygen storing foam. To load the foam with oxygen, it was placed in a pressure vessel and exposed to a 40 psig oxygen atmosphere for a week. This allowed full loading of the foam with oxygen, based on calculations of oxygen

diffusion rates. To test for toxicity, unpressurized foam was exposed to hybridoma cells cultured in serum free medium. The foam was obtained from a sterile package, and thus did not need further sterilization. Two cultures were started from a common stock, one with foam and one without foam. The foam was added to the cells when they were in early exponential growth and at a concentration of approximately 2×10^5 cell/mL. After two days of growth, the cells were sampled from each system, and concentration and viability were measured.

To test for the ability of the foam to meet the oxygen demands of cells in culture, a sealed, no headspace flask with 50 mL of hybridoma cells and serum free medium was chosen as the test system. The flask was agitated using a magnetic stir bar operating at 80 rpm. The vessel was sealed using a silicone rubber stopper. A dissolved oxygen probe was inserted through the stopper (Microelectronics, Inc.). The flask was operated at a cell density of approximately 1.0×10^6 cell/mL. First, the oxygen uptake rate was measured without the addition of the oxygenated foam. Next, the dissolved oxygen concentration was followed after the addition of 2.5 mL of oxygenated foam. From a combination of the two measurements, the true oxygen supply rate of the foam could be calculated.

4. THEORY

4.1 Model For Sparging Related Death

Tramper et al. (1986) found that sparging related death follows first order kinetics, and Tramper et al. (1987) modeled the death rate as being directly proportional to gas flow rate and inversely proportional to reactor volume (Equation 4-1). In experiments conducted to validate this model (Jöbses et al. 1991; Tramper et al. 1987; Tramper et al. 1988a; Tramper et al. 1986), the cell death rate was consistent with a hypothetical liquid killing volume, V_d, associated with the gas bubble. The killing volume was found to be a function of reactor volume, but not reactor geometry. The first order death rate,

$$k_d = \frac{QV_d}{V_b V_r}$$

Equation 4-1

is a function of gas flow rate, Q, reactor volume, V_r, bubble volume, V_b, and the killing volume. The same expression can be rearranged to give the death rate per bubble as a killing volume divided by the reactor volume,

$$\frac{k_d}{f_b} = \frac{V_d}{V_r}$$

Equation 4-2

where $f_b = \frac{Q}{V_b}$ represents the bubble frequency.

This model fits several experiments, mentioned above, designed to test whether sparging death could be attributed to bubble formation, rise, or burst. The data were found to be consistent with death from the bubble burst, but the data were inconsistent with

death from the bubble rise. However, some of these experiments (Tramper et al. 1987; Tramper et al. 1988a; Tramper et al. 1986) were carried out with insect cells in a medium containing 0.1% w/v methyl cellulose, and methyl cellulose is known to affect cell-bubble interactions (Michaels et al. 1995a). The conclusions that can be drawn from these experiments can not necessarily be generalized to sparging without protective additives. In fact, the experiments of Bavarian et al. (1991) conflict with the conclusions drawn from the experiments above. They observed that insect cells attach to rising bubbles and do not detach in a system with no protective additives. One would expect cells attached to these rising bubbles would die when the bubbles burst, based on the observations in the literature (Cherry and Hulle 1992; Garcia-Briones and Chalmers 1992; Trinh et al. 1994) and modeling of shear rates for bursting bubbles (Garcia-Briones et al. 1994).

Bavarian et al. (1991) suggested that a model from the ore flotation literature (Sutherland 1948) could be applied to cell attachment to rising bubbles, but cell attachment to rising bubbles does not explain the killing volume hypothesized by Tramper et al. (1987). When the death rate was plotted versus reactor height, with gas flow rate, bubble size, and reactor radius kept constant, Tramper et al. (1987) found that death rate decreased with increasing reactor height. If death was occurring only from flotation, Tramper et al. (1987) would have observed no change in death rate when varying reactor height. Thus, the killing zone found by Tramper et al. (1987) is not attributable to flotation. This discrepancy might be because Bavarian et al. (1991) found flotation in an insect cell system using only TNM-FH medium, while Tramper et al. added 0.1% w/v methyl cellulose and silicone antifoam to the medium. Alternatively, cell

death from flotation may be small compared to death from the killing zone proposed by Tramper et al. (1987).

To capture the behavior observed by both Bavarian et al. (1991) and Tramper et al. (1988a), it is necessary to reformulate the model proposed by Tramper et al. (1987). We propose the equation

$$\frac{k_d}{f_b} = \frac{V_{d,rise}}{V_r} + \frac{V_d}{V_r}$$

Equation 4-3

where a new killing volume, $V_{d,rise}$, has been added, representing a volume swept out by the rising bubble. Cells in this volume attach to the bubble and die when the bubble bursts. The cells are assumed to attach irreversibly, which is consistent with the observations of Bavarian et al. (1991), and the surface of the bubble is assumed to be far from saturated with attached cells. The swept volume can thus be represented as a cylinder, giving

$$V_{d,rise} = H_r \pi R_p^2$$

Equation 4-4

where H_r is the reactor height, and R_p is an effective radius projected by the rising bubble. Cells that fall within the projected area attach to the rising bubble and die when the bubble bursts at the top of the reactor. Using this formulation, and representing the reactor as a cylinder of radius R_r, we may simplify Equation 4-3 as follows:

$$\frac{k_d}{f_b} = \frac{R_p^2}{R_r^2} + \frac{V_d}{V_r}$$

Equation 4-5

It should be noted that this model applies only to non-interacting bubbles, i.e., those that do not break up or coalesce.

Several assumptions must be made to solve for the projected radius of the bubble: first, the bubble is assumed to behave as a hard sphere; second, the cell is assumed to be small relative to the bubble and to not significantly affect streamline flow around the bubble; and third, the cell is assumed to behave as a fluid element, without any significant momentum difference relative to the liquid. One can then assume that cells will follow the streamlines for flow around a sphere. Although cells are treated as moving like fluid elements, they project beyond their streamline. Thus, a cell following streamline flow can contact and attach to the bubble. Using the radius of the cell and the stream function for flow around a sphere, one can solve for the projected radius of the bubble (Figure 4-1). Both creeping flow and potential flow around a sphere need to be analyzed. Small bubbles move at velocities in the creeping flow regime; however, larger bubbles can exhibit circulation at the gas-liquid interface and have higher velocities, meaning they begin to fall in the potential flow regime.

4.1.1 Creeping Flow Solution

The stream function for creeping flow around a sphere, taking into account interfacial momentum transfer from Edwards et al. (1991), is

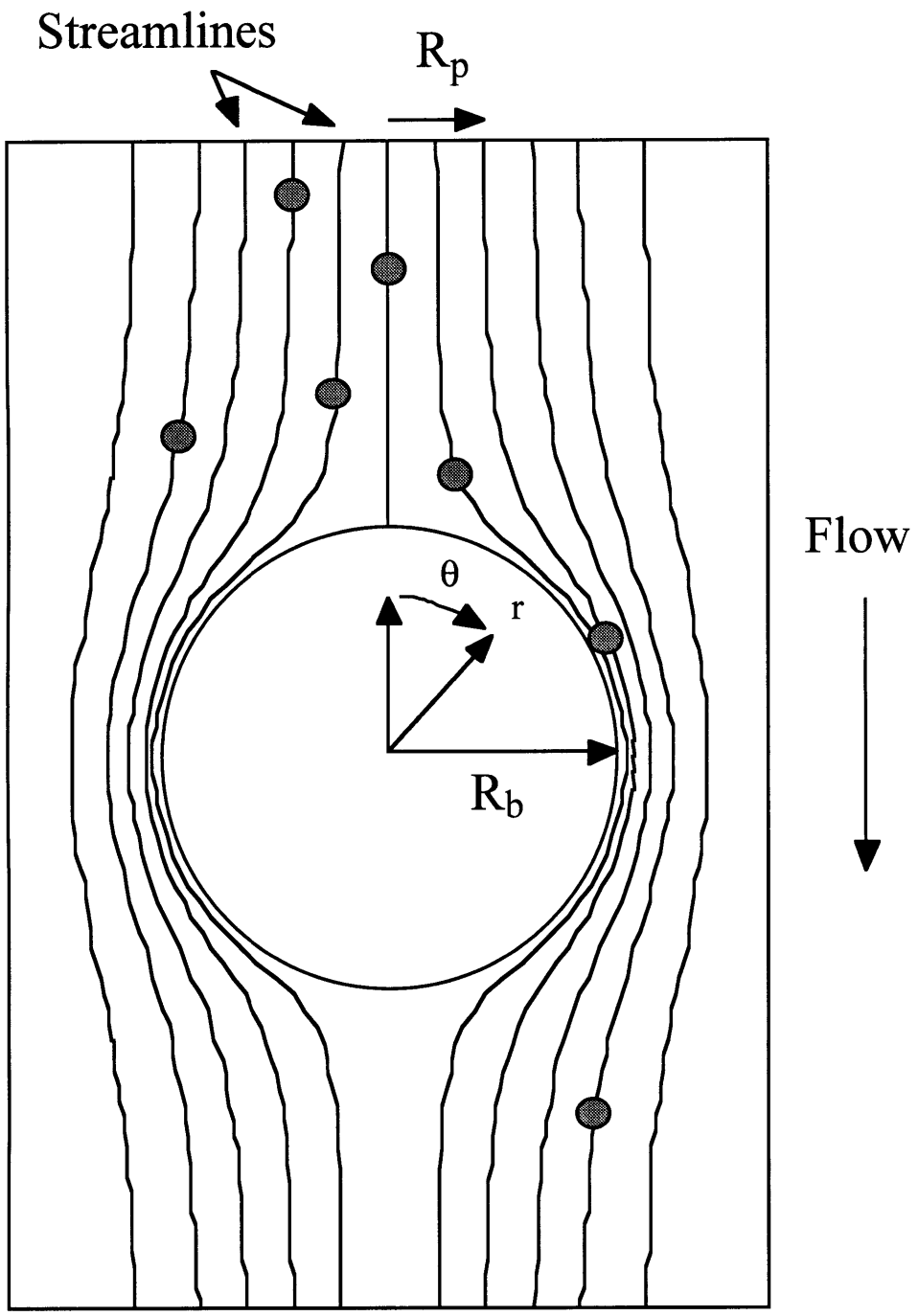

Figure 4-1 Cells following streamline flow around a rising bubble. Cell size is exaggerated for clarity. The bubble projects a radius, R_p, at a point far upstream of the bubble. Cells that are on streamlines which fall within this projected radius will contact and attach to the bubble. Inertial and diffusion effects have been ignored.

$$\Psi(r,\theta)=\left(\left(\frac{1}{2}-\frac{\left(\frac{3}{2}\mu_g+\frac{3\kappa^s}{R_b}+3\mu_l\right)}{\left(2\mu_g+\frac{4\kappa^s}{R_b}+6\mu_l\right)}\right)\frac{R_b^3}{r}+\left(\frac{\left(\frac{3}{2}\mu_g+\frac{3\kappa^s}{R_b}+3\mu_l\right)}{\left(2\mu_g+\frac{4\kappa^s}{R_b}+6\mu_l\right)}\right)R_b r-\frac{1}{2}r^2\right)v_\infty \sin^2\theta$$

Equation 4-6

Both the gas and liquid viscosities, μ_g and μ_l, respectively, are orders of magnitude lower than the surface dilatational viscosity, κ^s, divided by the bubble radius, R_b, for relevant systems (Michaels et al. 1995b). Thus, this stream function simplifies to the standard creeping flow stream function with a no slip boundary condition at the bubble-liquid interface:

$$\Psi(r,\theta)=\left(-\frac{1}{4}\frac{R_b^3}{r}+\frac{3}{4}R_b r-\frac{1}{2}r^2\right)v_\infty \sin^2\theta$$

Equation 4-7

The interception radius, R_i, a projected radius for the streamline where the cell will just touch the bubble at its equator, can be determined by solving the stream function at two different coordinates. Points at which the stream function has the same value represent the same surface in the flow field. The stream function evaluated at the bubble equator for a cell which just touches the surface,

$$\Psi\left(r=(R_b+R_c),\theta=\frac{\pi}{2}\right)=\left(-\frac{1}{4}\frac{R_b^3}{(R_b+R_c)}+\frac{3}{4}R_b(R_b+R_c)-\frac{1}{2}(R_b+R_c)^2\right)v_\infty$$

Equation 4-8

is set equal to the stream function evaluated far upstream from the bubble,

$$\lim_{r->\infty}\left[\Psi\left(r,\theta=\sin^{-1}\left(\frac{R_i}{r}\right)\right)\right]=-\frac{1}{2}\left(R_i\right)^2 v_\infty$$

Equation 4-9

where r and θ are spherical coordinates (there is no z dependence due to axial symmetry), and R_c is the cell radius. The equation can then be solved to give the interception radius:

$$R_i=\left(\frac{R_c^2\left(3R_b+2R_c\right)}{2\left(R_b+R_c\right)}\right)^{\frac{1}{2}}$$

Equation 4-10

All cells that are within the interception radius will contact the bubble. Contact with the bubble does not mean that the cell will attach, however. Michaels et al. (1995a) showed that a finite time is required before cell-bubble attachment will occur. Thus, it is necessary to take this into account.

There are two regions within the interception radius. In one region, cells will strike the bubble surface, but will not stay in contact with the bubble long enough to attach to it. In the other region, cells will contact the bubble and stay in contact long enough to attach to the bubble surface. The point given by $\left(r=\left(R_b+R_c\right),\theta\right)$ divides these two regions, and it is on the streamline that defines the projected radius for cell attachment. Using the definition for arcial velocity,

$$v_\theta=\left(1-\frac{3}{4}\frac{R_b}{r}-\frac{1}{4}\frac{R_b^3}{r^3}\right)v_\infty\sin\theta$$

Equation 4-11

it is possible to find an expression for the differential contact time of the cell:

$$dt = \frac{(R_b + R_c)d\theta}{v_\theta}$$

Equation 4-12

Equation 4-12 can be integrated to solve for the time the cell is on the bubble surface between contact at the dividing point and the point where the cell can leave the bubble surface:

$$\int_0^\tau dt = \int_\theta^{\frac{\pi}{2}} \frac{(R_b + R_c)d\theta}{\left(1 - \frac{3}{4}\frac{R_b}{(R_b + R_c)} - \frac{1}{4}\frac{R_b^3}{(R_b + R_c)^3}\right) v_\infty \sin\theta}$$

Equation 4-13

Since a cell which contacts the bubble can first detach when it reaches $\theta = \frac{\pi}{2}$, this integration limit is used as a conservative estimate, giving

$$\tau = \frac{(R_b + R_c)}{\left(1 - \frac{3}{4}\frac{R_b}{(R_b + R_c)} - \frac{1}{4}\frac{R_b^3}{(R_b + R_c)^3}\right) v_\infty} \log_e\left[\cot\frac{\theta}{2}\right]$$

Equation 4-14

An expression for θ can be found in a manner similar to the technique used to obtain Equation 4-10. The stream function at the points $\left(r = (R_b + R_c), \theta\right)$ and $\left(r \to \infty, \theta = \sin^{-1}\left(\frac{R_p}{r}\right)\right)$ are equated, and the equation is rearranged to solve for θ. The resulting expression simplifies to $\theta = \sin^{-1}\left(\frac{R_p}{R_t}\right)$. One can then insert the expression for θ

into Equation 4-14 and rearrange to find an expression for the projected radius for cell attachment. Cells on streamlines within the projected radius will both contact and attach to the rising bubble. We find

$$R_p = \left(\frac{R_c^2 \left(3R_b + 2R_c\right)}{2\left(R_b + R_c\right)} \right)^{\frac{1}{2}} \operatorname{sech}\left[\frac{\tau v_\infty \left(1 - \frac{3}{4} \frac{R_b}{\left(R_b + R_c\right)} - \frac{1}{4} \frac{R_b^3}{\left(R_b + R_c\right)^3} \right)}{\left(R_b + R_c\right)} \right]$$

Equation 4-15

The contact time, τ, can be thought of as defining a transition point. When cells are in contact with the bubble for less than τ, no attachment will occur, and when cells are in contact with the bubble for greater than τ, attachment will occur, as is reported by Michaels et al. (1995a) for direct cell-bubble contact experiments.

4.1.2 Potential Flow Solution

Sutherland (1948) performed a similar analysis for potential flow around a sphere and found that the interception radius is

$$R_i = \left(3R_b R_c\right)^{\frac{1}{2}}$$

Equation 4-16

However, Sutherland used a different integration limit when solving for projected radius. When using a conservative integration limit, as in Equation 4-13, we determined the projected radius to be

$$R_p = \left(3R_bR_c\right)^{\frac{1}{2}} \operatorname{sech}\left[\frac{3\tau v_\infty}{2R_b}\right]$$

Equation 4-17

The solutions for projected radii can be used in Equation 4-5 for analyzing experimental data and predicting cell death rates.

4.2 Analysis

4.2.1 Possible Protection Mechanism

In the creeping flow regime, the Reynolds number for flow around a bubble,

$$Re = \frac{2R_b v \rho_l}{\mu_l}$$

Equation 4-18

is less than or equal to one. For potential flow, the Reynolds number is typically greater than 1000. In the creeping flow regime, the terminal rise velocity of a bubble, v_t, can be estimated using Stokes Law:

$$v_t = \frac{4R_b^2 g\left(\rho_l - \rho_g\right)}{18\mu_l}$$

Equation 4-19

While for larger, oscillating bubbles, Maneri and Mendelson (1968) propose the correlation

$$v_t = \left(\frac{\gamma_{lv} g_c}{R_b \rho_l} + gR_b\right)^{\frac{1}{2}}$$

Equation 4-20

This correlation is not the solution one would obtain assuming potential flow around a hard sphere, since oscillations affect the rise velocity of the bubble.

Using a surface tension of 61 mN/m for a serum-free medium, measured by Michaels et al. (1995b), and the density and viscosity of liquid water at 37°C, Equations 19 and 20 provide estimates for the terminal rise velocity of a bubble in a bioreactor. As can be seen in Figure 4-2, there is a sizable transition region between creeping flow and potential flow conditions. The terminal rise velocity of the bubble increases rapidly in the creeping flow regime, and at bubble radii larger than 0.7 mm, Treybal (1980) suggests applying Equation 4-20. The velocities in the region between the creeping flow regime and Equation 4-20 are estimated by using a linear interpolation. Unfortunately, from an analytical viewpoint, the typical bubble sizes used for sparging are often in the transition region or the region where bubbles oscillate. Nevertheless, one can use the estimated velocities to make predictions about rise-related cell death rates.

Using the direct cell-bubble contact times necessary for attachment, reported by Michaels et al. (1995a), one is able to begin making realistic estimations of bubble rise-related death rates. Michaels et al. (1995a) found that cell attachment to bubbles can occur in as little as 10 ms in a serum-free medium, but cell attachment requires 50 ms or more in a medium with 0.1% w/v Pluronic® F68 and more than 1000 ms for a medium containing 0.1% w/v methyl cellulose. In Figure 4-3, several estimates for rise-related death rate have been made. The cell diameter was assumed to be 15 μm, and three cell-bubble attachment times, 0 ms, 25 ms, and 50 ms, were examined in both creeping and potential flow. To represent a laboratory scale reactor, a reactor volume of 100 mL was chosen, with a reactor radius of 1.5 cm. To represent typical sparging rates reported in the literature where death has been observed, a gas flow rate of 50 mL/min was chosen. Using the

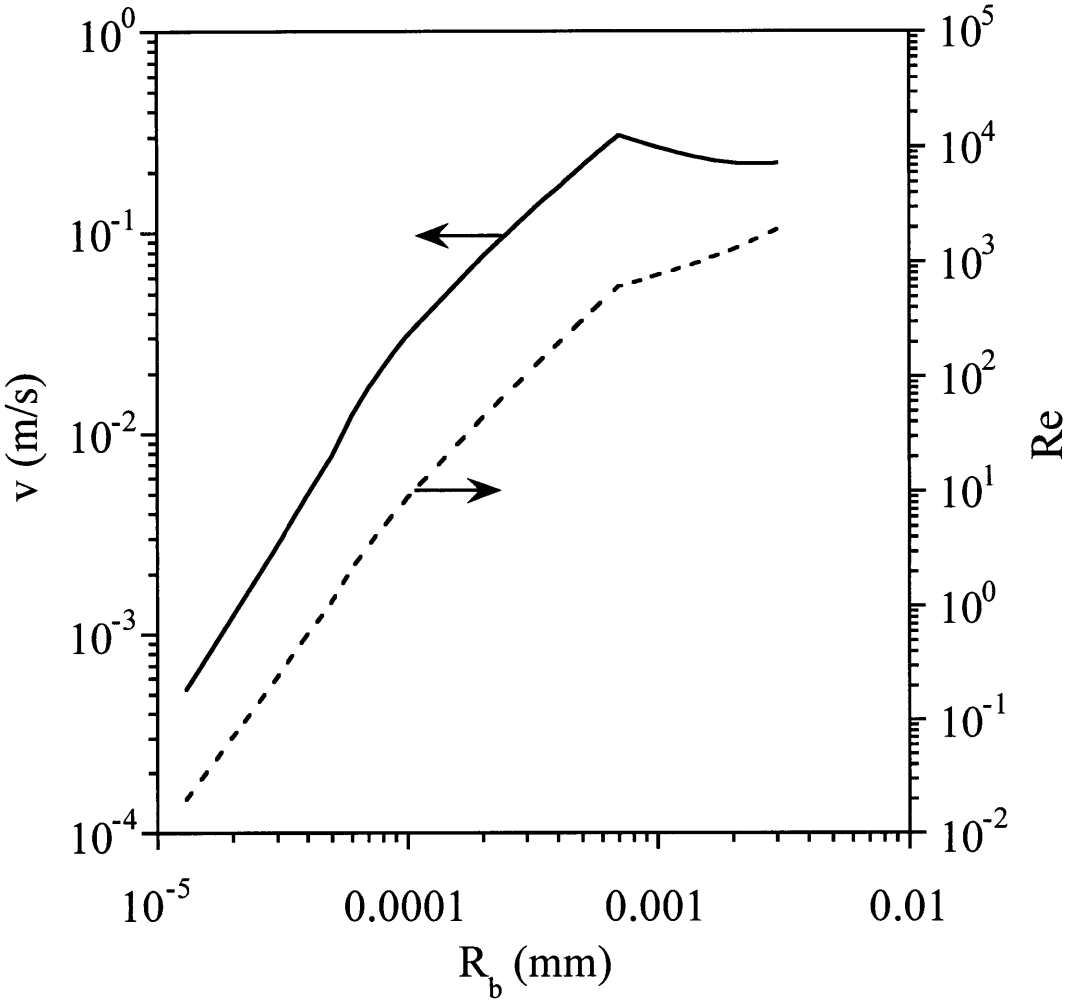

Figure 4-2 Bubble rise velocity (——) and Reynolds number (- - - -) estimated from correlations for the terminal rise velocity of a bubble. The calculations are based on serum free medium at 37°C. For Reynolds numbers below 1, Equation 4-19 is used. Treybal (1980) has suggested that Equation 4-20 (Maneri and Mendelson 1968) be applied for bubbles greater than 0.7 mm in radius. The transition region has been estimated using a linear interpolation.

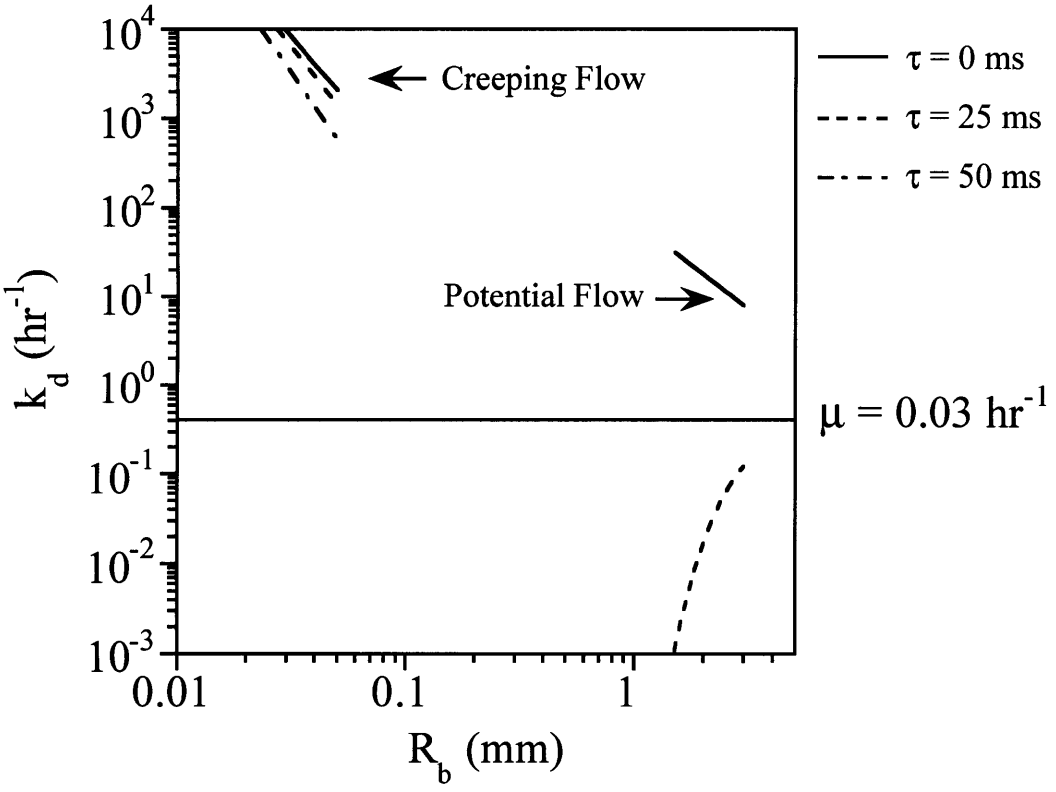

Figure 4-3 The death rates related to rising bubbles have been estimated for a reactor 1.5 cm in radius and 100 mL in volume, with a gas flow rate of 50 mL/min. Three cell-bubble attachment times, τ = 0 ms (——), 25 ms (- - - -), and 50 ms (- · - ·), were used in the calculations. The rise velocities were obtained from Figure 4-2. Equation 4-5 and Equation 4-15 were used to estimate death rates in the creeping flow regime, and Equation 4-5 and Equation 4-17 were used in the potential flow regime.

velocities from Figure 4-2, one can calculate the projected bubble radii from Equation 4-15 and Equation 4-17. The projected radii can then be used to calculate rise-related death rates using Equation 4-5. As can be seen in Figure 4-3, the death rates from bubbles in the creeping flow regime are predicted to be much larger than the typical growth rates for animal and insect cells, even when considering the cell-bubble attachment time of 50 ms. In the potential flow region, the cell death rates are predicted to be quite high for instantaneous cell-bubble attachment, but the death rates decrease dramatically as the cell-bubble attachment time increases. One might use a linear interpolation between the solutions for creeping and potential flow to obtain estimates for the death rates in the transition region, but the actual behavior might reflect a deep well instead. Also, the potential flow solution may not be strictly valid due to bubble oscillations.

Surface active molecules act to stabilize the gas-liquid interface of a bubble and prevent circulation. This makes the bubble behave more like a rigid sphere and keeps the boundary condition at the bubble surface close to a no slip condition. Under these conditions, the flow around the bubble will have a viscous boundary layer and it may be approximated by the creeping flow stream function. Thus, one could argue that since cell-bubble attachment is occurring in systems containing many different surface active molecules, the creeping flow solution for projected radius (Equation 4-15) might be applied to even the larger bubble sizes. In Figure 4-4, the creeping flow solution has been extended over the entire range of bubble sizes. The reactor operation parameters are the same as those for Figure 4-3. For all three attachment times, the predicted death rates remain significant throughout the entire range of bubble sizes. At the larger bubble sizes

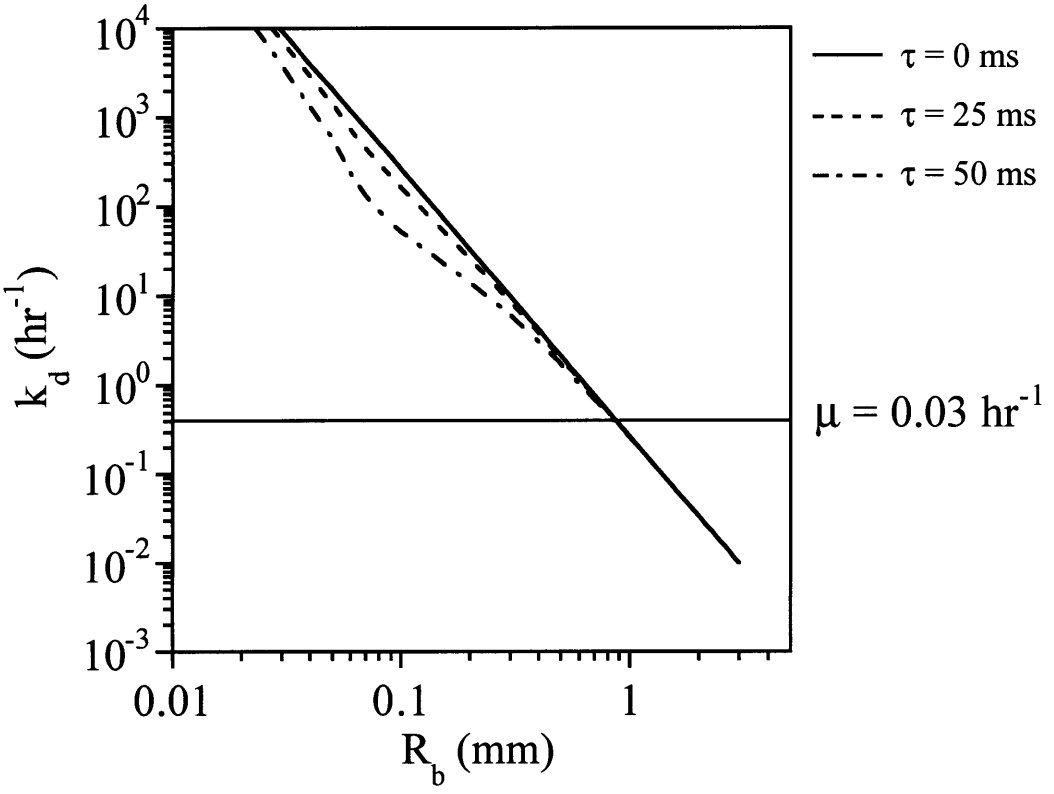

Figure 4-4 Equation 4-15 can also be used to estimate rise-related death rates beyond the creeping flow regime in the same reactor configuration as in Figure 4-3, under the assumption that surface active molecules make the gas-liquid interface more rigid, and thus extend the applicability of the creeping flow solution. Rise velocities were obtained from Figure 4-2. The death rates are shown for three attachment times: τ = 0 ms (——), 25 ms (- - - -), and 50 ms (- · - ·).

typical in bioreactors, the death rates collapse onto the curve for instantaneous cell-bubble attachment. It is not until the cell-bubble attachment time exceeds 500 ms or the bubble radius gets quite small that there is a significant deviation from the instantaneous cell-bubble attachment curve.

4.2.2 Reconciling Literature Observations

On the surface, it seems as if the observations of Tramper et al. (1988a) and (1988b) and Bavarian et al. (1991) are in conflict. Bavarian et al. found that cells attach to rising bubbles, and one would expect that cells attached to a bubble die when the bubble bursts (Cherry and Hulle 1992; Trinh et al. 1994). Yet, the experiments of Tramper et al. suggest that cell attachment to rising bubbles does not contribute to cell death. Tramper et al. (1988a) carried out experiments using bubbles ranging from 0.9-2.6 mm in radius, with insect cells in a medium containing 0.1% w/v methyl cellulose. From the cell-bubble attachment times measured by Michaels et al. (1995a) for Chinese Hamster Ovary cells in a medium containing 0.1% w/v methyl cellulose, it is possible to estimate the rise-related death rates for bubbles ranging from 0.9-2.6 mm in radius. The velocities can be estimated from Figure 4-2, used to evaluate Equation 4-15, and then Equation 4-5 can be used to estimate the rise-related death rates. The experimentally measured death rates were about 0.11 hr^{-1}, while the calculated rise-related death rates were negligible. Thus, one would not expect to measure rise-related cell death under their conditions. However, Bavarian et al. (1991) used 30-55 μm radius bubbles in a medium without methyl cellulose and observed freely suspended cells attaching to rising bubbles. As can be seen in Figure 4-3, one would

predict extensive cell-bubble attachment under those conditions. Thus, these experiments are consistent within the framework of this model.

The experiments of Orton (1992) and Wu and Goosen (1995) showed an increase in cell death rate with a decrease in bubble radius. Based on the experimental conditions of Orton (1992), one can predict rise-related death rates for this system (Figure 4-5). The data were obtained with hybridoma cells in IMDM, containing 5% v/v FBS and antifoam. A 100 mL bubble column, 2.8 cm in diameter, with a single orifice sparger was used. For these calculations, the cell-bubble attachment was assumed to be instantaneous, and the cells were assumed to be 15 μm in diameter. Under these conditions the rise velocity is unimportant, and no velocity assumptions need to be made. Since these data were taken at several different gas flow rates, they were normalized to a gas flow rate of 30 mL/min. Both the model presented by Tramper et al. (1987) and the model presented here are directly proportional to bubble frequency, and the normalization should not cause any artifacts. Assuming no rise-related death at the largest bubble size, one can estimate the basal death rate, which corresponds to the killing volume proposed by Tramper et al. (1987). Equation 4-15 is then evaluated at each bubble radius and inserted into Equation 4-5 to estimate the overall death rate. As can seen in Figure 4-5, the rise-related death rate increases as the bubble radius decreases and may account for the observed experimental behavior. The agreement is not perfect, but this may be a result of the assumptions made for cell size and cell-bubble attachment time.

Similarly, one can analyze the data of Wu and Goosen (1995) (Figure 4-6). These data were obtained at a gas flow rate of 10 mL/min, in a 35 mL bubble column, 2.3 cm in

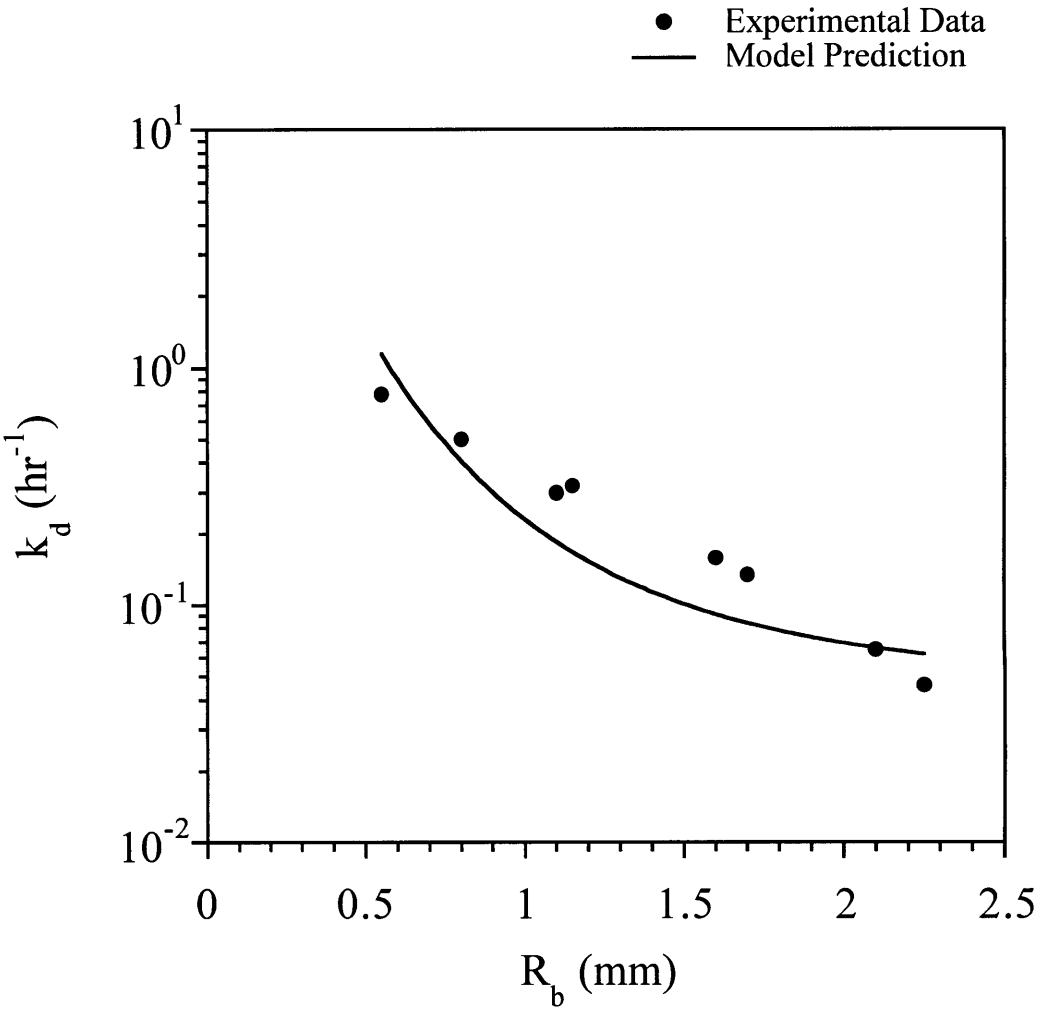

Figure 4-5 Sparging related death rates were measured by Orton (1992) (●) in a 100 mL reactor. The data were obtained at different gas flow rates, but have been normalized to a gas flow rate of 30 mL/min. The estimated sparging related death rates (——), calculated assuming that cell-bubble attachment was instantaneous and the cell diameter was 15 μm, follow the general trend of the data well.

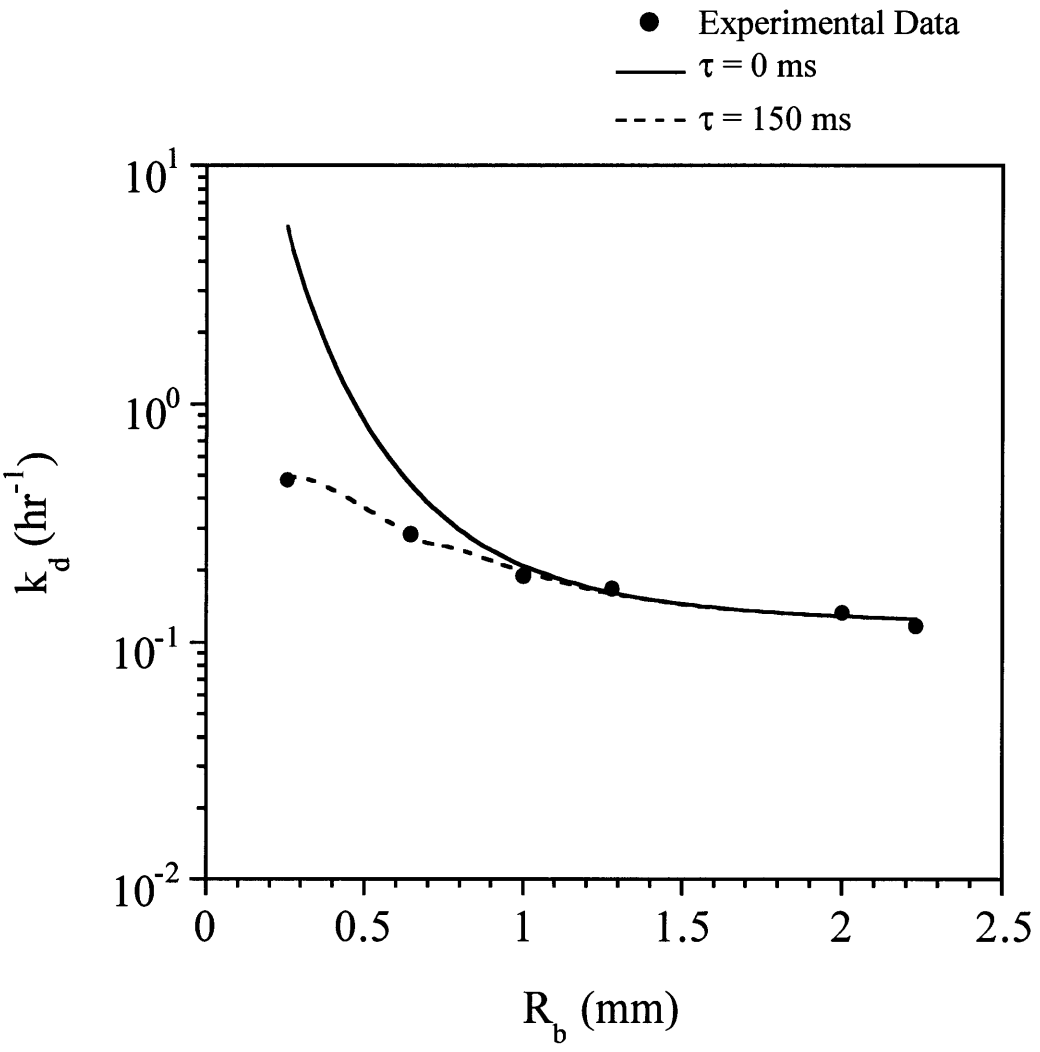

Figure 4-6 The sparging related death rates measured by Wu and Goosen (1995) (●), with a gas flow rate of 10 mL/min in a 35 mL reactor, compare reasonably well with the estimated sparging related death rates (——) obtained by assuming that cell-bubble attachment occurred instantaneously and by assuming that cells were 15 μm in diameter. The agreement breaks down at smaller bubble diameters. When an attachment time of 150 ms is incorporated (- - - -), the agreement improves.

diameter, with a single orifice sparger. Insect cells in IPL-41, containing 5% v/v FBS and antifoam were used in their experiments. For one set of estimates, cell-bubble attachment was again assumed to occur instantaneously, and the cells were assumed to be 15 μm in diameter. The data fit the model reasonably well, except for the smaller bubble radii. The data that do not agree with the model are for bubble radii that are smaller than those tested by Orton (1992).To improve agreement between the model and the data, it is necessary to take the cell-bubble attachment time into account. The bubble rise velocity is estimated using the same procedure that was used to generate Figure 4-2, except that a surface tension of 52 mN/m was used. This was obtained from Michaels et al. (1995b) for a 3% FBS medium and should reasonably reflect the conditions in this system. With the cell-bubble attachment time set at 150 ms, the agreement between the data and the model is very good. This cell-bubble attachment time is reasonable, based on comparisons to data from Michaels et al. (1995a). They found that for a 3% FBS medium, cell attachment begins at 100 ms and does not become significant until about 500 ms. Overall, these experiments are consistent within the modeling framework.

4.2.3 Implications for Industrial Operation

This model is useful for predicting sparging-related cell death rates in scale-up processes for industrial size bioreactors. For instance, consider the growth of insect cells in a medium formulation with 5% FBS, but no other protective additives, in a sparged reactor, with a height to diameter ratio of 3, with 1.5 mm radius bubbles, and with a gas flow rate of 0.01 vvm. Assume that the death rate measured by Wu and Goosen (1995) for the largest bubble did not contain measurable rise-related death. From Equation 4-5

and Equation 4-15, one can estimate the total death rate in the reactor, including rise-related death, at various reactor scales, again assuming instantaneous cell-bubble attachment. Figure 4-7 shows the ratio of the death rate including rise-related death to the death rate excluding rise-related death versus reactor volume. It is clear that at typical laboratory scales, rise-related death makes a small contribution to overall death, yet as reactor size increases, the death rate might be seriously underestimated by neglecting rise-related death.

Similar calculations can be made to assess the effect of additives on cell death rates in industrial bioreactors. We will assume the same conditions as above, except that 0.1% w/v methyl cellulose has been added to the medium. Tramper et al. (1988a) reported cell death measurements for insect cells under these conditions, and based on those experiments, one can assume no significant rise-related death at the laboratory scale. One can again estimate the relative death rates as a function of reactor volume, using Equation 4-5 and Equation 4-15. To make these calculations, Figure 4-2 can be used to estimated bubble rise velocities and the data reported by Michaels et al. (1995a) can be used for cell-bubble attachment time in a 0.1% w/v methyl cellulose medium. Since the cell-bubble attachment time with methyl cellulose is so long, the rise-related contribution to overall death is insignificant, and one would predict no change in death rate with increasing reactor size under the specified scale-up conditions (Figure 4-7).

4.3 Discussion

The application of the model clearly shows that seemingly conflicting experimental results can now be unified. Also, it is clear that protective additives' most

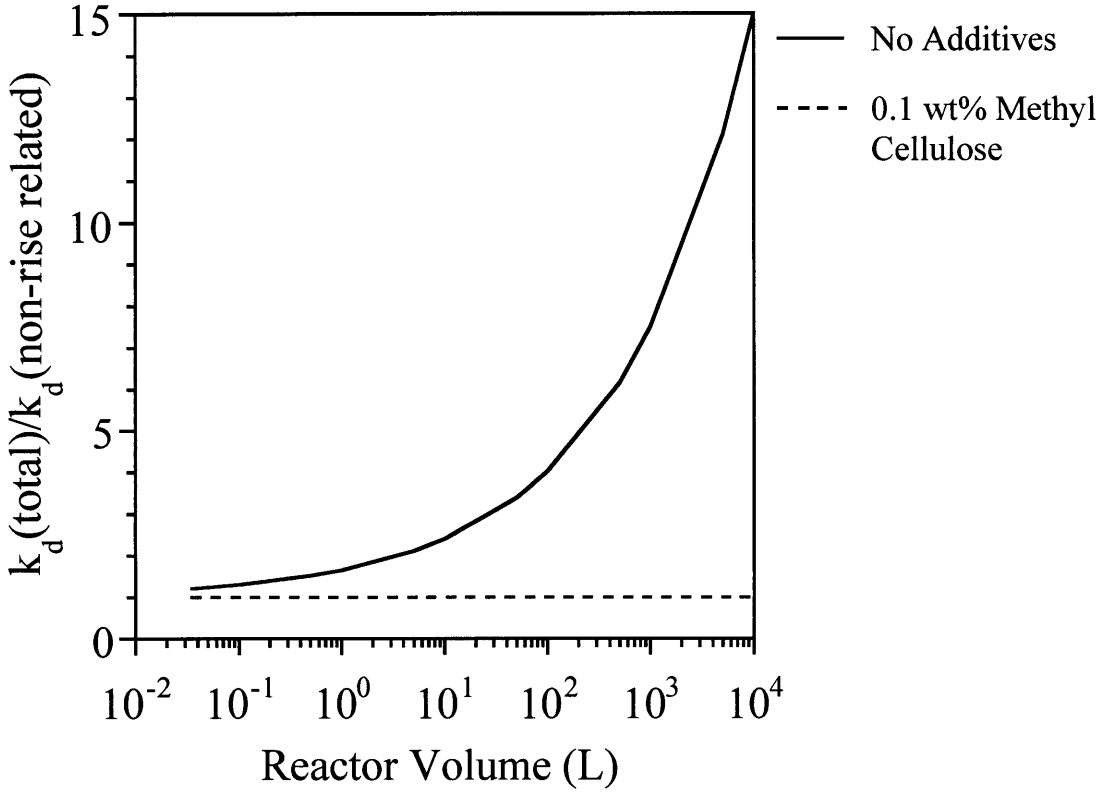

Figure 4-7 Overall death rate varies with reactor size when cell attachment to rising bubbles contributes to cell death. The ratio of death rate including rise-related death to death rate excluding rise-related death represents the ratio by which the death rate will be underestimated by neglecting cell-attachment to rising bubbles. The calculations are based on a bubble radius of 1.5 mm and a gas flow rate of 0.01 vvm. The reactor height to diameter ratio is kept constant at 3. For additive free media, based on the data of Wu and Goosen (1995) and the model, the death rate contributed by cell attachment to rising bubbles is significant and becomes the largest contributor to the death rate at large scale (——). For media with 0.1% w/v methyl cellulose, based on the data of Tramper et al. (1988a), Michaels et al. (1995a), and the model, the death rate from attachment to rising bubbles is insignificant and the death rate should not change noticeably with increasing reactor size (- - - -).

important mode of protection from sparging related death might be hidden in the existing experimental data. From Figure 4-7, one can see that bubble rise-related death might be relatively inconsequential at the laboratory scale, yet at large scales, it becomes the dominant mode of cell death. Thus, as can be seen in Figure 4-7, the major protective mechanism, at a large scale, for additives such as methyl cellulose and Pluronic® F68 may be to prevent cell attachment to rising bubbles. It is also clear from experiments such as those of Jöbses et al. (1991), that other protection mechanisms are at work, such as a reduction in the rise-independent killing volume.

The model suggests that at large scales, when working without protective additives, minimizing sparging related death means minimizing rise-related death by limiting reactor height. This is in direct conflict with the reactor design recommendations of Tramper and Vlak (1988b), who suggest that the optimal large scale reactor design maximizes the height of the reactor. For the cases where additives such as Pluronic® F68 or methyl cellulose are present, the model suggests that rise-related death will be insignificant, and thus the reactor design recommendations of Tramper and Vlak (1988b) are justified. However, the model suggests that for micro-bubbles, with radii of up to 100 μm, death from rising bubbles may again become significant. Thus, the use of very small bubbles might be inadvisable for industrial operation.

5. RESULTS

5.1 Physical Property Measurements

5.1.1 Viscosity

Methyl cellulose is typically used as a viscosity enhancer. The product used in these experiments is rated to result in a viscosity of 15 cP for a 2% w/v solution in water. The average molecular for this grade of methyl cellulose is approximately 14,000 Da. Since the concentrations of methyl cellulose that are typically used for shear protection are much lower than 2% w/v, the effect of methyl cellulose on viscosity was measured. For the serum free medium formulation, including 100 ppm silicone antifoam C and 0.1% w/v methyl cellulose, the viscosity was 0.85 cP at 37°C. When measuring the same medium formulation without the methyl cellulose, the viscosity was found to be 0.75 cP at 37°C. This agrees with the findings of Orton (1992) for IMDM without any additives. Orton (1992) also found that the addition of Pluronic® F68 did not substantially alter the medium viscosity. These data are similar to the viscosity for pure water at 37°C, 0.69 cP. Thus, at these low levels, methyl cellulose and Pluronic® F68 do not significantly increase the medium viscosity, and the medium viscosity is not substantially different from that of water.

5.1.2 Equilibrium Surface Tension for Media

The equilibrium surface tension was measured at 37°C for three different media. For serum free medium with antifoam, the surface tension was 41.8 mN/m. With the addition of 0.1% w/v Pluronic® F68 (Sigma), the surface tension dropped to 35.7 mN/m. When 0.1% w/v methyl cellulose was added to the serum free medium with antifoam

formulation, the surface tension was found to be 38.3 mN/m. The equilibrium surface tensions for all three medium formulations are significantly lower that the surface tensions for either pure water or additive free IMDM.

5.1.3 Surface Excess for Pluronic® F68

Two different sources of Pluronic® F68 were used in the course of these studies. One batch was obtained from Fluka and was several years old. The other batch was obtained from Sigma and used within one year of purchase. For each source of Pluronic® F68, a series of concentrations in aqueous solution were prepared. The surface tension was measured at 35°C for concentrations in the range of 10^{-4} to 3% w/v Pluronic® F68. From a plot of surface tension versus the logarithm of concentration, one can determine the critical micelle concentration and the surface area covered per molecule of surfactant in the sub-micelle concentration range. The surface excess,

$$\Gamma = \frac{-1}{RT}\left(\frac{d\gamma_{lv}}{d(\ln C)}\right)_T$$

Equation 5-1

is defined as a function of the gas constant, R, the absolute temperature, T, and the change in surface tension, $d\gamma_{lv}$, divided by the change in the natural logarithm of concentration, d(ln C), at constant temperature. The surface excess is constant below the critical micelle concentration in the region where a complete monolayer of surfactant is at the interface. The change in surface tension versus natural logarithm of surfactant concentration is linear in this region. The inverse of the surface excess represents the surface coverage per molecule at the interface. This allows for comparison of the surface coverage for different

surfactants. Surfactants of different molecular weights or structures would be expected to behave differently.

In Figure 5-1, the surface tension curve is plotted for the batch of Pluronic® F68 obtained from Fluka. The curve is linear in the region of 10^{-4} to 1% w/v Pluronic® F68. The critical micelle concentration appears to be between 1 and 3% w/v Pluronic® F68, but the data were not extended to high enough concentrations to make a strong assignment of critical micelle concentration. From a regression of the data, the surface area per molecule was determined to be 259 ± 8 $Å^2$/molecule (all variances are standard error unless otherwise noted). Figure 5-2 shows a plot for the batch of Pluronic® F68 obtained from Sigma. In this case, the surface area per molecule was determined to be 225 ± 7 $Å^2$/molecule. For the batch obtained from Sigma, the surface tensions at the same concentrations are slightly higher than the batch obtained from Fluka. It also appears that the critical micelle concentration is greater than 3% w/v Pluronic® F68 in this case. The surface areas per molecule are slightly different from each other. So, there appear to be slight differences in both critical micelle concentration and surface area per molecule for the two batches of Pluronic® F68, but these differences seem relatively small. One would not expect large differences in cell culture performance based on these differences.

5.1.4 Size Distribution for Pluronic® F68

The size distributions for these two batches of Pluronic® F68 were also examined to confirm their similarity. In Figure 5-3, the elution profiles for gel permeation chromatography are plotted for both the batch from Fluka and from Sigma. The batches appear to have nearly monodisperse distributions and the same average molecular weight.

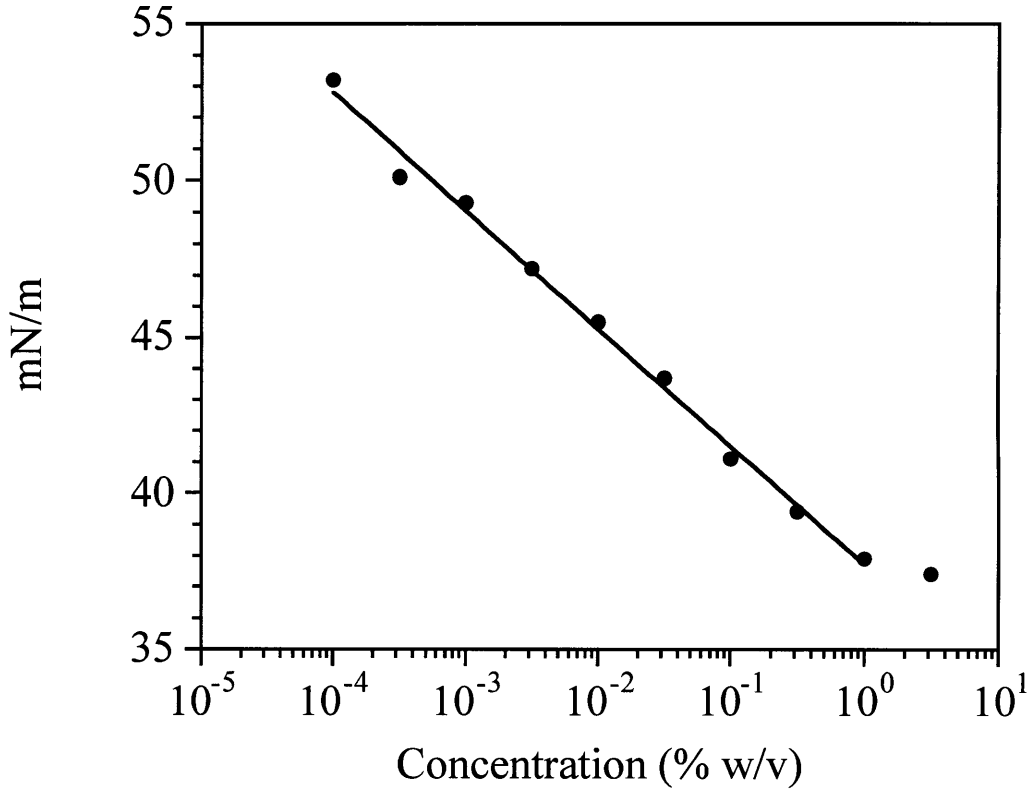

Figure 5-1 Surface tension as a function of Pluronic® F68 concentration for batch supplied by Fluka.

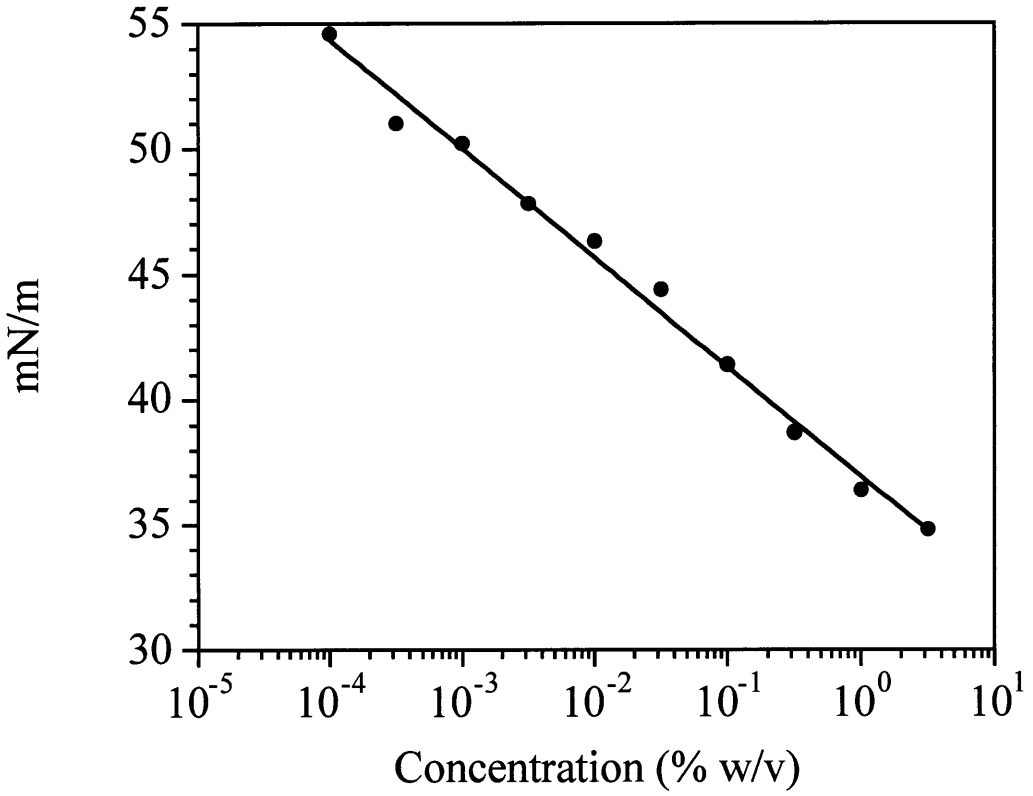

Figure 5-2 Surface tension as a function of Pluronic® F68 concentration for batch supplied by Sigma.

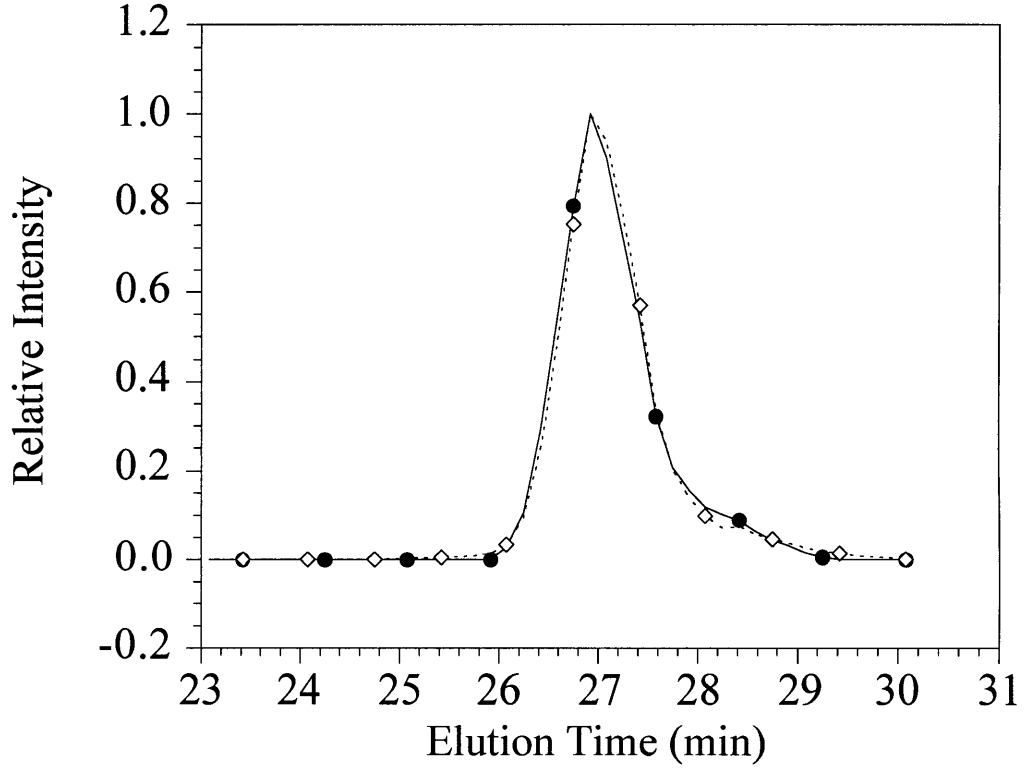

Figure 5-3 Elution profiles for two batches of Pluronic® F68. One curve represents a batch obtained from Fluka (—●—). The other curves represents a batch obtained from Sigma (····◇···).

For the batch from Fluka, the weight average molecular weight was determined to be 7178 Da with a polydispersity index of 1.08. For the batch from Sigma, the weight average molecular weight was found to be 7165 Da, and the corresponding polydispersity index was 1.10. By this standard, the two batches of Pluronic® F68 appear to be nearly identical.

It has been noted in the literature (Yu et al. 1997) that different manufacturers produce Pluronic® F88, a polymer related to Pluronic® F68, with differing physical properties. Yu et al. (1997) found that for two different manufacturers of Pluronic® F88, the chemical composition of the polymers was essentially identical as measured by NMR, but the size distributions by gel permeation chromatography and the critical micelle temperatures differed significantly. Thus, ostensibly identical compounds were found to exhibit different physical properties, and one would expect that large physical differences might have some effect on cell culture performance. However, large physical differences were not found for the two batches of Pluronic® F68 used in this work.

5.1.5 Rise Velocity

Rise velocity was measured in two media for two bubble sizes each. For serum free medium with antifoam, the rise velocity for a 1.60 ± 0.05 mm bubble was 0.22 ± 0.03 m/s at 37°C. Treybal (1980) suggests applying Equation 4-20 (Maneri and Mendelson 1968) to predict rise velocity for bubbles of this size. The surface tension for this system was 41.8 mN/m at 37°C, and the liquid density was assumed to be the same as water. The predicted rise velocity is 0.20 m/s, and it is in reasonable agreement with the experimental

result. For a bubble radius of 3.09 ± 0.16 mm, the rise velocity was 0.23 ± 0.02 m/s. This compares well to the predicted value of 0.21 m/s.

Rise velocity was also measured for serum free medium with antifoam and 0.1% w/v Pluronic® F68 (Fluka). For a bubble radius of 1.40 ± 0.05 mm, the rise velocity was 0.24 ± 0.03 m/s at 37°C. Based on the surface tension for this system, measured at 37°C, 35.7 mN/m, Equation 4-20 predicts a terminal rise velocity of 0.20 m/s. This is in reasonable agreement with the measurement. For the larger radius bubble, 2.31 ± 0.03 mm, the rise velocity was 0.26 ± 0.02 m/s. Equation 4-20 predicts a rise velocity of 0.20 m/s for this case as well. Equation 4-20 seems to slightly under predict the actual rise velocity. This could be because the bubbles have not reached their true terminal rise velocity or the fact that they do not reach a surface tension equilibrium. Jordan et al. (1994) measured the instantaneous rise velocity for 0.92 ± 0.01 mm radius bubbles at several heights in a bubble column. They saw that for low concentrations of Pluronic® F68 in water (4 mg/L or less), it can take tens of centimeters for the bubble to reach a steady rise velocity. The bubbles tended to slow down as they accumulated more surfactant on their interfaces. For concentrations approaching those in my experiments, the bubbles seemed to reach the terminal rise velocity much more quickly. Assuming similar equilibrium surface tensions, Equation 4-20 predicts a rise velocity of 0.22 m/s for their system, compared to the actual velocity of 0.16 m/s. So, for their system Equation 4-20 slightly over predicts the rise velocity. Although the agreement is not perfect, the expression proposed by Maneri and Mendelson (1968) seems to reasonably fit the data

for both media tested here and should be applicable to systems with other additives as well.

5.2 Variation of Culture Conditions

5.2.1 Comparison of Pre-sparging Growth Conditions

Cells grown under two sets of conditions were compared for sparging related death under identical sparging conditions. All experiments were performed at a 100 mL culture volume in a 1.3 cm radius reactor, operating at 37°C. The gas flow rate was 43 ± 2 mL/min, resulting in 1.60 ± 0.05 mm bubbles. Prior to experiments, all cells were centrifuged, rinsed in phosphate buffered saline, centrifuged again, and suspended in serum free medium with antifoam. The suspension was then used in the sparging experiments. One group of cells was grown in serum free medium supplemented with 5% v/v fetal bovine serum (FBS). The other group of cells was grown in serum free medium alone. Each bar represents the average of three to four independent experiments. As can be seen in Figure 5-4, the two growth conditions did not differ significantly in death rates when evaluated using a two sample t test that assumes equal variances (t statistic = 0.31, $p = 0.38$). If FBS were having a long acting metabolic effect on the cells, one would expect growth in this medium to produce stronger cells. Since the sparging experiments were approximately two hours in duration, whatever protective effect FBS has on the cells themselves must dissipate rapidly. FBS does have a protective effect on cells, however. When cells were grown in either the serum free medium or with FBS, but sparged in serum free medium with antifoam and 5% v/v FBS, they died, on average, at a rate of 0.58 ± 0.10 hr^{-1} compared to an average rate of 1.07 ± 0.06 hr^{-1} for cells that were sparged in

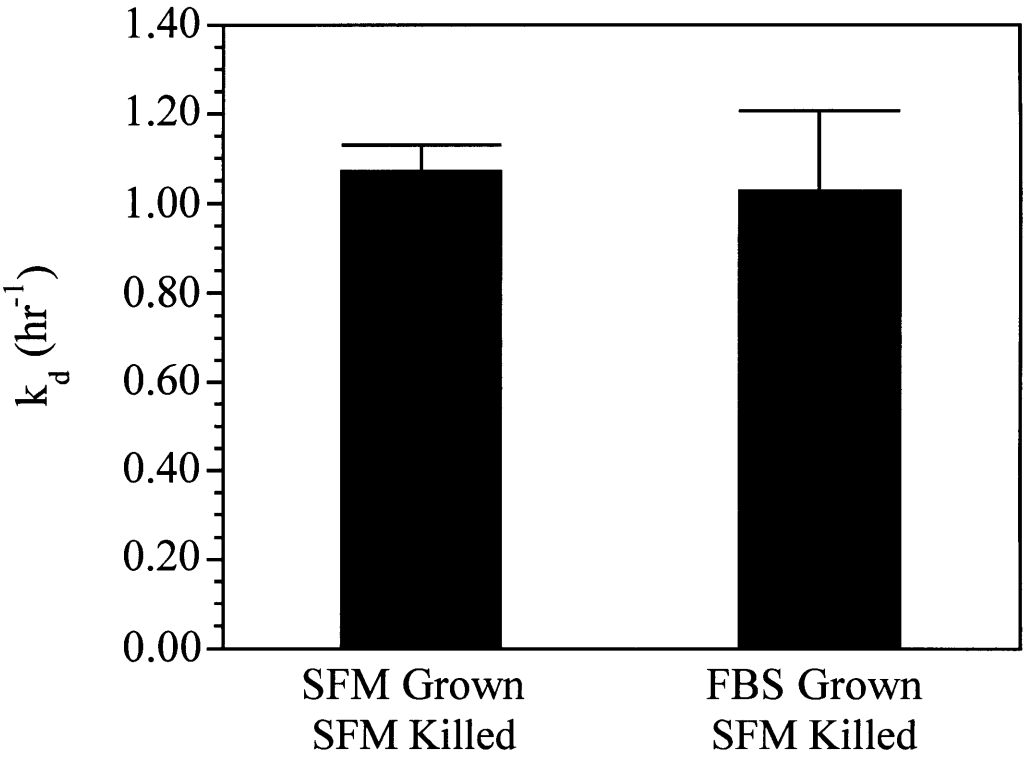

Figure 5-4 Comparisons of death rates for cells grown at two different conditions, but sparged under identical conditions. One group of cells were grown in serum free medium (SFM), separated, and suspended in serum free medium with antifoam for sparging experiments. The other group of cells were grown in the serum free medium supplemented with 5% v/v fetal bovine serum (FBS), separated, and suspended in serum free medium with antifoam for sparging experiments. Each bar represents the average of three to four independent experiments at 37°C. The error bars are the standard error. The difference between the two data sets is not statistically significant (t statistic = 0.31, p = 0.38).

serum free medium with antifoam. These data suggest that the role of serum in protection against sparging damage is fast acting, and probably related to effects at the gas-liquid interface.

5.2.2 Effect of Temperature on Sparging Death

For each of the three medium compositions tested, sparging death rate measurements were made at two temperatures, 24°C and 37°C. The 1.3 cm radius reactor was operated at a gas flow rate of 43 ± 2 mL/min and a volume of 100 mL. The 24 gauge needle was used as the sparger. Figure 5-5 shows the average of three independent experiments for serum free medium with antifoam. The bubbles in this case were 1.60 ± 0.05 mm. The death rate at 37°C is 3.4 times higher than the death rate at 24°C. The difference is statistically significant at the 95% confidence level (t statistic = 14.4, p = 6.7 x 10^{-5}). The results for 1.40 ± 0.05 mm bubbles in serum free medium with antifoam and 0.1% w/v Pluronic® F68 (Sigma) are shown in Figure 5-6. The data each represent the average of two independent experiments. Again, the death rate at 37°C is higher than the death rate at 24°C. This time the difference is 3.2 fold, which is statistically significant at the 95% confidence level (t statistic = 10.3, p = 0.005). Finally, the results for 1.40 ± 0.05 mm bubbles in serum free medium with antifoam and 0.1% w/v methyl cellulose are presented in Figure 5-7. Each bar represents the average of two independent experiments. The data shows the same trend with death rate, a 3.5 fold higher death rate for 37°C than for 24°C. This difference is statistically significant as well (t statistic = 19.1, p 0.001). These data show that a decrease in temperature can have a significant effect on sparging related death. The temperature effect is not specific to any type of protectant, however.

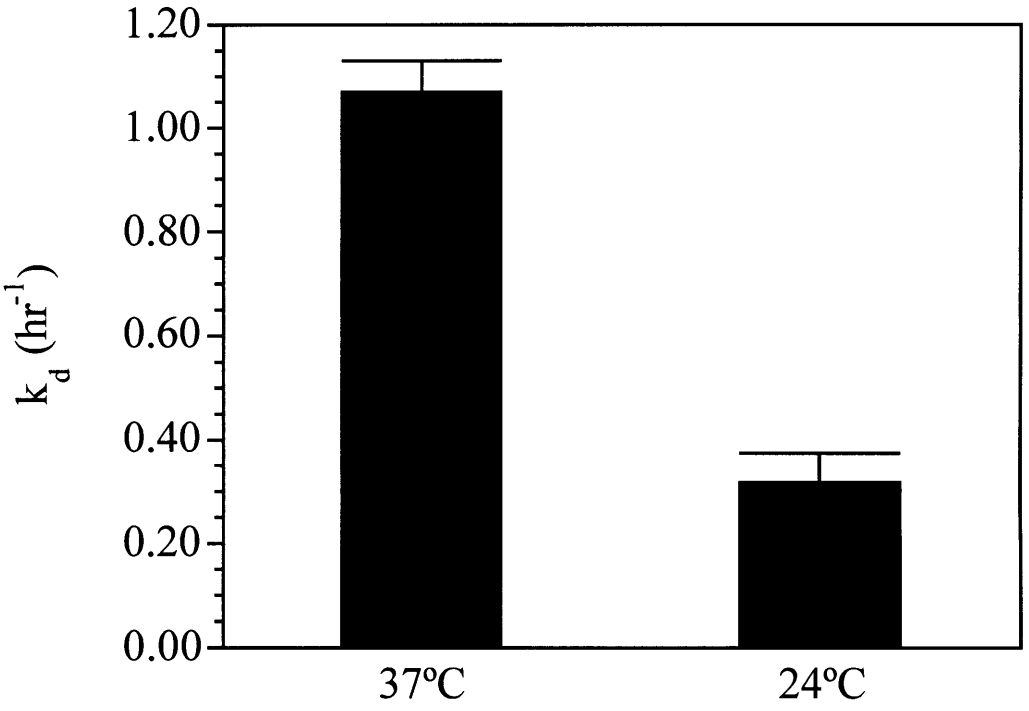

Figure 5-5 Comparison of death rate for two temperatures in serum free medium with antifoam. Data are for 1.60 ± 0.05 mm radius bubbles, and the error bars represent the standard error for three independent measurements. The higher temperature has a 3.4 fold higher death rate, which is significant at the 95% confidence level (t statistic = 14.4, p = 6.7×10^{-5}).

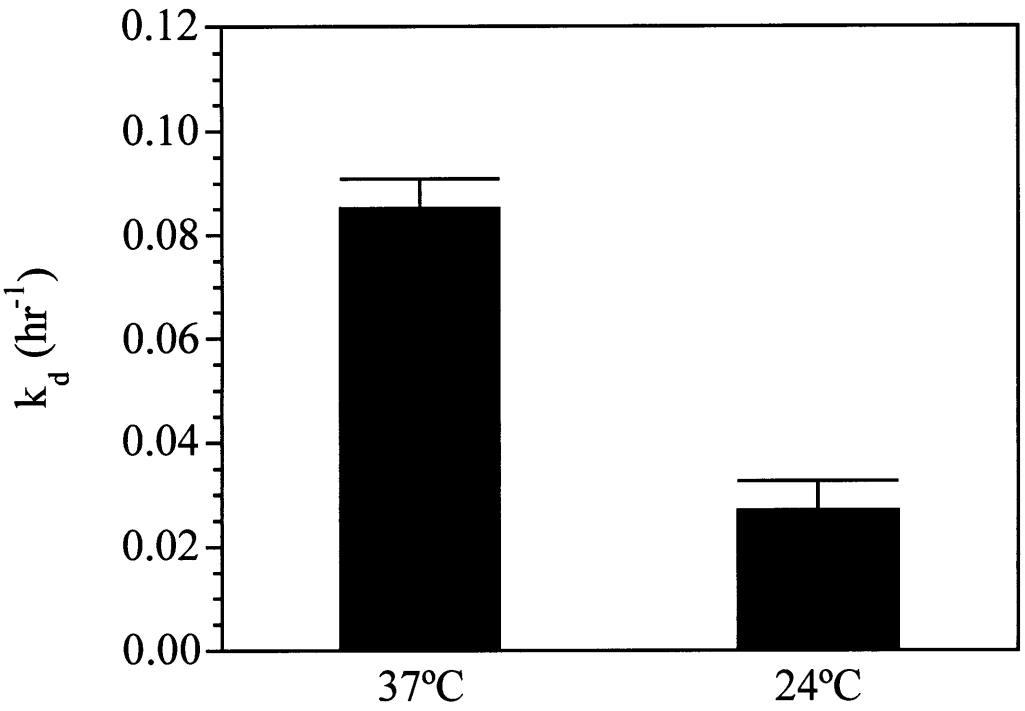

Figure 5-6 Comparison of death rates for two temperatures in serum free medium with antifoam and 0.1% w/v Pluronic® F68 (Fluka). Data are for 1.40 ± 0.05 mm radius bubbles, and the error bars represent the standard error for two independent measurements. The higher temperature has a 3.2 fold higher death rate, which is significant at the 95% confidence level (t statistic = 10.3, p = 0.005).

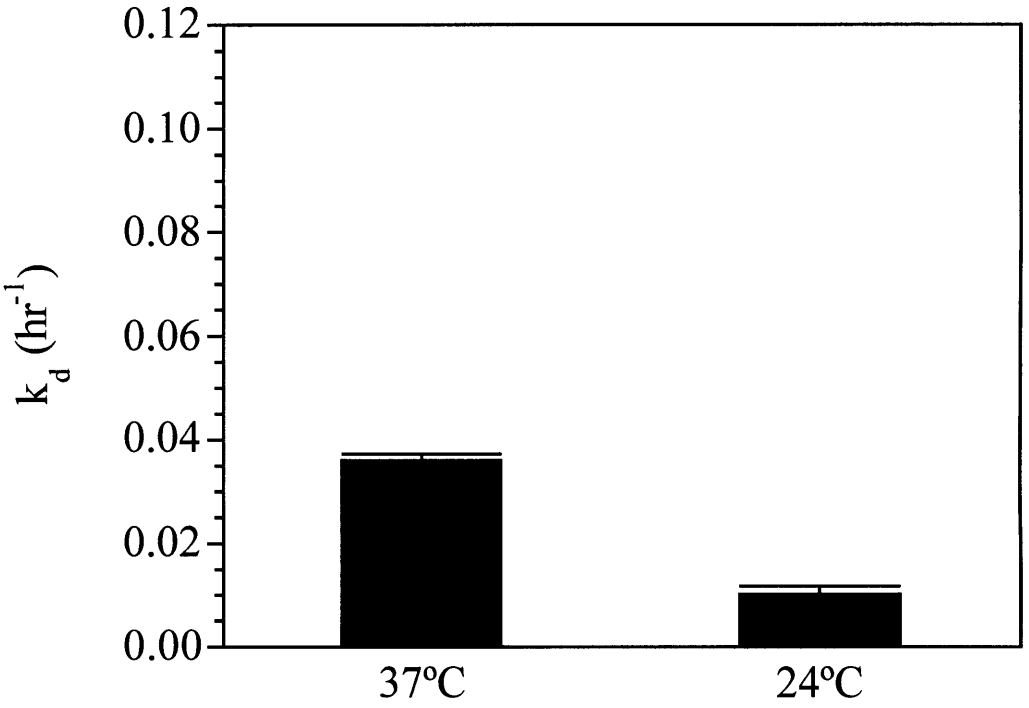

Figure 5-7 Comparison of death rates for two temperatures in serum free medium with antifoam and 0.1% w/v methyl cellulose. Data are for 1.40 ± 0.05 mm radius bubbles, and the error bars represent the standard error for two independent measurements. The higher temperature has a 3.5 fold higher death rate, which is significant at the 95% confidence level (t statistic = 19.1, p = 0.001).

The relative decrease in death rate for all three systems is similar. The difference does not reflect errors related to cell growth rate, as appropriate controls were performed. The reduction in sparging death may be due to an increase in cell strength. A temperature reduction decreases the plasma membrane fluidity of the cells, and this may result in a more shear resistant cell membrane. Ramirez and Mutharasan (Ramirez and Mutharasan 1990; Ramirez and Mutharasan 1992) observed such a plasma membrane fluidity decrease for both serum and Pluronic® F68 addition. This effect does not account for all of the protection afforded by these additives, but the experiments here suggest that it perhaps plays some role.

5.2.3 Comparison of Death for Two Pluronic® F68 Batches

The two batches of Pluronic® F68, one from Fluka and one from Sigma, were tested to determine the effect of Pluronic® F68 variability on protection. The 1.3 cm radius reactor was operated at 24°C with a gas flow rate of 43 ± 2 mL/min for both batches. The 24 gauge needle was used as the sparger and produced bubbles 1.40 ± 0.05 mm in radius. The medium consisted of serum free medium with antifoam and 0.1% w/v Pluronic® F68, supplied by either Fluka or Sigma. The reactors were operated at different reactor volumes, however. Thus, the death rates are normalized by dividing by the volumetric gas flow rate. This should not introduce any artifacts, as other experiments show that there is no height related effect for this system. Figure 5-8 shows the average of two independent experiments for each Pluronic® F68 source. The Pluronic® F68 supplied by Fluka exhibits a statistically significant increase in death rate relative to the Pluronic® F68 supplied by Sigma (t statistic = 3.79, p = 0.03). The surface tension data presented

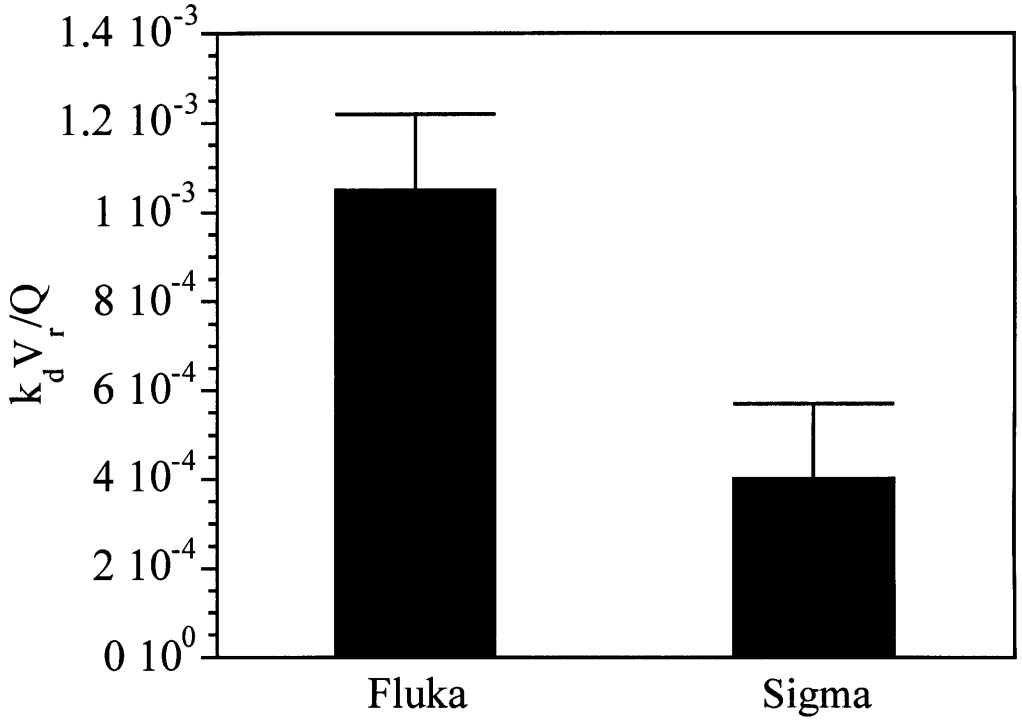

Figure 5-8 Comparison of death rates for two different sources of Pluronic® F68 at 24°C. The reactors were operated using serum free medium with antifoam and 0.1% w/v Pluronic® F68. At as gas flow rate of 43 ± 2 mL/min the bubble radius was 1.40 ± 0.05 mm. The reactor volumes were different, so the death rates are normalized on a volumetric gas flow basis. The error bars represent the standard error of two independent measurements. The death rate for the Pluronic® F68 supplied by Fluka is 2.6 fold higher than the death rate for the Pluronic® F68 supplied by Sigma. The difference is statistically significant at the 95% confidence level (t statistic = 3.79, p = 0.03).

previously only shows a slight difference between the two sources of Pluronic® F68, and the size distribution data shows no measurable difference. It is clear, however, that there is a significant difference in protection against sparging damage. Thus, is seems reasonable to suggest testing lots of Pluronic® F68 for protection against sparging damage before use in industrial bioreactors. The simple analytical tests do not provide a true guide to protective performance.

5.3 Variation of Reactor Height

5.3.1 Serum Free Medium with Antifoam

These experiments compare cell death rates measured in reactors operated at the same volume, gas flow rate, and bubble frequency. The tall reactor was 0.64 cm in radius and 142 cm in culture height. The short reactor was 1.3 cm in radius and 34 cm in culture height. For the experiments reported in Figure 5-9, the reactors were operated at a gas flow rate of 43 ± 2 mL/min with a bubble radius of 1.60 ± 0.05 mm. The average death rate for three independent experiments in the tall reactor was 0.49 ± 0.06 hr^{-1} while the average death rate for three independent experiments in the short reactor was 0.32 ± 0.06 hr^{-1}. The difference in the death rates is statistically significant at the 95% confidence level, (t statistic = 3.78, p = 0.01). From the difference in the death rates, one can solve for the projected radius using Equation 4-5. The projected radius is 7.5 ± 2.0 μm (S.E. from propagated measurement error). One can also determine the rise-independent killing volume from this data, and it is found to be $3.1 \times 10^{-4} \pm 0.4 \times 10^{-4}$ mL (propagated S.E.).

Using rise velocity, cell radius, bubble radius, and estimates of cell-bubble attachment time based on the measurements of Michaels et al. (1995a), one can calculate a

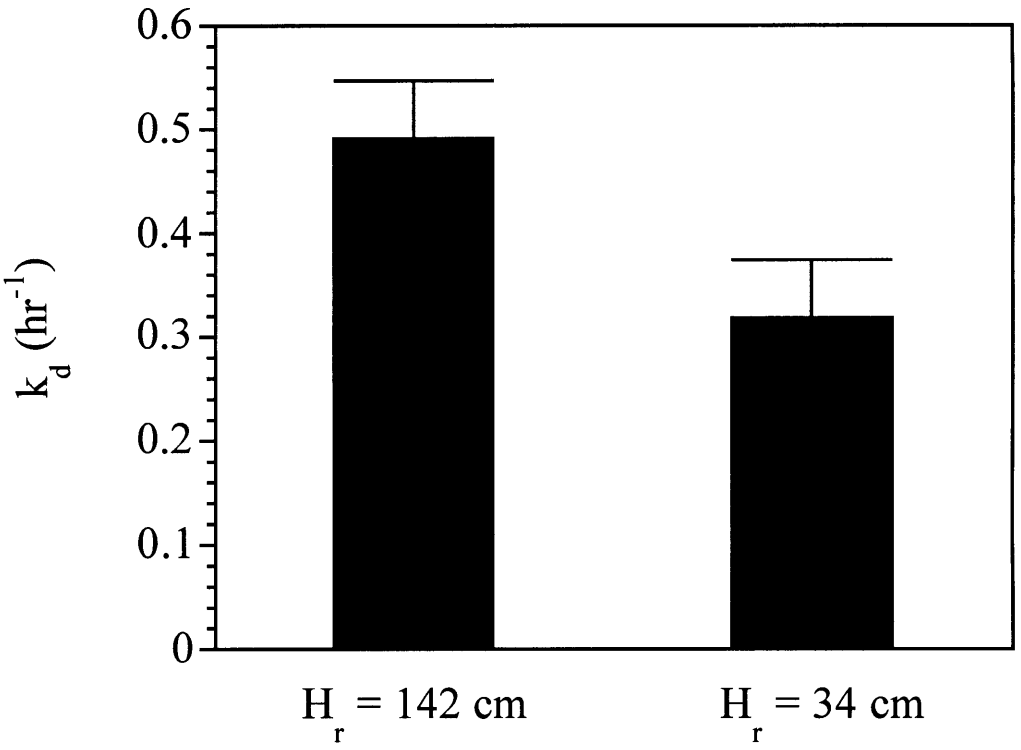

Figure 5-9 Comparison of death rates for tall and short reactors with serum free medium and antifoam at 24°C. The data represent the average of three independent reactor runs for each reactor height. Reactor volume was 180 ± 1 mL, gas flow rate was 43 ± 2 mL/min, and bubble radius was 1.60 ± 0.05 mm. The error bars represent the standard error. The difference in death rates between the two reactors is statistically significant at the 95% confidence level (t statistic = 3.78, p = 0.01). The projected radius based on these data is 7.5 ± 2 μm, compared to a projected radius of 8.0 ± 0.2 μm predicted by the model.

predicted projected radius. Rise velocity for a 1.6 mm bubble in serum free medium with antifoam was 0.22 ± 0.03 m/s at 37°C. One would not expect a significant change in rise velocity upon reducing the temperature to 24°C, so this data was used in the calculations. In addition, the projected radius is not very sensitive to small changes in rise velocity for this attachment time. The cell radius was measured to be 6.5 ± 0.5 μm. Using these data and an attachment time of 50 ms, from Michaels et al. (1995a) in serum free medium, the projected radius predicted by Equation 4-15 is 8.0 ± 0.2 μm (propagated S.E.). This agrees well with the experimentally determined projected radius.

5.3.2 Serum Free Medium with Antifoam and Pluronic® F68

In Figure 5-10, the death rates for tall and short reactors are compared for serum free medium with antifoam and 0.1% w/v Pluronic® F68 (Sigma). The bubble radius was 1.40 ± 0.05 mm. The other operating conditions are as above. The difference in death rates between the tall and short reactors is small, and each bar represents the average of two independent experiments. The difference is not statistically significant at the 95% confidence level (t statistic = 1.53, p = 0.13). This result is consistent with no significant cell attachment to rising bubbles. Bubble rise velocity for this system was 0.24 ± 0.03 m/s at 37°C. Again, since the attachment sensitivity to rise velocity is small and velocity would not be expected to change significantly upon reducing the temperature to 24°C, this velocity was used in the calculations. Using data for Pluronic® F68 from Michaels et al. (1995a), Equation 4-15 predicts that the projected radius of the bubble is negligible. The rise-independent killing volume thus accounts for all the death observed in this case. The killing volume was found to be $4.5 \times 10^{-6} \pm 0.2 \times 10^{-6}$ mL (propagated S.E.), indicating

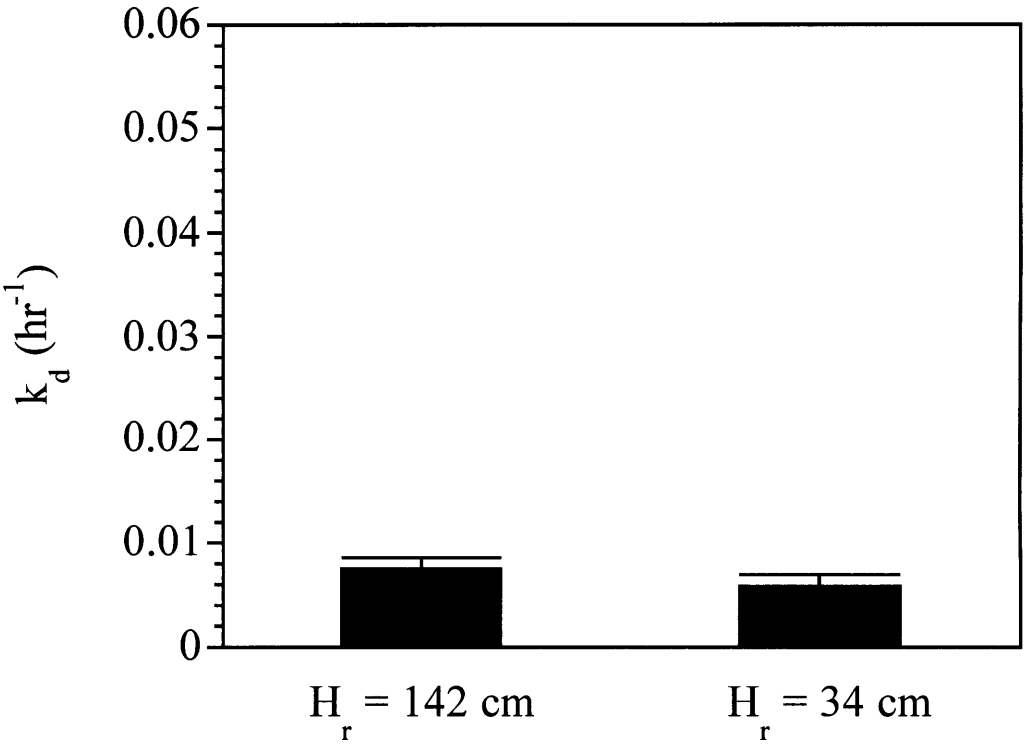

Figure 5-10 Comparison of death rates for short and tall reactors with serum free medium, antifoam, and 0.1% w/v Pluronic® F68 at 24°C. The data represent the average of two independent reactor runs for each reactor size. Reactor volume was 180 ± 1 mL, gas flow rate was 43 ± 2 mL/min, and bubble radius was 1.40 ± 0.05 mm. The error bars represent the standard error. The difference between death rates is not statistically significant at the 95% confidence level (t statistic = 1.53, p = 0.13).

that Pluronic® F68 protects by both reducing the rise-independent killing volume and by preventing rise-related death.

5.3.3 Serum Free Medium with Antifoam and Methyl Cellulose

Figure 5-11 compares the death rates in short and tall reactors for serum free medium with antifoam and 0.1% w/v methyl cellulose. Each bar represents the average of two independent experiments. In this case, the bubble radius was also 1.40 ± 0.05 mm. There is no significant difference between the death rates (t statistic = 0.35, p = 0.38), consistent with no cell attachment to rising bubbles. Michaels et al. (1995a) found that significant cell-bubble attachment takes at least 10 000 ms for a medium with methyl cellulose. This attachment time is longer than the residence time of the bubble in the reactor. Using the surface tension at 37°C, 38.3 mN/m, and the estimated rise velocity, Equation 4-15 predicts a negligible projected radius for the bubble. The rise-independent killing volume in this case is $9.0 \times 10^{-6} \pm 0.5 \times 10^{-6}$ mL (propagated S.E.). The protection mechanism for methyl cellulose is also consistent with two modes of action, reduction in rise-independent killing volume and prevention of rise-related death.

5.4 Variation of Reactor Volume

5.4.1 Serum Free Medium with Antifoam

For all the experiments reported below, a 1.3 cm radius reactor was operated at 37°C. In Figure 5-12, the death rates are plotted versus reciprocal reactor volumes for serum free medium with antifoam, a system with a bubble radius of 1.60 ± 0.05 mm. The gas flow rate was controlled at 43 ± 2 mL/min with a 24 gauge needle as the sparger. This is the same general experimental approach employed by Tramper et al. (1987) and

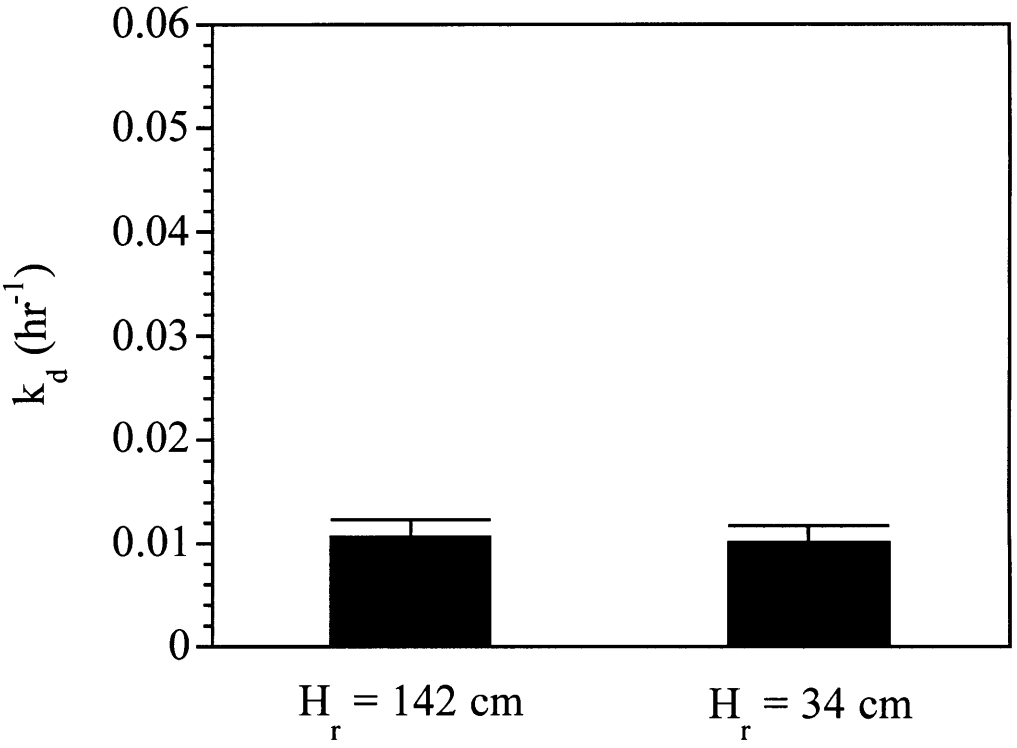

Figure 5-11 Comparison of death rates for short and tall reactors with serum free medium, antifoam, and 0.1% w/v methyl cellulose at 24°C. The data represent the average of two independent reactor runs for each reactor size. Reactor volume was 180 ± 1 mL, gas flow rate was 43 ± 2 mL/min, and bubble radius was 1.40 ± 0.05 mm. The error bars represent the standard error. As expected, the difference between death rates is not statistically significant at the 95% confidence level (t statistic = 0.35, p = 0.38).

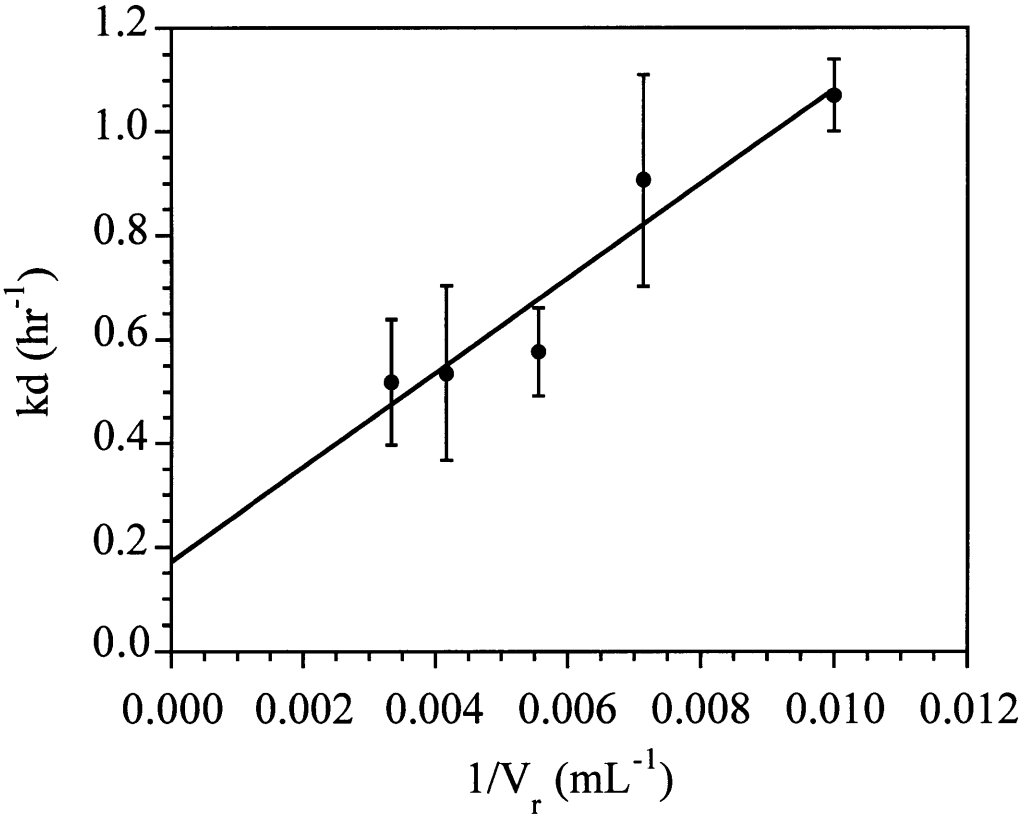

Figure 5-12 Death rate versus inverse reactor volume for serum free medium with antifoam at 37°C. Gas flow rate was 43 ± 2 mL/min, and bubble radius was 1.60 ± 0.05 mm. The error bars represent the standard error of three independent measurements. The slope of the graph represents the killing volume proposed by Tramper et al. (1987) multiplied by bubble frequency. The projected radius of the bubble may be calculated from the y-intercept of the graph, and it is 14 ± 4 μm. This value compares well to the model prediction of 8.0 ± 0.2 μm. However, due to the small contribution of rise-related death to overall death at this reactor scale and experimental variability, the y-intercept is not statistically significant at the 95% confidence level (t statistic = 1.71, p = 0.18).

Jöbses et al. (1991). Each data point represents the average of three independent experiments. Death rates were much greater than the typical growth rates for these cells, so no control cultures were employed. The data are fit using a linear regression. As can be seen from Equation 4-5, when death rate is plotted versus inverse reactor volume, the slope corresponds to the killing volume of Tramper et al. (1987) times the bubble frequency. The y-intercept of the graph corresponds to the bubble frequency times the square of the projected radius divided by the square of the reactor radius. Thus, a positive y-intercept is consistent with death resulting from cell attachment to rising bubbles. The rise-independent killing volume calculated from this data is $6.5 \times 10^{-4} \pm 1.1 \times 10^{-4}$ mL (propagated S.E.). The projected radius determined from this data is 14 ± 4 μm (propagated S.E.). This compares well with the predicted projected radius of 8.0 ± 0.2 μm (propagated S.E.) discussed previously. However, this type of experiment is somewhat more sensitive to experimental variability in death rate, since at these reactor heights, the rise-related death rate is small compared to the rise-independent death rate. The y-intercept does not meet the 95% confidence level for statistical significance (t statistic = 1.71, p = 0.18). The data are consistent with the experiments comparing death rates in reactors of two different heights and are also consistent with the model predictions.

The serum free medium with antifoam medium was also tested at a slightly larger bubble size. Using the same gas flow rate as above, but a 16 gauge needle as the sparger, a bubble radius of 1.78 ± 0.06 mm was achieved. Each data point in Figure 5-13 consists of the average of two or three independent experiments. The y-intercept for this data is

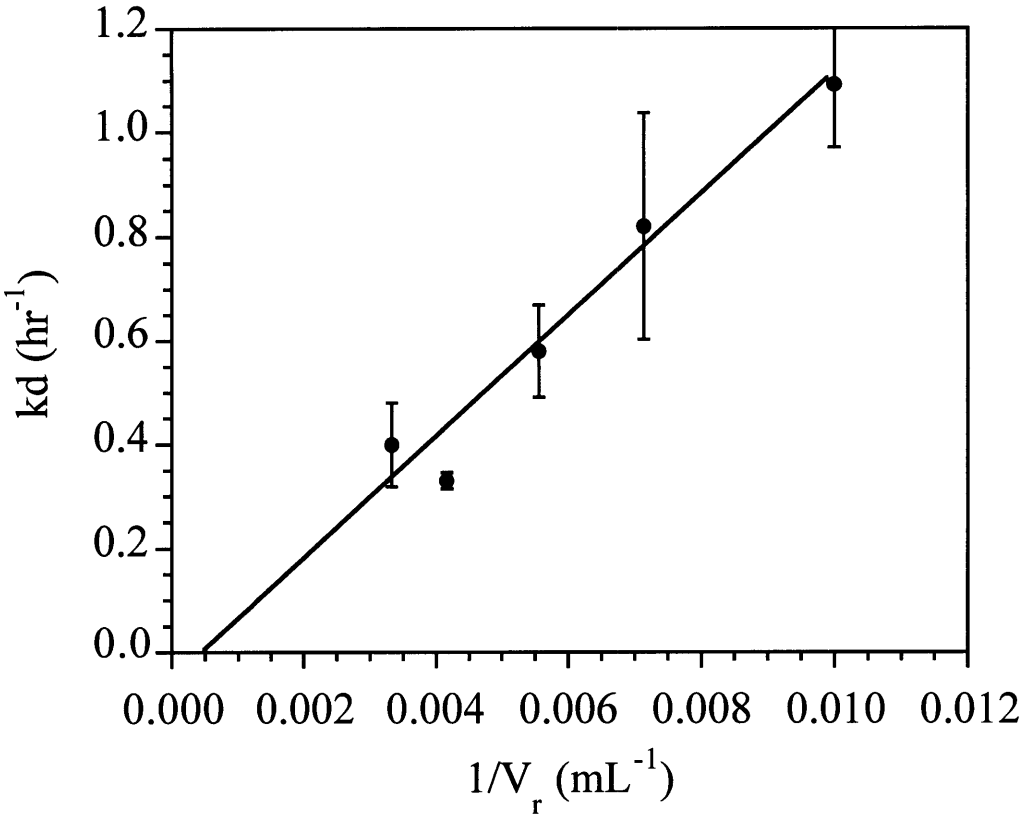

Figure 5-13 Death rate versus inverse reactor volume for serum free medium with antifoam at 37°C. Gas flow rate was 43 ± 2 mL/min, and bubble radius was 1.78 ± 0.06 mm. The error bars represent the standard error of two to three independent experiments. The slope of the graph represents the rise-independent killing volume multiplied by bubble frequency. The y-intercept of this curve is close to zero, indicating a negligible projected radius, compared to the model prediction of 8.0 ± 0.2 μm. However, the predicted value for y-intercept lies within the standard error for the value.

approximately zero, and thus this data suggests no projected radius for these experimental conditions. The model also predicts a projected radius of 8.0 ± 0.2 μm (propagated S.E.) for this data. This value lies within the standard error of the y-intercept, and this set of experiments demonstrates some of the problems with the previous approaches in the literature that discount rise-related death based on small scale reactors. The effect, which may become significant at large scales, is lost in the experimental scatter for typical lab scale reactors. The rise-independent killing volume calculated for this case is $11 \times 10^{-4} \pm 2 \times 10^{-4}$ mL (propagated S.E.).

5.4.2 Serum Free Medium with Antifoam and Pluronic® F68

Sparging related death as a function of reactor volume was also measured for serum free medium with antifoam and 0.1% w/v Pluronic® F68 (Fluka). Operating at a gas flow rate of 43 ± 2 mL/min, using a 24 gauge needle as a sparger, a bubble radius of 1.40 ± 0.05 mm was achieved. In Figure 5-14, two or three independent experiments were averaged for each data point. The y-intercept is positive, indicating rise-related death. The projected radius calculated from this data is 2.0 ± 1.2 μm (propagated S.E.), but the intercept is not statistically significant at the 95% confidence level (t statistic = 0.84, p = 0.46). The rise-independent death gives a killing volume of $3.7 \times 10^{-5} \pm 0.6 \times 10^{-5}$ mL (propagated S.E.). For a 16 gauge needle sparger, with a gas flow rate of 57 ± 2 mL/min, the bubble radius was 2.31 ± 0.03 mm. Each data point in Figure 5-15 represents the average of two independent experiments. In this case as well, the y-intercept is positive. The projected radius is 3.3 ± 2.5 μm (propagated S.E.), but it is also not statistically significant at the 95% confidence level (t statistic = 0.65, p = 0.56). The rise-independent

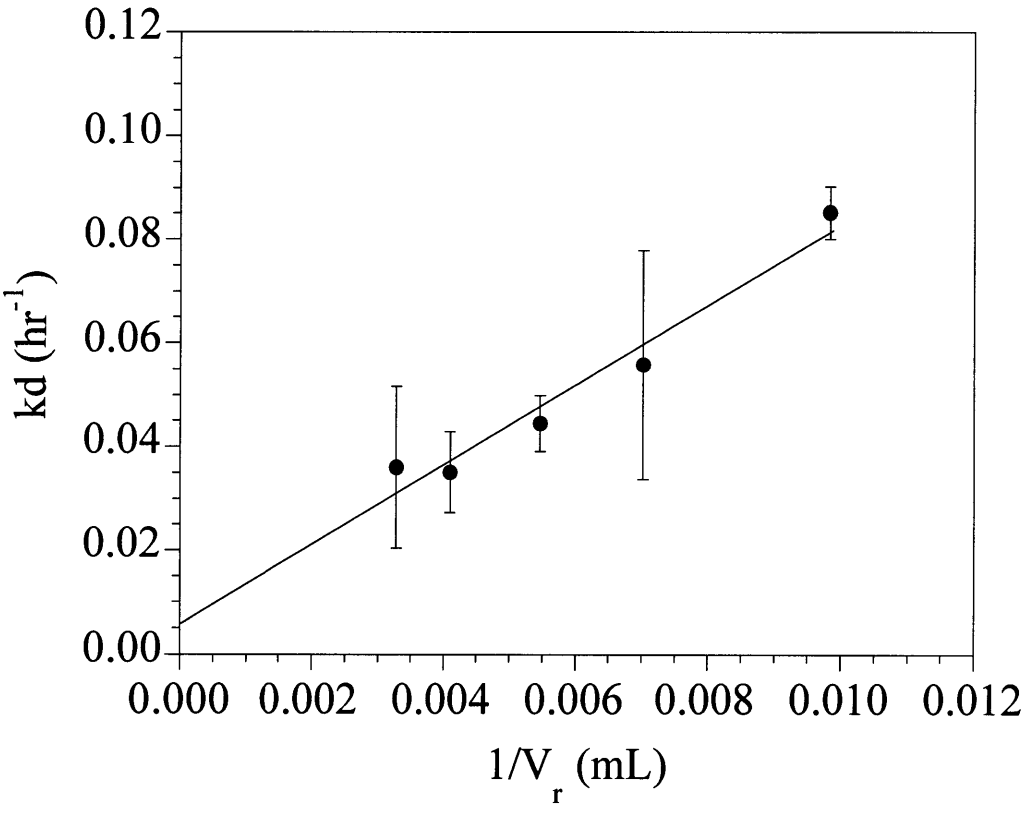

Figure 5-14 Death rate versus inverse reactor volume for serum free medium with antifoam and 0.1% w/v Pluronic® F68 (Fluka) at 37°C. The error bars represent the standard error of two to three independent experiments for 1.40 ± 0.05 mm bubbles. The gas flow rate was 43 ± 2 mL/min. The y-intercept represents a projected radius of 2.0 ± 1.2 μm, but it is not statistically significant at the 95% confidence level (t statistic = 0.84, p = 0.46).

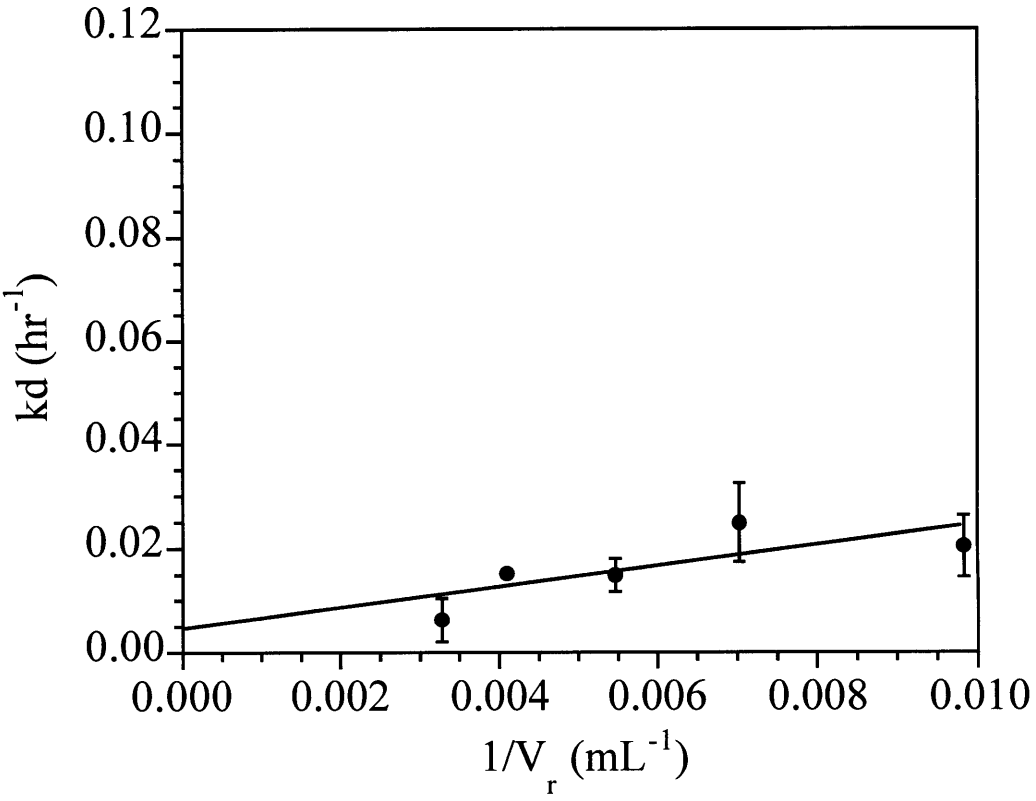

Figure 5-15 Death rate versus inverse reactor volume for serum free medium with antifoam and 0.1% w/v Pluronic® F68 (Fluka) at 37°C. The error bars represent the standard error of two independent experiments for 2.31 ± 0.03 mm bubbles. The reactor was operated at a gas flow rate of 57 ± 2 mL/min. The projected radius calculated from this data is 3.3 ± 2.5 μm, but it is not statistically significant at the 95% confidence level (t statistic = 0.65, p = 0.56).

killing volume for this case is $3.0 \times 10^{-5} \pm 1.5 \times 10^{-5}$ mL (propagated S.E.). The rise-independent killing volume is reduced compared to the serum free medium with antifoam case, and the rise-related death is also reduced. This is consistent with two protection mechanisms for Pluronic® F68.

If there is actually any cell attachment to rising bubbles, it is much smaller in magnitude than it is with serum free medium with antifoam. The data are reasonably consistent with the model predictions for Pluronic® F68, even though the model predicts a negligible projected radius. The measurements of Michaels et al. (1995a) have a broad range for attachment times, and if the true cell-bubble attachment time is towards the smaller end of the measurements, the model does predict the small projected radii measured. Also since there can be variability in different sources of Pluronics® (Yu et al. 1997), the cell-bubble attachment time might be expected to vary on this basis. Finally, this type of experiment is somewhat insensitive for measuring rise-related death, as was noted above. It was performed to compare to the experiments of Jöbses et al. (1991), which also used Pluronic® F68 and varied reactor volume. Their experiments also saw a small positive y-intercept when death rate was plotted versus inverse reactor volume.

5.4.3 Serum Free Medium with Antifoam and Methyl Cellulose

Finally in Figure 5-16, death rates are measured for various reactor volumes in serum free medium with antifoam and 0.1% w/v methyl cellulose. The gas flow rate was 43 ± 2 mL/min, using a 24 gauge needle sparger, This resulted in a bubble radius of 1.40 ± 0.05 mm, the same as with Pluronic® F68 above. Each data point represents the average of two to three independent experiments. When the death rates are plotted versus

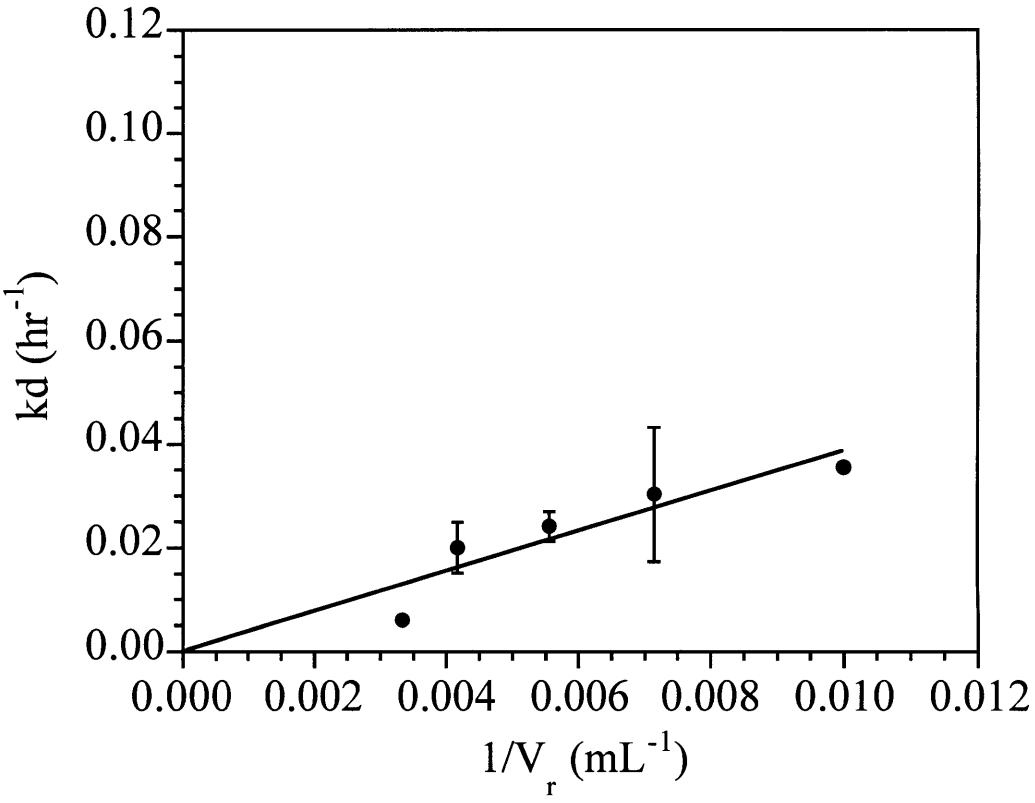

Figure 5-16 Death rate versus inverse reactor volume for serum free medium, antifoam, and 0.1% w/v methyl cellulose at 37°C. Gas flow rate was 43 ± 2 mL/min, and bubble radius was 1.40 ± 0.05 mm. The error bars represent the standard error of two to three independent experiments. The slope of the graph represents the killing volume proposed by Tramper et al. (1987) multiplied by bubble frequency. The y-intercept contains the projected radius of the bubble, which, as expected, is insignificant (t statistic = -0.05, p = 0.96).

reciprocal reactor volume, the rise-independent killing volume is determined to be 1.8 x $10^{-5} \pm 0.5 \times 10^{-5}$ mL (propagated S.E.). This is much smaller than for the case without methyl cellulose or Pluronic® F68, thus it can be inferred that methyl cellulose acts to reduce this killing volume. The y-intercept on this graph, which corresponds to rise-related death rate, is insignificant (t statistic = -0.05, p = 0.96). Consistent with the data, the model predicts a negligible rise-related death rate. This indicates that methyl cellulose is protecting by two mechanisms: reducing the rise-independent killing volume and preventing rise-related death.

5.5 Discussion

This is the first work to measure an increase in sparging related death rate with an increase in reactor height (at fixed gas flow rate, bubble radius, and reactor volume). This observation is consistent with cell attachment to rising bubbles resulting in cell death. Although the observations of cell attachment to rising bubbles in Bavarian et al. (1991) are consistent with our model, cell attachment to rising bubbles does not account for the killing volume proposed by Tramper et al. (1987). If cell attachment to rising bubbles accounted for the killing volume observed by Tramper et al. (1987), they would have observed no change in death rate when they increased reactor height with gas flow rate, bubble radius, and reactor radius fixed. The experimental death rates measured by Tramper et al. (1987) did not show this effect for two reasons: one, the experiments were conducted in a medium containing methyl cellulose; and two, relatively short reactors were used. Methyl cellulose would be expected to virtually eliminate rise-related death based on the data of Michaels et al. (1995a) and the model. It is clear from the

experimental data presented here that methyl cellulose eliminates any cell death which could be attributed to the bubble rise. For the reactor size used in the experiments of Tramper et al. (1987), one would predict that even for instantaneous cell-bubble attachment, rise-related death would be relatively minor, and thus, difficult to measure. Jöbses et al. (1991) measured sparging related death in various reactor configurations using hybridoma cells in media without methyl cellulose. They did not observe significant levels of death which could be attributed to rising bubbles. However, at the bubble and reactor sizes they used, the model suggests that bubble rise-related death would also be minor. The experiments in this paper where reactor volume was varied were conducted with reactor heights similar to those in previous publications. It is clear that for this size of reactor, rise-related death is a minor contributor to death, even though when reactor height is large enough, rise-related death can become significant.

Michaels et al. (1995a) observed that there is a dramatic increase in cell-bubble attachment time for Chinese Hamster Ovary cells when comparing serum free medium to a medium with either Pluronic® F68 or methyl cellulose. Using these data, the model correctly predicts rise-related death for the serum free medium case and predicts no rise-related death for the Pluronic® F68 and methyl cellulose cases. This model should be applicable for both animal and insect cell lines. While the experimental death rates measured here are consistent with the cell-bubble attachment times measured by Michaels et al. (1995a), the experiments lack sufficient precision to determine a reliable cell-bubble attachment time. This is because projected radius at these bubble sizes does not become sensitive to changes in attachment time until attachment time reaches the order of tenths

of seconds. It is possible that cell-bubble attachment time is dependent on cell line. Surface energies for animal and insect cells are approximately the same (Absolom 1986; Chattopadhyay et al. 1995b), but it is clear that protective additives which have similar surface energies at the gas-liquid interface can have profoundly different cell-bubble attachment times (Michaels et al. 1995a; Michaels et al. 1995b). Since this work tested conditions at the two extremes in cell-bubble attachment time, cell line effects might not be observable. The model suggests that for intermediate attachment times, like those for media with serum or polyethylene glycol, the rise-related death rate becomes sensitive to changes in attachment time. Thus, one might see cell line dependent differences in rise-related death rates for those systems. It is also possible, although not probable, that not all cells that are attached to a bubble die when the bubble bursts, and cell line differences may be observed on this basis.

The prevention of cell-bubble attachment is not the only protective action of these additives. The death that is attributable to the killing volume of Tramper et al. (1987) can be compared for the experimental conditions presented in this paper. When comparing the serum free medium case to the Pluronic® F68 and methyl cellulose cases, the killing volume was seen to decrease from $3.1 \times 10^{-4} \pm 0.4 \times 10^{-4}$ mL to $4.5 \times 10^{-6} \pm 0.2 \times 10^{-6}$ mL and $9.0 \times 10^{-6} \pm 0.5 \times 10^{-6}$ mL, respectively (bubble radii were similar for these data). Killing volumes can also be obtained from several published sources. At a bubble size of 1.4 mm, Tramper et al. (1988a) found the killing volume to be 2.2×10^{-5} mL in an insect cell system with methyl cellulose. Wu and Goosen (1995) found a killing volume of 8.6×10^{-5} mL for insect cells in a 5% v/v FBS medium at a similar bubble radius. The killing

volumes we report here were obtained at a similar temperature as those obtained in the insect cell systems. The bubble radii for our data are also comparable. The killing volume with methyl cellulose is the same order of magnitude for both animal and insect cells. The unprotected cases do not agree as well, but the insect cell case had a medium with 5% v/v FBS, while our hybridoma system was serum free. One would expect a larger killing volume for serum free medium, as serum has been shown to provide some protection against sparging damage (Kilburn and Webb 1968; Michaels et al. 1991b). Jöbses et al. (1991) reported data for hybridoma cells and bubbles 2.5 mm in radius. One can examine the relative effect of adding Pluronic® F68, but direct comparisons of killing volume are not warranted. They found the killing volume was 4.9×10^{-4} mL for a 1% v/v newborn calf serum medium and was reduced to 2.5×10^{-5} mL in a medium containing Pluronic® F68. The killing volume is reduced by a factor of 20, which compares to a reduction factor of 70 for our experiments. This difference might be attributed to cell line, batch of Pluronic® F68, or medium composition. The serum free environment used in our studies is most likely harsher for cells than the serum containing environment used by Jöbses et al. (1991). Thus, even if the final protection level afforded by Pluronic® F68 is the same, the improvement will be greater when comparing to a lesser initial standard.

6. NOVEL OXYGEN SUPPLY

6.1 Background and Calculations

Even in the presence of protective polymers, some sparging death still occurs. Thus, a novel bubble-free oxygen supply method is proposed. Oxygen solubilities in media are typically quite low, and this makes oxygen supply a critical issue in cell culture. Since mass transfer across the free liquid surface is typically insufficient to meet oxygen demand in large scale reactors, it is proposed that oxygen be supplied in a highly concentrated form. Most solids or liquids which release oxygen as part of a chemical reaction, hydrogen peroxide for example, are toxic to animal cells. Pressurizing the reactor to several atmospheres above ambient conditions using pure oxygen would improve the mass transfer. However, high concentrations of oxygen in media can cause damage to cells, including DNA degradation, lipid peroxidation, polysaccharide depolymerization, and hydroxylation of aromatics (Fee 1981), and therefore direct exposure of media to high pressure oxygen gas is not desired. Thus, to supply high concentrations of oxygen to the media, it is proposed that high pressure oxygen gas be encapsulated in a thin polymer film. This supply strategy shields the cells from high oxygen concentrations, but still ensures high mass transfer rates.

The polymer particles can be fabricated as hollow spheres (Figure 6-1), or as a foam consisting of many small, hollow spheroids. The particles can be sterilized and loaded with oxygen by diffusion through the polymer. As long as the particles are kept in a high pressure oxygen environment, they will retain the oxygen. When exposed to ambient conditions, the oxygen will begin to diffuse out from the particles. The particles

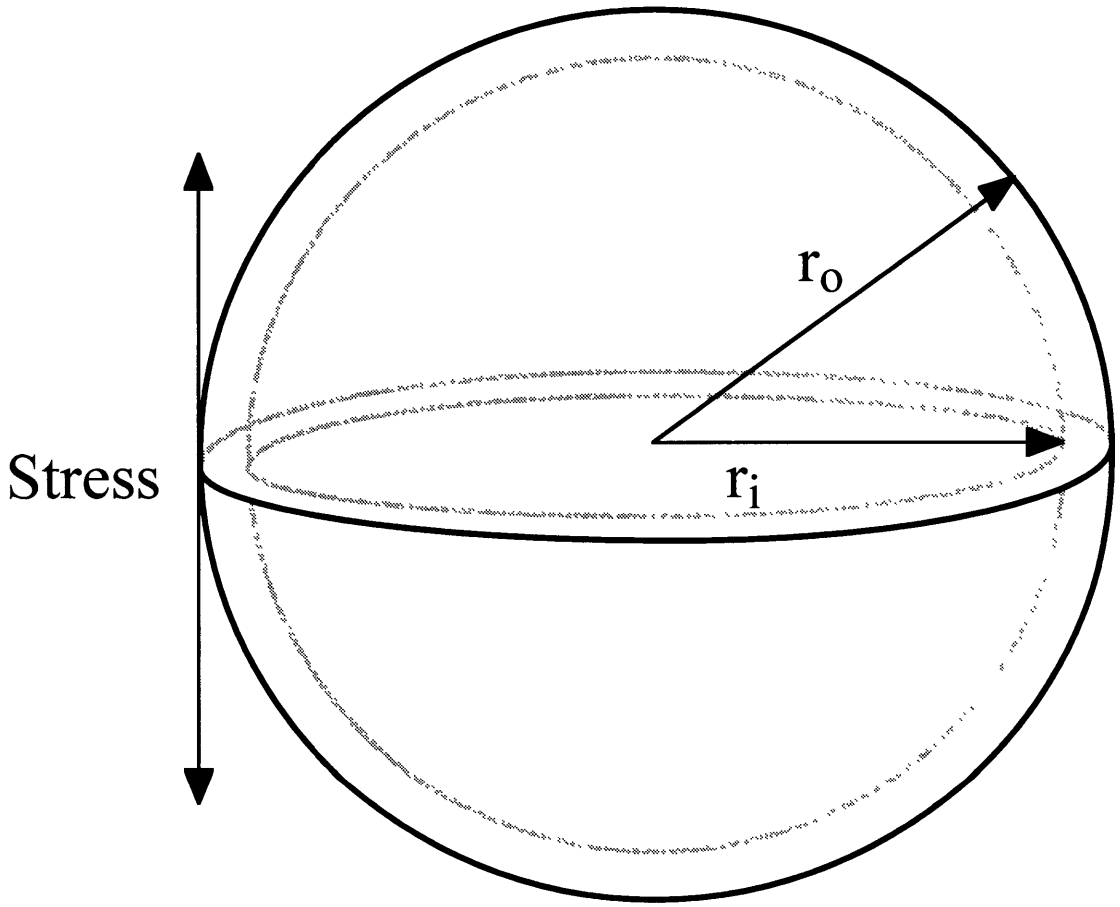

Figure 6-1 Diagram of oxygen containing particle. High pressure oxygen is contained in a thin polymer film. Internal pressure creates stress on the polymer, and the stress is dependent on the ratio of inner to outer radii of the particle.

would be treated as a fed batch nutrient and added to the media as needed to meet oxygen demand. With proper monitoring of the dissolved oxygen concentrations, cells should never experience adversely high oxygen levels. Even at the particle boundary layer, the oxygen concentration will not become dangerous if the reactor is maintained near ambient pressure exposed to a normal air atmosphere. As long as the mass transfer rate from the particle to the liquid does not exceed the mass transfer rate from the liquid boundary layer to the liquid bulk, the oxygen tension in the liquid can be kept low enough to avoid serious oxygen toxicity. Individual particles will expend their oxygen supply before the end of reactor operation. If the oxygen density in the particles is high enough, the buildup of particles should not be a problem. Alternatively, the oxygen particles could be removed semi-continuously during reactor operation.

To be practical, the polymer needs to be non-toxic and to be relatively non-adsorbent for cells and protein. The final volume fraction of particles in the reactor must be small or moderate in order to ensure a reasonable operating liquid volume fraction. There are several polymers that meet these criteria. Polyethylene is well known as a non-toxic biocompatible polymer. The polymer must also have sufficient oxygen permeability and tensile strength. The stress on the polymer in a sphere is given by

$$\text{Stress} = \frac{(\Delta P) r_i^2}{\left(r_o^2 - r_i^2\right)}$$

Equation 6-1

and it depends on the pressure difference, ΔP, the inner radius of the particle, r_i, and the outer radius of the particle, r_o. Stress on the polymer does not depend on the thickness of

the polymer; it depends on the relative thickness of the polymer. Figure 6-2 depicts the trade-off between gas loading and stress. The data are for a pressure of 1 MPa (10 atmospheres) over ambient. As the thickness of the polymer wall decreases, the stress on the polymer increases dramatically. The typical yield stress for polymers is in the range of 40-80 MPa (Krisher and Siebert 1984). The ratio of gas loading to polymer should be maximized in order to limit the volume of particles that need to be added to a reactor over the course of a batch cultivation. By setting 5 MPa as the maximum acceptable stress on the polymer and setting 1 MPa as the maximum net internal pressure for oxygen, it is possible to solve for the optimum ratio of inner and outer radii for the oxygen particles. Thus, to keep the stress on the polymer in a reasonable range, the gas loading is limited to 1.2×10^{-3} moles of oxygen per cubic centimeter polymer or less. Using this gas loading, one can calculate the total volume of particles that must be added to a reactor to support the growth of the cells. For a final cell density of 1×10^{7} cell/mL, the volume of particles added should be in the range of 5-50% of the liquid volume of the reactor, based on the range of oxygen uptake rates typical for animal cells (Miller and Blanch 1991). For the cell lines that are commonly used in industrial production, the holdup volume of oxygen particles would be about 10%.

For the conditions specified above, calculations were performed to evaluate the relative mass transfer rates between diffusion through the polymer and transport in the liquid boundary layer. Based on data and correlations in Geankoplis (1983), the mass transfer rates were calculated assuming that buoyant flow was dominating mass transfer at the particle-liquid interface. The oxygen concentration at the particle liquid interface

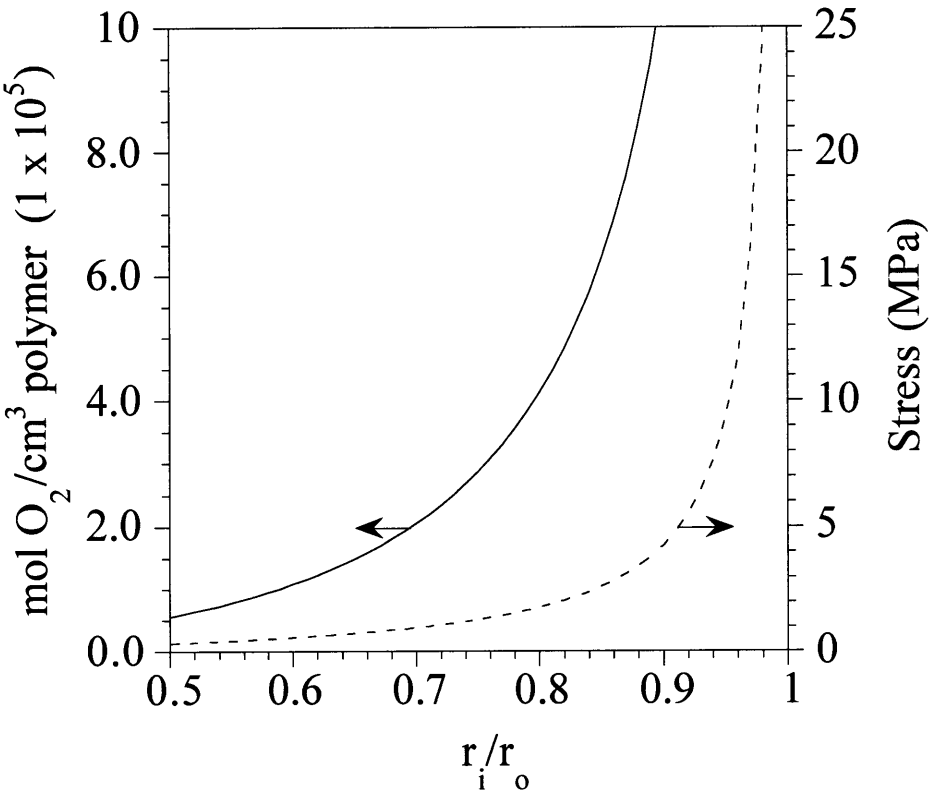

Figure 6-2 Comparison of oxygen loading and stress as a function of relative wall thickness for a spherical particle with an internal pressure of 1 MPa (10 atmospheres) over ambient. The ratio of inner to outer radii is the key parameter in determining loading and stress. The actual thickness of the polymer film is not important. As the ratio of inner to outer radii becomes large, the gas loading improves significantly; however, the stress on the polymer also increases significantly. Since the stress on the polymer must be kept well below the typical yield stress of 40-80 MPa, the oxygen loading of the particles is limited.

was assumed to be the air saturation value. The calculations showed that most polymers had sufficient oxygen diffusion rates to meet or exceed the liquid mass transfer rate when the particle size was on the order of 5 mm or less.

6.2 Experiments

The feasibility of using oxygen pressurized particles to supply oxygen was tested using hybridoma cells in serum free medium. The oxygen pressurized particles used for the test consisted of expanded polystyrene foam. This foam was tested for toxicity to the growing hybridoma cells and was found to have no effect on growth or viability. The foam was pressurized to 40 psig with oxygen and used in the experiments. When depressurized, the foam remained intact. When the foam was pressurized to 80 psig, it burst upon depressurization. A 50 mL flask was used as the test system. The cells were mechanically agitated using a magnetic stir bar operating at 80 rpm. The flask was operated with no gas headspace. The experiments consisted of two parts. First, the flask was loaded with approximately 1.0×10^6 cell/mL of cells in exponential growth, and the oxygen uptake rate was measured. Second, approximately 2.5 mL of oxygen loaded foam was added to the flask. In Figure 6-3, the cell concentration was 9.7×10^5 cell/mL. The oxygen uptake rate was 1.3×10^{-10} mmol O_2/cell-hr, which is in the normal range for animal cells (Miller and Blanch 1991). After approximately 45 min, the oxygen loaded foam was added. The 2.5 mL of foam was removed from the 40 psig oxygen atmosphere immediately prior to immersion in the culture. The foam was able to significantly exceed the oxygen demand of the culture. In Figure 6-4, the cell concentration was 9.4×10^5 cell/mL. The oxygen uptake rate in this case was 0.91×10^{-10} mmol O_2/cell-hr.

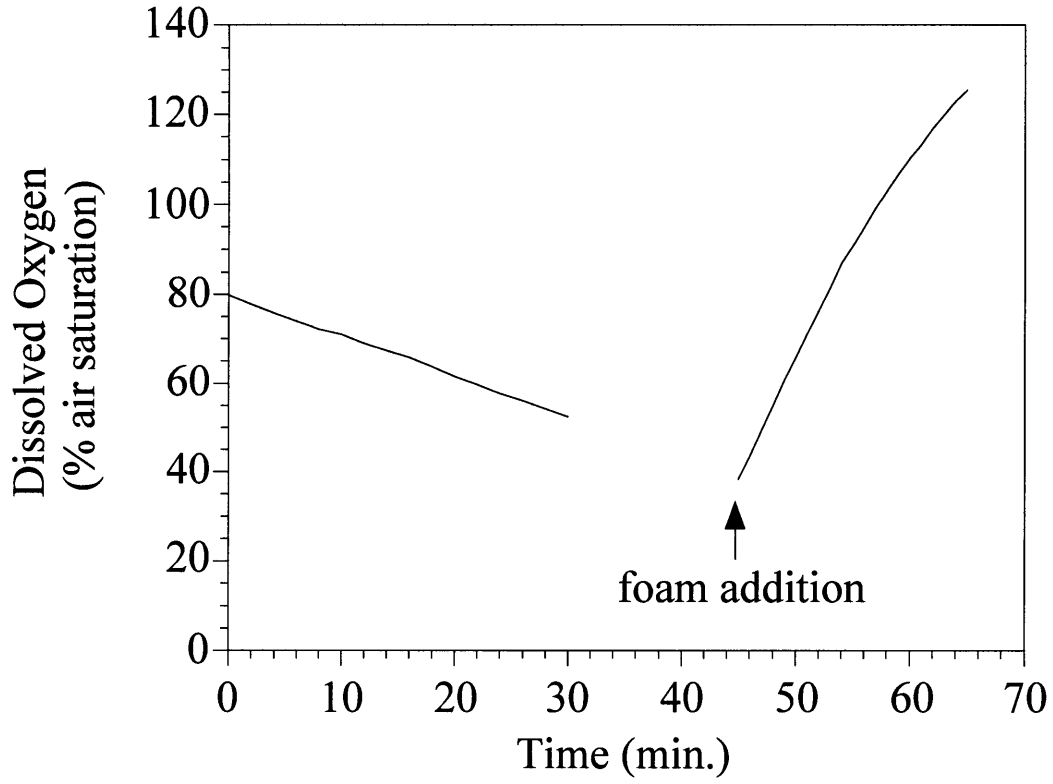

Figure 6-3 Dissolved oxygen concentrations before and after the addition of oxygenated foam. The cell concentration is 9.7 x 10^5 cell/mL. The oxygen uptake rate is 1.3 x 10^{-10} mmol O_2/cell-hr. The foam was used immediately after removal from the 40 psig oxygen atmosphere. The oxygen supply rate exceeds the oxygen demand after foam addition.

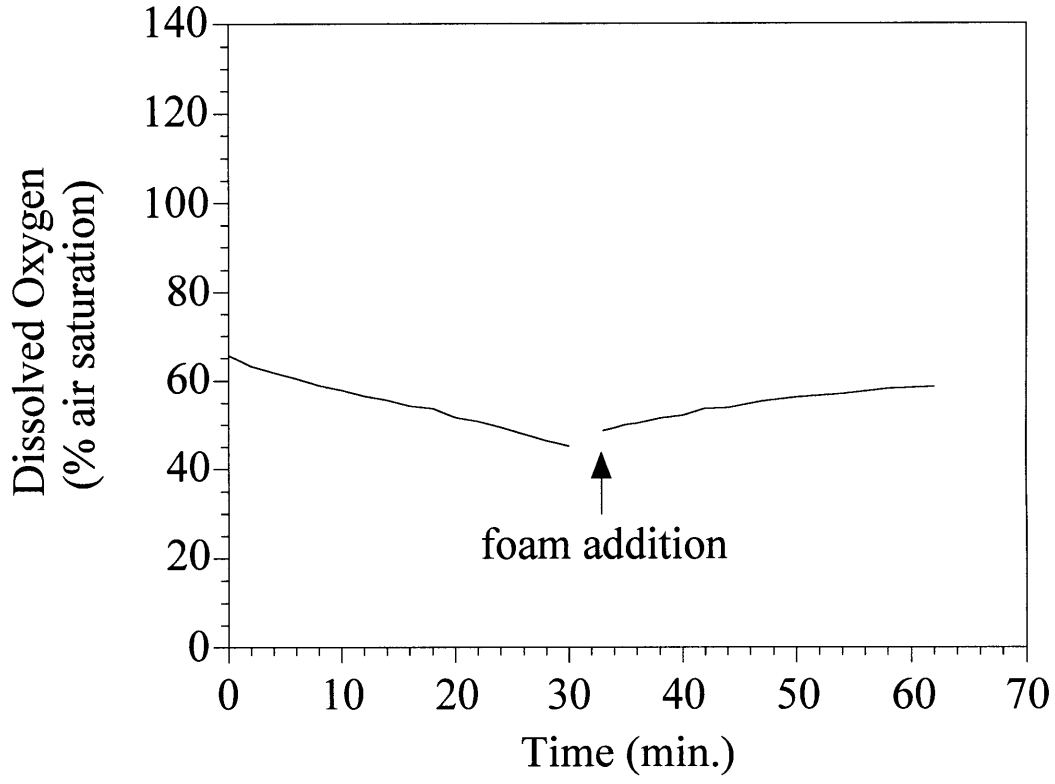

Figure 6-4 Dissolved oxygen concentrations before and after the addition of oxygenated foam. The cell concentration is 9.4 x 10^5 cell/mL. The oxygen uptake rate is 0.91 x 10^{-10} mmol O_2/cell-hr. The foam had been exposed to ambient conditions for approximately one hour and does not meet the oxygen demand as well as in Figure 6-3.

At approximately 32 min, the same foam used in the experiment in Figure 6-3 was added to the culture. It had been exposed to ambient conditions for approximately 1 hr. The foam was still able to exceed the oxygen demands of the culture. However, the oxygen supply rate was dramatically lower than in the previous case, indicating that the oxygen supply in the foam was being depleted.

Thus, the oxygen loaded particle appears to be a feasible method for supplying oxygen to an animal cell culture. It does not introduce the cell death associated with sparging, and it is easy to scale-up. The foam tested in the experiments would not be practical for an industrial system since significant amounts of protein might adsorb to the polymer. Also, each piece of foam would be depleted of oxygen after only a few hours, and the total volume of foam necessary to support a culture would be impractical. These problems are not insurmountable, however. They could be addressed with the proper polymer and good fabrication techniques. This approach does not address the other major benefit that results from sparging: removal of carbon dioxide. This is perhaps the more important issue. This approach for oxygen supply faces two obstacles for industrial application: one, there are regulatory concerns with adding a new component to the culture media; and two, with existing sparging protectants, cell death is not a problem at the cell densities currently achieved. This oxygen supply strategy may be desirable in some specialized cell culture applications, or it might by employed in other systems that need contained and sustained oxygen supply.

7. CONCLUSIONS

A model for cell attachment to rising bubbles has been developed. This new rise-related term for sparging death has been added to a model previously proposed in the literature. The previous model assumed that sparging death results solely from a volume associated with the bubble, and that the volume is independent of the reactor. The new model is dependent on the reactor, and it is consistent with behavior that has been observed in the literature but could not be explained by previous models for sparging related death. Three sets of sparging death rates measured at various bubble radii that are available in the literature were analyzed using the new model. For the case of hybridoma cells in a medium with 5% serum, the model is able to correctly predict that as bubble radius decreases, the sparging death rate increases under the assumption of nearly instantaneous cell-bubble attachment, as suggested in the literature. For the case of insect cells in a 5% serum medium, the model also correctly predicts an increase in sparging death rate as bubble radius decreases, assuming a cell bubble attachment time of 150 ms. This attachment time is consistent with published data obtained from a direct attachment time experiment. For the case of insect cells in a medium with 0.1% w/v methyl cellulose, the model correctly predicts no sparging death rate dependence on bubble radius.

This new model, which includes rise-related sparging death, was also used to predict sparging death rates as a function of reactor size. The model predicts that for lab scale reactors and large bubbles, rise-related death is a small contributor to sparging death. For lab scale reactors and small bubbles, the model predicts that rise-related death is a significant contributor to sparging related death when there are no protective additives.

For large scale reactors without a protective additive in the medium, the model predicts that rise-related death is the dominant form of sparging death. For large scale reactors with protective additives, the model predicts that rise-related death is insignificant. Thus, scale-up calculations vary according to whether protective additives are in the system. When they are present, lab scale death rates are representative of the death rates that would be observed in large scale reactors. When protective additives are absent, scale-up calculations must account for rise-related death, or there is a risk of seriously underestimating the sparging death rates at large scales.

Two types of lab scale experiment confirmed that rise-related death is significant in systems without protective additives. For hybridoma cells in serum free medium with antifoam and 1.60 ± 0.05 mm radius bubbles, the model predicts that the projected radius of the bubble is 8.0 ± 0.2 μm. The experiments found statistically significant projected radii of 14 ± 4 μm and 7.5 ± 2 μm. These data are in good agreement with the model, and they are also consistent with the attachment times found in direct attachment time measurements reported in the literature. For hybridoma cells in serum free medium with antifoam and either 0.1% w/v Pluronic® F68 or 0.1% w/v methyl cellulose, the model predicts no significant rise-related death, in good agreement with the experimental data in both systems. The data also demonstrate that Pluronic® F68 and methyl cellulose protect through two mechanisms. Both prevent cell attachment to rising bubbles, and thus prevent rise-related death. However, each also reduces rise-independent death.

Experiments with Pluronic® F68 obtained from two different sources found a statistically significant, 2.6 fold difference in death rates. When the different batches of

Pluronic® F68 were compared using gel permeation chromatography, the two batches had the same average molecular weight and polydispersity. Surface tensions for a variety of concentrations of each batch of Pluronic® F68 were also measured. There were no significant differences in surface tension until a concentration of over 3% w/v was reached. This is also the range of concentration where a change in the slope of the surface tension versus concentration curve suggests that the critical micelle concentration is being approached. The data suggest that there might be a difference in the critical micelle concentration between the two batches of Pluronic® F68, but due to a shortage of one batch of Pluronic® F68, it was not possible to determine if there was a true difference in the critical micelle concentration. No clear difference between the two batches of Pluronic® F68 can be determined from gel permeation of surface tension data. Thus, it is advisable to test different batches of Pluronic® F68 for performance in protecting against sparging related death before using them in large scale culture.

When comparing the sparging death rates obtained for the three media compositions mentioned above, cells that were sparged at 37°C had a death rate that was three fold higher that cells sparged at 24°C. This is consistent with a temperature reduction resulting in a decrease in plasma membrane fluidity. A reduction in plasma membrane fluidity has been found by other researchers to increase cell strength. Since the addition of serum can decrease plasma membrane fluidity, other researchers have also proposed that growth of cells in serum will increase cell strength. However, cells that were grown in 5% FBS and sparged in serum free medium had the same death rate as cells

that were grown and sparged in serum free medium, suggesting that serum does not affect cell strength for hybridoma cells grown under these experimental conditions.

A novel oxygen supply method was proposed and evaluated. Oxygen is charged into a porous solid polymer beads by diffusion. The beads supply cellular oxygen demands by diffusion of oxygen gas through the polymer and convective mass transfer at the bead liquid interface. An expanded polystyrene bead was pressurized using 40 psig oxygen and used to supply oxygen to cells. A volume fraction of 0.05 beads to culture was able to exceed the oxygen demands for a culture at a cell density of approximately 1×10^6 cell/mL. The foam was found to rapidly lose oxygen and is only able to supply oxygen for two to three hours at ambient conditions. The experimental data, supported by theoretical calculations, demonstrate that this approach is feasible for supplying oxygen to cultures that approach a final cell density of 1×10^7 cell/mL.

8. RECOMMENDATIONS FOR FUTURE WORK

The model for rise-related sparging death has been verified at one bubble radius and is able to explain published data obtained over a range of bubble radii. It is recommended that the model be further verified at several bubble radii using the constant volume, varied reactor height approach reported in this work. This method allows for greater accuracy in determining rise-related death. The model has only been tested at the extremes of attachment time. It would also be wise to test systems that fall in the range of intermediate attachment times, such as systems with serum. It is also recommended that for all future experiments, direct attachment times be obtained using an induction timer. This would allow unambiguous model predictions of rise-related death rates and better evaluation of the model.

It is also recommended that additional modeling work be pursued. Literature reports have found that animal and insect cells can become trapped in the draining thin films of bubble lamellae. The addition of Pluronic® F68 was reported to prevent this phenomenon. A longer cell-bubble attachment time would explain the behavior in this case as well. The drainage of the thin film and film-cell encounters could be modeled in a fashion analogous to that employed for rising bubbles. Cell attachment in the lamellae could be measured using confocal microscopy. It is likely that the reduction in rise-independent death found with Pluronic® F68 corresponds directly to the reduction of cells trapped in the lamellae.

The model might also be further verified by large scale reactor experiments. Specific death rates could by measured using the same bubble sizes in a large industrial

reactor of 2000 to 10 000 L and in a smaller, shorter reactor of 10 L. The gas flow rates should be high enough to induce significant death. These experiments could be conducted in an industrial reactor during validation runs when the product would not be used. When the data are normalized by bubble frequency and reactor volume, the large reactor should have a higher specific death rate if no additives are present. The difference in normalized death rates could then be used to determine the rise-related death, as explained in this thesis. With protective additives present, the normalized death rates for the large and small reactors should be the same.

No further research is recommended for the oxygen supply beads. It appears to be impractical due to regulatory concerns. It is also unnecessary at present, as sparging with protective additives is able to support the cell densities currently achieved in industry.

9. NOMENCLATURE

C = concentration
f_b = bubble frequency
g = acceleration of gravity
g_c = conversion factor
H_r = reactor height
k_d = first order death rate
Q = volumetric gas flow rate
r = spherical radial coordinate
R = gas constant
Re = Reynolds number
R_b = bubble radius
R_c = cell radius
r_i = inner radius of oxygen particle
R_i = interception radius
r_o = outer radius of oxygen particle
R_p = projected radius
R_r = reactor radius
t = time
T = temperature
v = velocity
v_t = terminal rise velocity
v_θ = arcial velocity
v_∞ = unbounded free stream velocity
V_b = bubble volume
V_d = death volume
$V_{d,rise}$ = death volume from rising bubbles
V_r = reactor volume
γ_{lv} = surface tension of gas-liquid interface
Γ = surface excess
ΔP = pressure difference
θ = spherical angular coordinate
κ^s = surface dilatational viscosity
μ_g = gas viscosity
μ_l = liquid viscosity
π = Pi
ρ_l = liquid density
ρ_g = gas density
τ = contact time
Ψ = stream function

10. REFERENCES

Absolom, D. R. 1986. Measurement of surface properties of phagocytes, bacteria, and other particles. Methods in Enzymology. **132:** 16-95.

Absolom, D. R. 1988. Erythrocyte adhesion to polymer surfaces: physicochemical and hydrodynamic factors. In: B. D. Ratner, Surface Characterization of Biomaterials, Elsevier Science Publishers, Amsterdam.

Absolom, D. R., Lamberti, F. V., Policova, A., Aingg, W., van Oss, C. J. and Neumann, W. 1983. Surface thermodynamics of bacterial adhesion. Applied Environmental Microbiology. **46:** 90-97.

Al-Rubeai, M., Oh, S. K. W., Musaheb, R. and Emery, A. N. 1990. Modified cellular metabolism in hybridomas subjected to hydrodynamic and other stresses. Biotechnology Letters. **12:** 323-328.

Al-Rubeai, M., Singh, R. P., Emery, A. N. and Zhang, Z. 1995b. Cell cycle and cell size dependence of susceptibility to hydrodynamic forces. Biotechnology and Bioengineering. **46:** 88-92.

Al-Rubeai, M., Singh, R. P., Goldman, M. H. and Emery, A. N. 1995a. Death mechanisms of animal cells in conditions of intensive agitation. Biotechnology and Bioengineering. **45:** 463-472.

Augenstein, D. C., Sinskey, A. J. and Wang, D. I. C. 1971. Effect of shear on the death of two strains of mammalian tissue cells. Biotechnology and Bioengineering. **13:** 409-418.

Bavarian, F., Fan, L. S. and Chalmers, J. J. 1991. Microscopic visualization of insect cell-bubble interactions. I: Rising bubbles, air-medium interface, and the foam layer. Biotechnology Progress. **7:** 140-150.

Born, C., Zhang, Z., Al-Rubeai, M. and Thomas, C. R. 1992. Estimation of disruption of animal cells by laminar shear stress. Biotechnology and Bioengineering. **40:** 1004-1010.

Chalmers, J. J. and Bavarian, F. 1991. Microscopic visualization of insect cell-bubble interactions. II: The bubble film and bubble rupture. Biotechnology Progress. **7:** 151-158.

Chattopadhyay, D., Rathman, J. F. and Chalmers, J. J. 1995a. The protective effect of specific medium additives with respect to bubble rupture. Biotechnology and Bioengineering. **45:** 473-480.

Chattopadhyay, D., Rathman, J. F. and Chalmers, J. J. 1995b. Thermodynamic approach to explain cell adhesion to air-medium interfaces. Biotechnology and Bioengineering. **48:** 649-658.

Cherry, R. S. 1991. A system for photographing cell-sized particles moving at high velocities. Biotechnology Techniques. **5:** 233-236.

Cherry, R. S. and Hulle, C. T. 1992. Cell death in the thin films of bursting bubbles. Biotechnology Progress. **8:** 11-18.

Edwards, D. A., Brenner, H. and Wasan, D. T. 1991. Interfacial Transport Processes and Rheology. Butterworth-Heinemann, Boston.

Fee, J. A. 1981. In: Oxygen and Life, Royal Society of Chemistry, London.

Freshney, R. I. 1987. Culture of Animal Cells, A Manual of Basic Technique. 2nd. Wiley-Liss, New York.

Garcia-Briones, M. and Chalmers, J. J. 1992. Cell-bubble interactions: Mechanisms of suspended cell damage. In: H. Pedersen, R. Mutharasan and D. DiBiaso, Annals of the New York Academy of Science, New York Academy of Science, New York.

Garcia-Briones, M. A., Brodkey, R. S. and Chalmers, J. J. 1994. Computer simulations of the rupture of a gas bubble at a gas-liquid interface and its implications in animal cell damage. Chemical Engineering Science. **49:** 2301-2320.

Gardner, A. R., Gainer, J. L. and Kirwan, D. J. 1990. Effects of stirring and sparging on cultured hybridoma cells. Biotechnology and Bioengineering. **35:** 940-947.

Geankoplis, C. J. 1983. Transport Processes and Unit Operations. 2nd. Allyn and Bacon, Inc., Boston.

Goldblum, S., Bae, Y.-K., Hink, W. F. and Chalmers, J. J. 1990. Protective effect of methylcellulose and other polymers on insect cells subjected to laminar shear stress. Biotechnology Progress. **6:** 383-390.

Handa, A., Emery, A. N. and Spier, R. E. 1987a. On the evaluation of gas-liquid interfacial effects on hybridoma viability in bubble column bioreactors. Developments in Biological Standardization. **66:** 241-253.

Handa, A., Emery, A. N. and Spier, R. E. 1987b. Detrimental effects of sparger aeration on suspended mammalian cell cultures - and their prevention. In: Proceedings, 4th European Congress on Biotechnology, Elsevier Science Publishers B.V., Amsterdam.

Handa-Corrigan, A., Emery, A. N. and Spier, R. E. 1989. Effect of gas-liquid interfaces on the growth of suspended mammalian cells: mechanisms of cell damage by bubbles. Enzyme and Microbial Technology. **11:** 230-235.

Jöbses, I., Martens, D. and Tramper, J. 1991. Lethal events during gas sparging in animal cell culture. Biotechnology and Bioengineering. **37:** 484-490.

Jordan, M., Sucker, H., Einsele, A., Widmer, F. and Eppenberger, H. M. 1994. Interactions between animal cells and gas bubbles: The influence of serum and Pluronic® F68 on the physical properties of the bubble surface. Biotechnology and Bioengineering. **43:** 446-454.

Kilburn, D. G. and Webb, F. C. 1968. The cultivation of animal cells at controlled dissolved oxygen partial pressure. Biotechnology and Bioengineering. **10:** 801-814.

Krisher, A. S. and Siebert, O. W. 1984. Materials of Construction. In: D. W. Green, Perry's Chemical Engineer's Handbook, 6th. McGraw-Hill, Inc., New York.

Kunas, K. T. and Papoutsakis, E. T. 1989. Increasing serum concentrations decrease cell death and allow growth of hybridoma cells at higher agitation rates. Biotechnology Letters. **11:** 525-530.

Kunas, K. T. and Papoutsakis, E. T. 1990a. The protective effect of serum against hydrodynamic damage of hybridoma cells in agitated and surface-aerated bioreactors. Journal of Biotechnology. **15:** 57-70.

Kunas, K. T. and Papoutsakis, E. T. 1990b. Damage mechanisms of suspended animal cells in agitated bioreactors with and without bubble entrainment. Biotechnology and Bioengineering. **36:** 476-483.

Lakhotia, S., Bauer, K. D. and Papoutsakis, E. T. 1992. Damaging agitation intensities increase DNA synthesis rate and alter cell-cycle phase distributions of CHO cells. Biotechnology and Bioengineering. **40:** 978-990.

Leverett, L. B., Hellums, J. D., Alfrey, C. P. and Lynch, E. C. 1972. Red blood cell damage by shear stress. Biophysical Journal. **12:** 257-273.

Maneri, C. C. and Mendelson, H. D. 1968. The rise velocity of bubbles in tubes and rectangular channels as predicted by wave theory. AIChE Journal. **14:** 295-300.

Martens, D. E., de Gooijer, C. D., Beuvery, E. C. and Tramper, J. 1992. Effect of serum concentration on hybridoma viable cell density and production of monoclonal antibodies in CSTRs and on shear sensitivity in air-lift loop reactors. Biotechnology and Bioengineering. **39:** 891-897.

McQueen, A. and Bailey, J. E. 1989. Influence of serum level, cell line, flow type and viscosity on flow-induced lysis of suspended mammalian cells. Biotechnology Letters. **11:** 531-536.

McQueen, A., Meilhoc, E. and Bailey, J. E. 1987. Flow effects on the viability and lysis of suspended mammalian cells. Biotechnology Letters. **9:** 831-836.

Mercille, S. and Massie, B. 1994. Induction of apoptosis in nutrient-deprived cultures of hybridoma and myeloma cells. Biotechnology and Bioengineering. **44:** 1140-1154.

Michaels, J. D., Kunas, K. T. and Papoutsakis, E. T. 1992. Fluid-mechanical damage of freely-suspended animal cells in agitated bioreactors: Effects of dextran, derivatized celluloses and polyvinyl alcohol. Chemical Engineering Communications. **118:** 341-360.

Michaels, J. D., Mallik, A. K. and Papoutsakis, E. T. 1996. Sparging and agitation-induced injury of cultured animal cells: Do cell-to-bubble interactions in the bulk liquid injure cells? Biotechnology and Bioengineering. **51:** 399-409.

Michaels, J. D., Nowak, J. E., Mallik, A. K., Koczo, K., Wasan, D. T. and Papoutsakis, E. T. 1995a. Analysis of cell-to-bubble attachment in sparged bioreactors in the presence of cell-protecting additives. Biotechnology and Bioengineering. **47:** 407-419.

Michaels, J. D., Nowak, J. E., Mallik, A. K., Koczo, K., Wasan, D. T. and Papoutsakis, E. T. 1995b. Interfacial properties of cell culture media with cell-protecting additives. Biotechnology and Bioengineering. **47:** 420-430.

Michaels, J. D. and Papoutsakis, E. T. 1991a. Polyvinyl alcohol and polyethylene glycol as protectants against fluid-mechanical injury of freely-suspended animal cells (CRL 8018). Journal of Biotechnology. **19:** 241-258.

Michaels, J. D., Petersen, J. F., McIntire, L. V. and Papoutsakis, E. T. 1991b. Protection mechanisms of freely suspended animal cells (CRL 8018) from fluid-mechanical injury. Viscometric and bioreactor studies using serum, Pluronic® F68 and polyethylene glycol. Biotechnology and Bioengineering. **38:** 169-180.

Miller, W. M. and Blanch, H. W. 1991. Regulation of Animal Cell Metabolism in Bioreactors. In: C. S. Ho and D. I. C. Wang, Animal Cell Bioreactors, Butterworth-Heinemann, Boston.

Mizrahi, A. 1984. Oxygen in human lymphoblastoid cell line cultures and effect of polymers in agitated and aerated cultures. Developments in Biological Standardization. **55:** 93-102.

Murhammer, D. W. and Goochee, C. F. 1988. Scaleup of insect cell cultures: Protective effects of Pluronic® F-68. Bio/Technology. **6:** 1411-1418.

Murhammer, D. W. and Goochee, C. F. 1990a. Structural features of nonionic polyglycol polymer molecules responsible for the protective effect in sparged animal cell bioreactors. Biotechnology Progress. **6:** 142-148.

Murhammer, D. W. and Goochee, C. F. 1990b. Sparged animal cell bioreactors: Mechanism of cell damage and Pluronic® F-68 protection. Biotechnology Progress. **6:** 391-397.

Newitt, D. M., Dombrowski, N. and Knelman, F. H. 1954. Liquid entrainment 1. The mechanism of drop formation from gas or vapour bubbles. Transactions of the Institution of Chemical Engineers. **32:** 244-261.

Oh, S. K. W., Nienow, A. W., Al-Rubeai, M. and Emery, A. N. 1989. The effects of agitation intensity with and without continuous sparging on the growth and antibody production of hybridoma cells. Journal of Biotechnology. **12:** 45-62.

Orton, D. R. 1992. Quantitative and mechanistic effects of bubble aeration on animal cells in culture. Doctoral Thesis. Massachusetts Institute of Technology.

Passini, C. A. and Goochee, C. F. 1989. Response of a mouse hybridoma cell line to heat shock, agitation, and sparging. Biotechnology Progress. **5:** 175-188.

Petersen, J. F., McIntire, L. V. and Papoutsakis, E. T. 1988. Shear sensitivity of cultured hybridoma cells (CRL-8018) depends on mode of growth, culture age and metabolite concentration. Journal of Biotechnology. **7:** 229-246.

Petersen, J. F., McIntire, L. V. and Papoutsakis, E. T. 1990. Shear sensitivity of hybridoma cells in batch, fed-batch, and continuous cultures. Biotechnology Progress. **6:** 114-120.

Ramirez, O. T. and Mutharasan, R. 1990. The role of the plasma membrane fluidity on the shear sensitivity of hybridomas grown under hydrodynamic stress. Biotechnology and Bioengineering. **36:** 911-920.

Ramirez, O. T. and Mutharasan, R. 1992. Effect of serum on the plasma membrane fluidity of hybridomas: an insight into its shear protective mechanism. Biotechnology Progress. **8:** 40-50.

Sato, M., Levesque, M. J. and Nerem, R. M. 1987. Micropipette aspiration of cultured bovine aortic endothelial cells exposed to shear stress. Arteriosclerosis. **7:** 276-286.

Shürch, U., Einsele, A., Kramer, H., Widmer, F. and Eppenberger, H. M. 1987. Influence of shear-forces on proliferation and antibody-production of hybridoma cells grown in mass culture. In: Proceedings, 4th European Congress on Biotechnology.

Smith, C. G. and Greenfield, P. F. 1992. Mechanical agitation of hybridoma suspension cultures: Metabolic effects of serum, Pluronic® F68, and albumin supplements. Biotechnology and Bioengineering. **40:** 1045-1055.

Smith, C. G., Greenfield, P. F. and Randerson, D. H. 1987. A technique for determining the shear sensitivity of mammalian cells in suspension culture. Biotechnology Techniques. **1:** 39-44.

Stathopoulos, N. A. and Hellums, J. D. 1985. Shear stress effects on human embryonic kidney cells in-vitro. Biotechnology and Bioengineering. **27:** 1021-1026.

Sutherland, K. L. 1948. Physical Chemistry of Flotation. XI. Kinetics of the Flotation Process. Journal of Physical Colloid Chemistry. **52:** 394-425.

Tramper, J., Joustra, D. and Vlak, J. M. 1987. Bioreactor design for growth of shear-sensitive insect cells. In: C. Webb and F. Mavituna, Plant and Animal Cell Cultures: Process Possibilities, Ellis Horwood, Chichester.

Tramper, J., Smit, D., Straatman, J. and Vlak, J. M. 1988a. Bubble-column design for growth of fragile insect cells. Bioprocess Engineering. **3:** 37-41.

Tramper, J. and Vlak, J. M. 1988b. Bioreactor design for growth of shear-sensitive mammalian and insect cells. In: A. Mizrahi, Advances in Biotechnological Processes, Alan R. Liss, Inc., New York.

Tramper, J., Williams, J. B. and Joustra, D. 1986. Shear sensitivity of insect cells in suspension. Enzyme and Microbial Technology. **8:** 33-36.

Treybal, R. E. 1980. Mass Transfer Operations. 3rd. McGraw-Hill Publishing Company, New York.

Trinh, K., Garcia-Briones, M., Hink, F. and Chalmers, J. J. 1994. Quantification of damage to suspended insect cells as a result of bubble rupture. Biotechnology and Bioengineering. **43:** 37-45.

van der Pol, L., Bakker, W. A. M. and Tramper, J. 1992. Effect of low serum concentrations (0%-2.5%) on growth, production, and shear sensitivity of hybridoma cells. Biotechnology and Bioengineering. **40:** 179-182.

van der Pol, L., Zijlstra, G., Thalen, M. and Tramper, J. 1990. Effect of serum concentration on production of monoclonal antibodies and on shear sensitivity of a hybridoma. Bioprocess Engineering. **5:** 241-245.

van der Pol, L. A., Beeksma, I. and Tramper, J. 1995a. Polyethylene glycol as protectant against damage caused by sparging for hybridoma suspension cells in a bubble column. Enzyme and Microbial Technology. **17:** 401-407.

van der Pol, L. A., Bonarius, D., van de Wouw, G. and Tramper, J. 1993. Effect of silicone antifoam on shear sensitivity of hybridoma cells in sparged cultures. Biotechnology Progress. **9:** 504-509.

van der Pol, L. A., Paijens, I. and Tramper, J. 1995b. Dextran as protectant against damage caused by sparging for hybridoma cells in a bubble column. Journal of Biotechnology. **43:** 103-110.

Wang, N. S., Yang, J.-D., Calabrese, R. V. and Chang, K.-C. 1994. Unified modeling framework of cell death due to bubbles in agitated and sparged bioreactors. Journal of Biotechnology. **33:** 107-122.

Wu, J. and Goosen, M. F. A. 1995. Evaluation of the killing volume of gas bubbles in sparged animal cell culture bioreactors. Enzyme and Microbial Technology. **17:** 1036-1042.

Wudke, M. and Shugerl, K. 1987. Investigation of the influence of physical environment on the cultivation of animal cells. In: R. E. Spier and J. B. Griffiths, Modern Approaches to Animal Cell Technology: ESCAT, European Society for Animal Cell Technology, 8th General Meeting, Butterworths, Boston.

Yu, G.-E., Altinok, H., Nixon, S. K., Booth, C., Alexandridis, P. and Hatton, T. A. 1997. Self-association properties of oxyethylene/oxypropylene/oxyethylene triblock copolymer F88. European Polymer Journal. **33:** 673-677.

Zhang, S., Handa-Corrigan, A. and Spier, R. E. 1992. Foaming and media surfactant effects on the cultivation of animal cells in stirred and sparged bioreactors. Journal of Biotechnology. **25:** 289-306.

Zhang, Z., Al-Rubeai, M. and Thomas, C. R. 1992b. Mechanical properties of hybridoma cells in batch culture. Biotechnology Letters. **14:** 11-16.

Zhang, Z., Al-Rubeai, M. and Thomas, C. R. 1992c. Effect of Pluronic® F-68 on the mechanical properties of mammalian cells. Enzyme and Microbial Technology. **14:** 980-983.

Zhang, Z., Al-Rubeai, M. and Thomas, C. R. 1993a. Comparison of the fragilities of several animal cell lines. Biotechnology Techniques. **7:** 177-182.

Zhang, Z., Al-Rubeai, M. and Thomas, C. R. 1993b. Estimation of disruption of animals cells by turbulent capillary flow. Biotechnology and Bioengineering. **42:** 987-993.

Zhang, Z., Ferenczi, M. A., Lush, A. C. and Thomas, C. R. 1991. A novel micromanipulation technique for measuring the bursting strength of single mammalian cells. Applied Microbiology and Biotechnology. **36:** 208-210.

Zhang, Z., Ferenczi, M. A. and Thomas, C. R. 1992a. A micromanipulation technique with a theoretical cell model for determining mechanical properties of single mammalian cells. Chemical Engineering Science. **47:** 1347-1354.